Topical Review

Zonal flows and pattern formation

Ö D Gürcan[1] and P H Diamond[2,3]

[1] LPP, Ecole Polytechnique, CNRS, F-91128 Palaiseau, France
[2] WCI Center for Fusion Theory, NFRI, Daejeon, Korea
[3] CMTFO and CASS, UCSD, California 92093, USA

E-mail: ozgur.gurcan@lpp.polytechnique.fr

Abstract

The general aspects of zonal flow physics, their formation, damping and interplay with quasi two dimensional turbulence are explained in the context of magnetized plasmas and quasi-geostrophic fluids with an emphasis on formation and selection of spatial patterns. General features of zonal flows as they appear in planetary atmospheres, rotating convection experiments and fusion plasmas are reviewed. Detailed mechanisms for excitation and damping of zonal flows, and their effect on turbulence via shear decorrelation is discussed. Recent results on nonlocality and staircase formation are outlined.

Keywords: zonal flows, drift waves, plasma turbulence, geophysical fluid dynamics, staircases

(Some figures may appear in colour only in the online journal)

1. Introduction: zonal flows in nature and laboratory

There are a range of problems in nature where an open dynamical system, usually a fluid, displays irregular behavior that results from free energy sources driving instabilities leading to a chaotic or turbulent state as the system evolves nonlinearly. These nonlinear systems typically create and destroy, a large number of different kinds of structures corresponding to different configurations of a field variable at different hierarchical levels that are nonlinearly coupled. Spatial structures that are generated by external drive in a turbulent fluid, and are destroyed by cascading to smaller or larger scales of a spectral hierarchy is an example of this.

Such systems, when driven far from equilibrium, can in fact explore a wide range of possible configurations of their phase space. A far from equilibrium system will go through many different configurations, and will generate more exotic structures as compared to a fluid near equilibrium. While the emergence of these structures are usually related to the particulars of the free energy source, and how the system taps this source microscopically, there are some

general features of how these 'large scale' structures adapt to the microphysics of the problem. Advective nonlinearities in a fluid system for instance, tend to decorrelate spatial points that may initially be correlated, by mixing the fluid elements via swirling eddy motions. However, every now and then, the out of equilibrium system, as it explores the phase space of all possible configurations in a nonlinear way, finds an interesting configuration that may be called a 'coherent structure', which is an emergent configuration of the turbulent fields that is preferred by the dynamics and the external constraints because of its distinct properties.

A particular spatial configuration of a fluid may, for example, transport heat most efficiently. Or it may be that the way the dissipation acts on a system makes it such that a particular flow configuration is unaffected by dissipation. In other cases, it may be that a spatial pattern arises because it is favored by the intrinsic nonlinear dynamics of the system.

One may speculate that part of the story of formation of coherent structures in a nonlinearly evolving system, can be understood via a process akin to 'natural selection': *those structures that are fittest in the sense that they can withstand the action of the nonlinearity, or transform the abundant free energy sources most efficiently, last longer, while the others die and keep generating other structures nonlinearly until they find a similar coherent configuration that is preferred by the nonlinearity, the dissipation or the externally imposed constraints.*

One implication of this view is that a strongly nonlinear open dynamical system, is expected to eventually be populated by coherent structures especially in regions of the hierarchy that are farther away from the drive. Homogenization of potential vorticity (PV) in quasi-geostrophic fluids [1] or quasi-two dimensional description of plasmas, formation of dipolar vortex solutions in quasi-geostrophic fluids [2, 3] and in drift wave turbulence [4], magnetic relaxation [5, 6] or the process of dynamic alignment in magnetohydrodynamics (MHD) [7–9] can all be considered as examples of this kind of evolution towards a nonlinear structure that is least prone to the action of the nonlinearities.

The rest of the story involves how different structures that are most effective in sometimes opposing roles such as transforming free energy sources and withstanding nonlinear stresses, co-evolve and adapt collectively to the environmental pressures that they themselves create or modify. As is the case in what are called 'complex adaptive systems' [10], the structures are not only affected by their environment which define them, but form collectively an ecosystem that sustains their own subsistence and evolve towards new equilibria that are better adapted to the environmental constraints and pressures.

Similar to species evolution, complex multiscale dynamical behavior may appear in nonlinear systems. For instance, a competition between two kinds of structures, one that can absorb the free energy very effectively, and another that can withstand the nonlinearity for long periods of time is not all that surprising. Such a competition may turn into an evolutionary 'arms race', and may end up developing very effective coherent structures leading to one species wining the arms race. Such a drastic change appears, when a dynamical system goes through a phase transition.

Possibly, one of the most striking phase transition phenomenon observed in plasma turbulence, is that of low to high confinement (L–H) transition in fusion plasma devices called tokamaks. In these systems, a certain class of coherent structures, called zonal flows, usually form and coexist with the underlying turbulence that is driven unstable by background gradients of heat and particles that are being confined. A particular class of instabilities that appear in these systems, generically called drift-instabilities (or drift-waves), drive these structures via Reynolds stresses, while these structures regulate the underlying drift-waves that drive them. Today we know that the L–H transition in tokamaks is preceded by limit cycle oscillations, that may be modeled as predator-prey (PP) dynamics.

Such large scale, long lived coherent structures, usually exist in systems that allow inverse cascade. The 'great red spot' of the Jovian atmosphere is a remarkable example. Gulfstream, or meandering jet streams in the atmosphere may be cited as other, more down to earth examples. While it is important to understand how these structures form, it is clear that once they form, they are relatively stable, as they can avoid complex distortions due to nonlinear stresses. Both atmospheres display atmospheric zonal flows, mesoscale alternating meridional flow patterns in addition to these convective structures. The subject of the current review is the formation and damping of these flows, characterization and qualitative understanding of their dynamics, and their influence on the environment, and the turbulence that drives them.

Even though they are a member of the cosmic family of coherent structures, with a possible underlying general principle such as the one discussed above, the zonal flows are also very specific in their flow patterns. The fact that they appear in physically very different natural systems imply that more concrete similarities may exist between these different problems. In other words, in addition to the rather general common nature of formation of coherent structures in open, nonlinear, far from equilibrium systems, formation of zonal flow patterns in quasi-two dimensional systems require particular attention to detail, in order to understand their particular 'universal' character.

1.1. Dynamics of drift wave/quasi-geostrophic turbulence with zonal flows

The complexity of turbulent dynamics, necessitates using a statistical description. While a straightforward application of the statistical methods leads to a solution with zero energy flux among spatial scales associated with the equipartition of energy, the physical solution of the energy budget equations in a driven (or internally unstable) system with a well defined inertial range (or a similar range of scales with regular character) is the case of fixed spectral flux. This leads to various types of spectra akin to the celebrated Kolmogorov spectrum [11].

The presence of large scale flow structures such as zonal flows, modify this picture substantially by turning it into a problem of mesoscale dynamics. In this view, neither the spectrum, nor the fluctuation level (i.e. mixing length), are *a priori* statistically stationary. There is no necessary 'steady state', and therefore the meso-scale dynamics of zonal jets and fluctuations has to be resolved at the same footing with the establishment of the wave-number spectra and radial profiles of average density, angular momentum, temperature as well as the fluctuations themselves. Here we will discuss how this difficult problem can be formulated for drift waves in magnetized confinement devices and quasi-geostrophic fluids in planetary atmospheres, and how it can be tackled in various different limiting cases with concrete applications from fusion plasmas.

Notice that this does not preclude the existence of steady states with zonal flows. This is the case, for instance, in the atmosphere of Jupiter, with a zonal flow pattern that seems to vary little over the years [12]. Similar staircase patterns are known to exist in the ocean [13], and have been observed in basic plasma devices [14] and gyrokinetic simulations of fusion plasmas [15].

Turbulence in a rotating frame can be approximately formulated as a PV conservation, or in the more general case as a PV budget, generated via barotropic pumping and dissipated via frictional drag or viscous stresses. This formulation is applicable to a surprisingly wide variety of examples from planetary atmospheres to the ocean and to sloping bottom and rotating convection experiments, due to the fact that the relation is exact for the Navier–Stokes equation in a rotating frame of reference, and therefore is respected in various approximate forms or expansions such as the quasi-geostrophic approximation.

There are various descriptions of plasma turbulence to varying degrees of realism from the Klimontovich, to Vlasov–Boltzmann, to two fluid, to gyro or drift-kinetics. Reduced drift equations can be obtained either by taking the moments of gyro or drift-kinetic equations [16], or by using a drift expansion of the velocities in two-fluid equations. Since each of the two-fluid equations are isomorphic to the Navier–Stokes equation in rotating frame (with Lorentz force playing the role of Coriolis force), it is easy to show that one can define a PV for each species (ions or electrons) that is conserved as it is advected by the velocity of that species. In the case of simplified dynamics for ions or electrons (such as adiabatic ions, or a simple generalized Ohm's law), one can write a single PV that is conserved by the plasma velocity. Substituting the drift expansion into these conserved potential vorticities and using other equations such as the equation of continuity etc we can derive a wide range of equations from ion temperature gradient driven instability (ITG) to Hasegawa–Wakatani or to Charney–Hasegawa–Mima, with proper treatment of zonal flows, in the form of sheared flows which form out of the stresses exerted on the fluid by the wave turbulence.

PV mixing can be thought of as a unifying framework that can be used to describe the formation of staircases. We discuss how the plasma and the geophysical cases are similar in certain aspects with certain key differences in others. We note that the Rhines scale defines a scale at which the standard 2D dual cascade picture at smaller scales, switch to wave turbulence interacting primarily with the zonal flows. One can define an anisotropic generalization of this, as a curve in k_x, k_y space inside of which the drift or Rossby wave turbulence display the character of wave turbulence. Note that the Rhines scale, critical balance and mixing length estimates are related as they all describe balance between linear and nonlinear processes defining a critical scale, or a critical curve in k space.

PV is important for the turbulence/ZF evolution since it is a mixed quantity (i.e. background+fluctuation+zonal) that is exactly conserved by the full nonlinear dynamics. Therefore it is the square of the PV, the potential enstrophy (PE), that is really exchanged between the zonal and the fluctuating components. The spectral evolution can be described more accurately as a local dual cascade, competing with a nonlocal PE forward cascade mediated by the zonal flows through which the zonal flows acquire their energy. A description leading to PP oscillations by these processes can be introduced using the wave-kinetic formulation.

Because the basic form of drift/Rossby group propagation is backwards with respect to its radial phase propagation they carry wave momentum towards the stirring region resulting in momentum convergence. Thus, if a seed velocity shear is introduced, the sheared flow leading to a tilting of the eddies results in an increase of the initial shear. This mechanism forms the basis of the modulational instability analysis based on a wave-kinetic formulation.

The modulational instability framework also allows the derivation of amplitude equations describing the self-focusing and the wave-collapse phenomena for the coupled drift-wave/zonal flow dynamics. The amplitude equations can also be derived to describe the two dimensional evolution of this system and therefore describing and anisotropic wave-collapse. Using more and more anisotropic scalings to describe the anisotropic collapse leading to the formation of the zonal flows.

During the cycle of the PP evolution, one important stage, which determines how the cycle advances, is the phase where the zonal flow slowly dissipates its energy. This happens due to a damping, or a drag mechanism on the large scale flow. Different linear and nonlinear mechanisms for the damping of zonal flows exist. In particular the effect of passing-trapped particle friction, can be mentioned as a linear neoclassical mechanism for the zonal flow damping.

Another key phase in the PP cycle is the quenching of the turbulence by the zonal flows by shearing apart, or by refracting (in k_r) the underlying turbulence. This is a well-known

mechanism which is due to the shearing of the eddies by zonal flow shear, which can be described also as an exchange of enstrophy between the large scale flow and the small scale turbulence. One not so obvious mechanism of shear decorrelation come actually from the effect of sheared flow on the three-wave resonance process. The sheared flow acts as a differential Doppler shift on the frequency of each of the three interacting waves. This reduces the resonance manifold, while decreasing the nonlinear three-wave interaction coefficients, making the direct three-wave interactions less efficient, and thus forcing the turbulence to interact exclusively via the zonal flows.

The stages of initial growth, the secondary growth of the sheared flow, the suppression of the primary instability by the flow shear, and the damping of the sheared flow consequently constitute a PP cycle. The first being the growth phase of a linear instability, which is usually well studied. The second stage being the formation of sheared flows for instance via the modulational instability, which is caused by Reynolds stresses (but could be Maxwell or kinetic stresses as well). The last stage, being the damping of the zonal flow. Surprisingly, such a cycle can be modeled by simplifying the linear pieces of the physics (putting a constant growth rate for the turbulence and damping rates for both the turbulence and the zonal flows), and using a basic description of the enstrophy transfer such as cascade models or shell models. It is clear in this picture that the cascade that is mediated by the zonal flows and the PP dynamics are inherently tied.

Zonal flows are probably key players also in the transition to the H-mode in magnetically confined plasmas. Limit cycle oscillations, possibly linked to PP oscillations between zonal flows, mean flows, and turbulent fluctuations have been observed in a number of tokamaks during the transition phase (also called the I-phase). Simple L–H transition models based on self-consistent mean $E \times B$ shear and its suppression of turbulent transport have been studied starting from the early 90s. Such models can be extended to include the PP dynamics, leading to the formation of limit cycle oscillations or radially propagating zonal flow waves via coupling to momentum transport physics.

PV staircases, are well-known features in geophysical fluid dynamics, which give rise to the formation of zonal jets. Zonal jets can be described by inverting these PV staircases for the zonal flow component. While in the equivalent plasma system (either the Hasegawa–Wakatani, or the generalized Hasegawa–Mima problems) it is not possible to simply invert the PV in order to obtain the flow, the fact remains that the zonal flow equation is a simple Euler equation even in the plasma case, which makes it possible that the zonal PV can be inverted to obtain zonal flows.

One final subject related to the zonal flow physics is the question of non-locality in turbulent transport in magnetically confined plasmas. A turbulent patch localized in space due to the localization of its drive or free energy naturally spreads in space. It is the basic swirling motion of turbulent eddies themselves that spread the turbulence. Zonal flows play a key role in turbulent spreading either by inhibiting it, or by dynamically coupling to it and generating zonal flow-avalanche (of poloidal momentum transport) waves.

1.2. Planetary atmospheres

There is no uniformity in terms of atmospheric dynamics of planets in the solar system. Mercury has little atmosphere and the wind patterns around it are dominated by an outward flow away from the sun, much like a comet's. Venus has a dense atmosphere that rotates much faster than the rotation of the planet itself (super-rotation), two features shared also by Saturn's moon Titan, the only moon in the solar system to have a substantial atmosphere. Earth's atmosphere has interesting turbulent dynamics and complex wind patterns, with appearance of
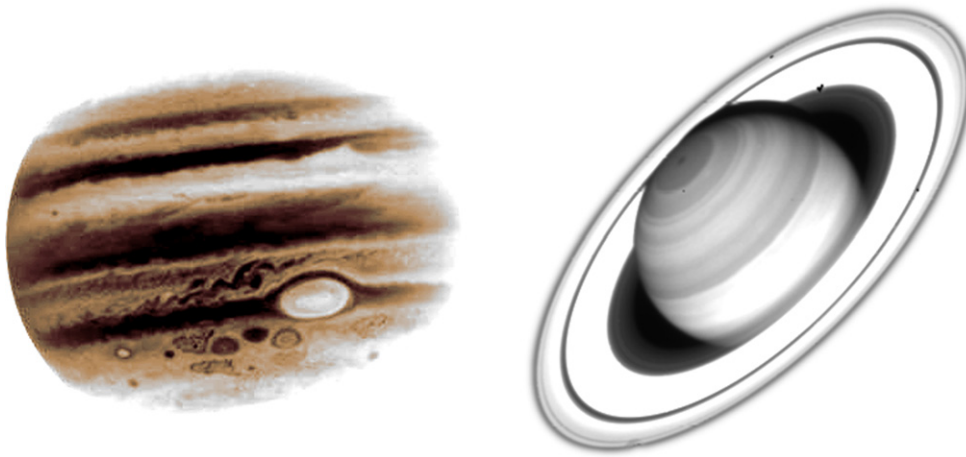
Figure 1. Jupiter, with the banded flow pattern of its atmosphere and its giant red spot on the left, and Saturn with its disk and finer banded structure of its atmosphere on the right as observed by the Hubble Space Telescope.
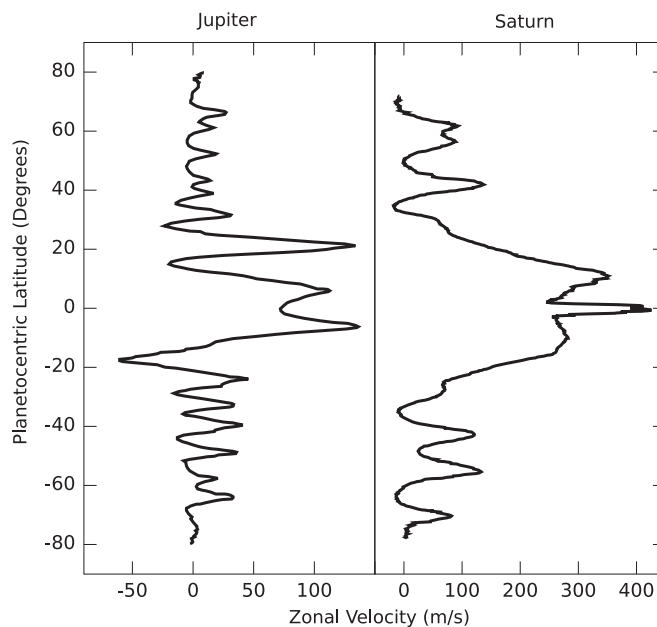

Figure 2. Atmospheric wind patterns of Jupiter on the left [18] and Saturn on the right [19] from the Cassini ISS (Imaging Sub-System) data.

intermittent cyclones, hurricanes and other phenomena, which incidentally gets more interesting as we keep pumping CO_2 into it. However the speeds of these winds barely ever reach 10–20% of the rotation speed of the earth. As any fan of science fiction knows; one of the most striking features of the Martian atmosphere, is the existence of sudden giant sandstorms.

In an interesting contrast to those, are the gas giants, like Jupiter and Saturn. Jupiter's atmosphere is very particular with persistent characteristic features. Yet it is very dynamic and

rotates differentially with a rather remarkable banded cloud structure resulting from the zonal winds that dominate the flow pattern of the atmosphere (see figure 1). Saturn has a similar banded cloud structure of its atmosphere, which seems relatively finer than that of Jupiter. However, its differential flow pattern is rather similar (see figure 2) with banded, sheared flows.

Observations of features of Jupiter's atmosphere, go back to the 17th century, to the time of Giovanni Cassini who was apparently aware of the giant red spot. The realization of its differential rotation came about as a kind of acceptance of defeat in the face of a series of failed attempts to determine its rotation speed based on the rotation of characteristic features visible on its surface [17].

Determination of the atmospheric flow patterns of Jupiter date back to 50 s from ground based observations [20]. Images from Voyager missions [12], Hubble Space Telescope [21] and Cassini spacecraft's Imaging Sub-System (ISS) [18] have been used to determine the atmospheric velocities, verifying and increasing the confidence in earlier observations. The images from these missions give us a very detailed picture of the turbulence at the top layers of Jupiter's atmosphere as a very rich complex dynamical problem [22].

One obvious feature of the atmospheres of these planets is the existence of zonal flow structures, a feature incidentally shared by the atmosphere of our earth in the form of mid-latitude westerlies. Banded zonal flows are also observed in the Earth's oceans [13, 23, 24], in the form of coherent flow structures elongated in the east-west direction.

While the giant planets and earth have very different atmospheres, sufficient parallels exist between these systems that a uniform mathematical formulation is possible at the simplest level. In fact, with slight differences on the equations of state and the approximations on compressibility, the same basic mathematical set of equations can be used to describe the dynamics of the atmosphere and of the oceans at the same time.

1.2.1. β-plane turbulence. From Rossby [25]:

In a barotropic atmosphere it is possible to eliminate the pressure between the two equations governing the horizontal components of motion. The resulting equation expresses the fact that vertical atmospheric columns, moving across the surface of the earth, must preserve their individual absolute vorticity after allowence has been made for such vorticity changes as may result from horizontal shrinking or stretching.

Large scale chaotic motions in a planet's atmosphere can be described using a fluid formulation similar to Navier–Stokes equations to a very good approximation. Electromagnetic fluctuations and kinetic effects can safely be neglected when dealing with flow patterns at atmospheric scales. Instead, there are two ingredients, which are essential in order to describe atmospheric turbulence: rotation and granulation. To describe basic fluid motion in a rotating atmosphere, we can write the basic equations in the form:

$$\left(\frac{\partial}{\partial t} + \mathbf{v} \cdot \nabla \right) \mathbf{v} + 2\Omega \times \mathbf{v} = -\frac{\nabla P}{\rho} \tag{1}$$

and derive the equation for the component of vorticity that is normal to the planet surface: $\zeta \equiv \hat{\mathbf{n}} \cdot (\nabla \times \mathbf{v})$

$$\left(\frac{\partial}{\partial t} + \mathbf{v}_\perp \cdot \nabla \right) \zeta + (\zeta + f) \nabla_\perp \cdot \mathbf{v}_\perp + v_y \frac{\partial}{\partial y} f = 0, \tag{2}$$

where $\mathbf{v}_\perp$ is the horizontal component of the velocity, $f = 2\Omega \sin\theta$ is the local component of the planetary vorticity (Ω is the planetary rotation rate and θ is the latitude) $\hat{\mathbf{n}}$ is the vector normal to the planet's surface and P and ρ are the pressure and mass density of the atmosphere. Note that the normal component of the curl of the term on the right hand side (i.e. $\rho^{-2}\hat{\mathbf{n}} \times \nabla\rho \cdot \nabla P$) vanishes by virtue of the equation of state $P = P(\rho)$, independent of its particular functional form. Fluids that satisfy this condition (i.e. $\nabla\rho \times \nabla P = 0$) in general are called 'barotropic fluids'. Here x and y are local longitudinal and latitudinal directions respectively. Hence, f is taken to be a function of y.

If we consider thickness of the fluid layer, an equation of continuity can be written:

$$\left(\frac{\partial}{\partial t} + \mathbf{v}_\perp \cdot \nabla\right)h + h\nabla_\perp \cdot \mathbf{v}_\perp = 0 \tag{3}$$

which together with (2) implies conservation of

$$\frac{\mathrm{d}}{\mathrm{d}t}\left[\frac{\zeta + f}{h}\right] = 0 \tag{4}$$

which means for an individual fluid element $(\zeta + f) \propto h$.

In other words, as Rossby describes in the above quotation, the absolute vorticity $\zeta + f$ of a fluid element, changes only with horizontal shrinking or stretching. This is in fact a particular version of what has come to be called the Ertel's theorem:

$$\frac{\mathrm{d}}{\mathrm{d}t}\left[\frac{\omega_a \cdot \nabla\lambda}{\rho}\right] = 0, \tag{5}$$

where $\omega_a = \Omega + \nabla \times \mathbf{v}$ is the absolute vorticity, and λ is a Lagrangian conserved quantity which is a function of density, pressure or both (usually $\lambda = s$, where s is entropy), with possible sources and sinks. In the above example for example the λ corresponds to density itself with a constant stratification of height h in the direction normal to the planet's surface.

The above quantity is called 'PV', probably in analogy with the concept of 'potential temperature' that was already commonly used in atmospheric physics at the time when it was first introduced. *It indicates the vorticity the air column would have had, had it been at the reference latitude f_0 with a reference height of h_0.*

1.2.2. Freezing in laws. Freezing in laws in the form of

$$\frac{\partial}{\partial t}\omega = \nabla \times (\mathbf{v} \times \omega), \tag{6}$$

where ω is a freezing in quantity, are important ingredients of mixed conservation laws such as PV conservation. Considering together with an equation of continuity of the form

$$\frac{\partial n}{\partial t} + \mathbf{v} \cdot \nabla n + n\nabla \cdot \mathbf{v} = 0$$

we can write:

$$\left(\frac{\partial}{\partial t} + \mathbf{v} \cdot \nabla\right)\frac{\omega}{n} = \frac{\omega}{n} \cdot \nabla\mathbf{v} \tag{7}$$

Following Vallis [26], consider a Lagrangian conserved quantity χ. The difference in values of χ between two infinitesimally separated points on a line element $\delta\ell$ is also conserved:

$$\frac{\mathrm{d}}{\mathrm{d}t}\delta\chi = \frac{\mathrm{d}}{\mathrm{d}t}(\nabla\chi \cdot \delta\ell) = 0$$

and since the equation of an infinitesimal line element can be written as $\mathrm{d}\delta\ell/\mathrm{d}t = \delta\mathbf{v}$ or:

$$\left(\frac{\partial}{\partial t} + \mathbf{v} \cdot \nabla\right)\delta\ell = \delta\ell \cdot \nabla\mathbf{v} \tag{8}$$

since (7) and (8) are isomorphic, the vorticity and the line element evolve exactly the same way, which means that we can write:

$$\frac{\mathrm{d}}{\mathrm{d}t}\left(\nabla\chi \cdot \frac{\omega}{n}\right) = 0.$$

1.2.3. Geostrophic balance. The simplest formulation, which includes a basic form of planetary rotation and granulation is the so-called β-plane model. This model is commonly used in geophysical fluid dynamics as a crude model of geophysical turbulence. Its simplicity comes from a number of assumptions and approximations.

It relies on a particular condition called the geostrophic balance:

$$\mathbf{v}_\perp = \frac{\hat{\mathbf{n}} \times \nabla P}{f\rho}$$

which is a statement of the local balance between the vertical components of the Coriolis force $-2\boldsymbol{\Omega} \times \mathbf{u}$ and the pressure gradient force $-\nabla P/\rho$.

It is mathematically equivalent to the so called 'drift approximation' in magnetized plasmas. For example, the $E \times B$ drift:

$$\mathbf{v}_E = \frac{\hat{\mathbf{b}} \times \nabla\Phi}{B}c$$

which is a balance between the Lorentz force (i.e. $q\mathbf{v} \times \mathbf{B}/c$) and the electric force (i.e. $-q\nabla\Phi$) is in fact a lowest order force balance when the magnetic field is large. The analogy between the magnetized plasmas and planetary atmospheres is based partly on the fact that Coriolis and Lorentz forces have the same mathematical forms.

Both of these expression for the lowest order balance, can be extended by adding other similar terms. Both correspond to the zeroth order equation in a perturbation expansion with a small parameter (introduced by strong rotation in one case, and strong magnetic field in the other). The small parameter in the case of geophysical fluid dynamics is the Rossby number

$$\varepsilon = \frac{U}{2\Omega L},$$

where U and L are characteristic velocity and length scale respectively.

A similar balance exists in the horizontal direction between the horizontal pressure gradient and the gravity force. This allows us to write the horizontal component of the velocity as $\mathbf{v}_\perp = gf^{-1}\hat{\mathbf{n}} \times \nabla h$, where the thickness of the fluid layer $h = h_0(x, y) + h_1(x, y, t)$ plays the role of the stream function [27].

The critical simplification of the beta plane approximation is the assumption that the projection of the planetary vorticity in the direction perpendicular to the surface of the planet varies roughly linearly in the latitudinal direction (i.e. $f = f_0 + \beta y$). The assumption is approximately valid for mid latitudes as long as the characteristic latitudinal extent of

fluctuations remains small compared to the scale at which the local component of the planetary vorticity changes.

The strength of the PV conservation becomes apparent when we note that within these approximations, the PV to be conserved takes the form:

$$q \approx \frac{\zeta + f_0 + \beta y}{h_0 + h_1} \approx \frac{\zeta + f_0 + \beta y - f_0 h_1 / h_0}{h_0}, \tag{9}$$

where the advection velocity is $\mathbf{v}_\perp = g f_0^{-1} \hat{\mathbf{n}} \times \nabla h_1$ (i.e. assuming h_0 is constant for the sake of argument). Due to its approximate nature q is sometimes called the quasi-geostrophic PV, whose conservation equation that can be written explicitly as:

$$\left(\frac{\partial}{\partial t} + \hat{\mathbf{n}} \times \nabla_\perp \psi \cdot \nabla_\perp \right) \left(\nabla_\perp^2 \psi - \psi \right) + \beta' \frac{\partial}{\partial x} \psi = 0, \tag{10}$$

where the temporal and spatial variables are scaled by f_0^{-1} and $R = \sqrt{h_0 g} f_0^{-1}$ (i.e. the so-called Rossby deformation radius) respectively, the normalized streamfunction is the height deviation ratio $\psi = h_1 / h_0$ and $\beta' = \frac{R}{f_0} \beta$ is the ratio of the Rossby radius to the local planetary vorticity gradient length. Note that (10) is the Charney equation, or the Charney–Hasegawa–Mima (CHM) equation as it is called in plasma physics. We obtained it here using a constant bottom height and a linear variation of the local horizontal planetary vorticity.

However as can be seen from the definition of PV, the same equation can be obtained with a constant f_0 but with a linear variation of the bottom height $h_0(y)$, in which case, one would write $\beta' = -\frac{R}{h_0} \frac{dh_0}{dy}$ which is the ratio of the Rossby deformation radius to the gradient length for the bottom height. It is not surprising given that the PV can change either with an increase in absolute vorticity (i.e. for instance due to a linearly varying locally vertical planetary vorticity) or with a decrease in fluid height (i.e. for instance due to a linearly varying profile of bottom height). The two give exactly the same equation. In fact any combination of those would work also in which case one would define β' using the gradient length of the equilibrium PV.

One can introduce mesoscale flows explicitly into the above picture, simply by adding the mesoscale vorticity (which is mostly zonal for geophysical problems, but we leave it general) to the definition of total PV:

$$q \approx q_0 + \bar{q} + \tilde{q},$$

where $q_0 = f_0 + \frac{\beta}{h_0} y$, $\bar{q} = \bar{\zeta}$, $\tilde{q} = \tilde{\zeta} - \frac{f_0}{h_0^2} \tilde{h}_1$, where $\bar{q}$ is the mesoscale (e.g. zonal) vorticity, which in principle varies in a slower time scale compared to the fluctuations $\tilde{q}$, but in a faster time scale compared to the mean q_0. In this case the advection velocity is also a sum of mesoscale and fluctuation velocities $\mathbf{v}_\perp = \tilde{\mathbf{v}}_\perp + \bar{v}_\perp$, where the mesoscale velocity and vorticity are linked via $\bar{\zeta} = \nabla \times \bar{\mathbf{v}}_\perp$. We leave the discussion of zonal flow physics to section 3.

The PV conservation is useful in particular due to the fact that one can invert it, to obtain physical quantities such as velocity, pressure etc. This feature is called the 'principle of invertibility' [28]. This is possible in the problem that is discussed above, so that the CHM problem can be analyzed completely in terms of PV alone. Adding any Lagrangian conserved quantity with sources and sinks (such as entropy) do not break this invertibility but changes the definition of PV.

1.3. Rotating convection

The idea that the same equation can be obtained using either the β effect, or using a constant vorticity but a variation of the bottom height may seem like a mathematical curiosity.
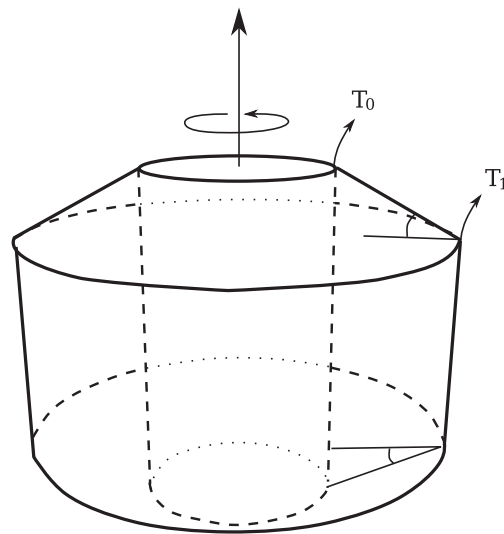
Figure 3. A characteristic rotating annulus setup for the rotating convection experiments. The system rotates with a rotation frequency Ω, the inner and outer plates of the cylinder are kept at T_0 and T_1 respectively, providing a temperature gradient for the convection, and the slope at the top and bottom of the container provides a β effect as discussed in section 1.3.

However this fact can actually be used to model planetary dynamics under laboratory conditions. This can be done in practice, using rotating platforms, where the rotation speed can be controlled and different kinds of fluid containers with varying bottom heights can be used. In the context of geophysical fluid dynamics, what is particularly interesting is the so called 'rotating convection' experiments. These can be set-up in different ways, using cylindrical or spherical containers with free or constrained top surfaces and some kind of temperature difference or fluid granulation to provide the convective drive. A large number of such experiments has been performed over the years starting from the mid 50s [29, 30] instigated partly by the theoretical works of S Chandrasekhar [31]. Today, the study of rotating convection continue to progress, especially with the advent of new measurement, analysis and visualization techniques. The large, rotating turntable experiment of Laboratoire des Ecoulements Gophysiques et Industriels in Grenoble is an example of a setup where such experiments are being performed today under different configurations. Figure 4 shows the zonal flow structures in an experiment when a small scale convective driving is supplied by spraying the upper free surface with salty (denser) water in this setup [32]. A review of the earlier experimental work on this subject can be found in [33].

One particular setup that is commonly studied in this context is the cylindrical annulus with sloping top and bottom surfaces (see figure 3) to provide the β effect where the inner and outer surfaces are kept at different temperatures to provide a temperature gradient and hence the free energy for forming convective cells [34].

Another interesting setup is the Grenoble experiment which has a sloping bottom surface and a free top surface and the convective drive is obtained by spraying salty (denser) water from the top. The observed zonal jets and their dynamics can be seen in figure 4.

You can find a detailed (and rather standard) derivation of the equations describing the evolution of rotating convection system of figure 3 in the appendix A. While for a viscous fluid with free energy injection, PV is not really conserved, one can still think in terms of a
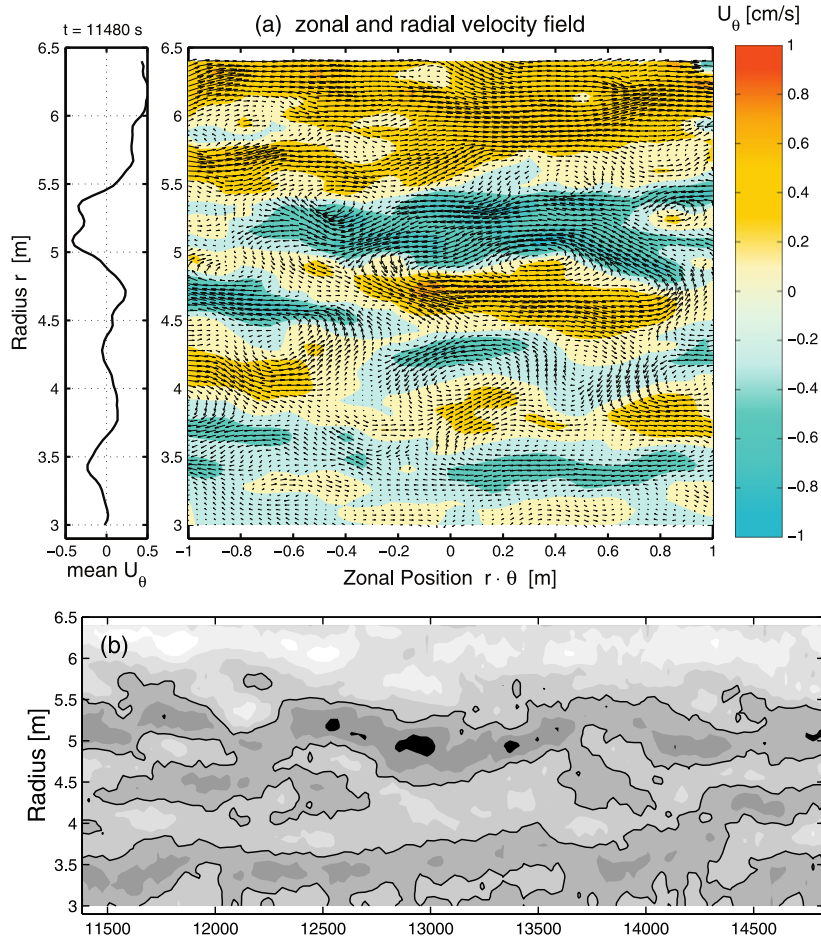
Figure 4. The velocity field from the sloping bottom experiment in Grenoble [32]. Here the snapshot of the velocity field (right) and the spatially averaged zonal velocity (left) are shown in (a) and the time evolution of the mean zonal velocity is shown in (b). Figure used with permission from Read P L *et al* 2004 *Geophys. Res. Lett.* **31** L22701. Copyright 2004 Wiley and Sons.

PV budget:

$$\frac{\mathrm{d}q}{\mathrm{d}t} = P_q - D_q, \tag{11}$$

where P_q is the production and D_q is the dissipation of q. For a Newtonian fluid, we can write the dissipation as $D_q = -\nu \nabla_{\perp}^2 q$. The production of PV comes from the so-called baroclinic term, the normal component of the curl of the term on the right hand side of equation (1) divided by height (i.e. $\rho^{-2}h^{-1}\hat{\mathbf{n}} \times \nabla\rho \cdot \nabla P$). The equation of state for the rotating convection problem is (e.g. [31]):

$$\rho = \rho_0 \big[1 - \alpha\big(T - T_0\big) \big]$$

which suggest that the density perturbation is linked to temperature perturbation, which is governed by the heat equation rather than the pressure perturbation, which is linked to

velocity through the geostrophic balance and is therefore determined by the vorticity equation. Since these two are functionally independent (albeit being dynamically coupled), the baroclinic term does not vanish, giving rise to a source of PV, which can be written to the lowest order as:

$$P_q = -\frac{1}{h\rho_0^2}\frac{\mathrm{d}P_0}{\mathrm{d}r}\frac{\partial}{\partial y}\delta\rho$$

which becomes

$$P_q = -\frac{\alpha\Omega^2 r_0}{h}\frac{\partial}{\partial y}\delta T$$

using the equation of state and the lowest order balance between pressure gradient and the centrifugal force. Here δT is the temperature perturbation as discussed in appendix A. In the setup that is considered above the PV varies only due to variations in fluid height, which is usually not fluctuating (i.e. the fluid volume is constrained both at the bottom and at the top). This means, we can write the PV as:

$$q \approx \frac{\zeta + f_0}{h_0 - 2\eta_0 x} \approx \frac{\zeta}{h_0} + \frac{f_0}{h_0}\left(1 + \frac{2\eta_0}{h_0}x\right),$$

where η_0 is the tangent of the angle that the conical top and bottom surfaces make with the horizontal. We also assumed that both angles are the same so that they add up to give $h = h_0 - 2\eta_0 x$. With this, the PV budget equation given in (11) becomes:

$$\left(\frac{\partial}{\partial t} + \hat{\mathbf{n}} \times \nabla_\perp\psi \cdot \nabla_\perp\right)\nabla_\perp^2\psi - \eta_*\frac{\partial}{\partial y}\psi = -Ra\partial_y\Theta + \nabla_\perp^4\psi \tag{12}$$

in dimensionless variables (see appendix A), which is coupled to the temperature perturbation equation of the Rayleigh–Bénard convection [35].

$$\mathcal{P}\left(\frac{\partial}{\partial t} + \hat{\mathbf{n}} \times \nabla_\perp\psi \cdot \nabla_\perp\right)\Theta + \frac{\partial}{\partial y}\psi = \nabla_\perp^2\Theta. \tag{13}$$

The system ((12)–(13)) describes the nonlinear evolution of thermal Rossby waves.

1.4. Fusion devices, tokamaks

Excellent comprehensive reviews of zonal flow physics, from the point of view fusion plasma turbulence [36], and their experimental studies in basic plasmas, tokamaks and stellarators [14] are already available. Therefore, here we will limit ourselves to developments that are relevant for the common aspects of zonal flow physics.

Zonal flows, in the context of fusion plasmas, are radially localized, poloidally elongated $E \times B$ flow structures (see figure 5). Since the radial motion associated with these flow structures is negligible by definition, zonal flows do not contribute to the radial transport. Because of this, they are usually linearly stable, or even damped and therefore has to be driven by turbulence via Reynolds stresses that the complex turbulent motions generate. We will discuss the details of the generation mechanism in the next section. Here we content ourselves to citing some physical and numerical observations of zonal flows in fusion devices, and in particular in tokamaks.

ZFs can be directly detected in the plasma by measuring the electrostatic potential. This can be achieved by measuring the floating potential using Langmuir probes near the plasma edge [38–40] or using remote diagnostic systems such as the heavy ion beam probes at the
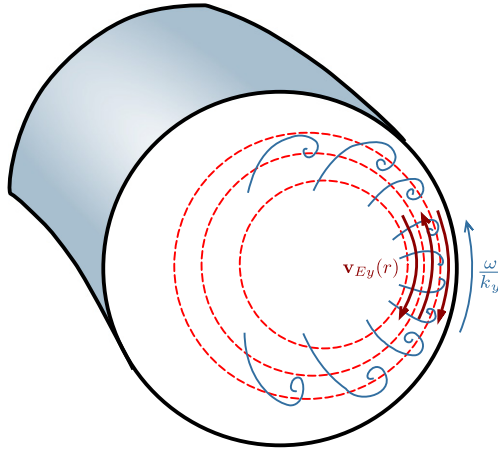
Figure 5. A cartoon, showing the basic rotating convection pattern due to diamagnetic drift, temperature inhomogeneity and curvature in a tokamak, and the zonal flows that are driven by the Reynolds stresses that are generated (in red).

core of the plasma where the physical access is limited [41, 46]. However most measurements of zonal flows in tokamak plasmas, is done on a particular class of oscillating zonal flows, called geodesic acoustic modes (GAMs). Because GAMs have a frequency of the order of few *kHz* in most tokamaks, they are much easier to detect. They have been observed on DIII-D [47, 48], JIPP T-IIU [49], ASDEX Upgrade [50], JFT-2M [51], T-10 [52], HL-2A [53] and recently on Tore Supra using a special detection technique [54]. Note that, since their oscillation is rather generic to toroidal geometry, we will not discuss specifics of GAM physics in this review. Some aspects of GAMs are, nonetheless, similar to the low frequency zonal flows that are related to the zonal flows that are observed in the geophysical setting.

Various diagnostic systems that measure fluctuation characteristics in tokamaks measure density fluctuations directly. These fluctuations show structures that propagate in the poloidal direction. This apparent movement is due to a combination of wave propagation and the actual plasma velocity. While it is not possible to separate wave propagation and plasma velocity looking only at density fluctuations, it is generally accepted that the radial profile of this speed corresponds roughly to the radial profile of the plasma velocity and the wave-number dependence of this observed velocity corresponds roughly to the wavenumber dependence of the phase speed, i.e.:

$$v_{fl}(r, k_\theta) \approx v_E(r) + v_{ph}(k_\theta).$$

Figure 6 shows the two dimensional profile of the poloidal velocity as inferred from the movement of density fluctuations observed using the beam emission spectroscopy system in the DIII-D tokamak [37]. Here the shear in the radial direction comes mostly from the shear in the $E \times B$ velocity.

1.5. Basic plasma devices

Zonal poloidal plasma flows have also been observed in various basic plasma devices, from small stellerators such as CHS [41], TJ-II [42] and TJK [43] to linear machines such as CSDX [44], CLM [45] among others. Because of the relatively large values of collisionality, the dynamics in these small devices (in particular the linear ones) is mostly dominated by

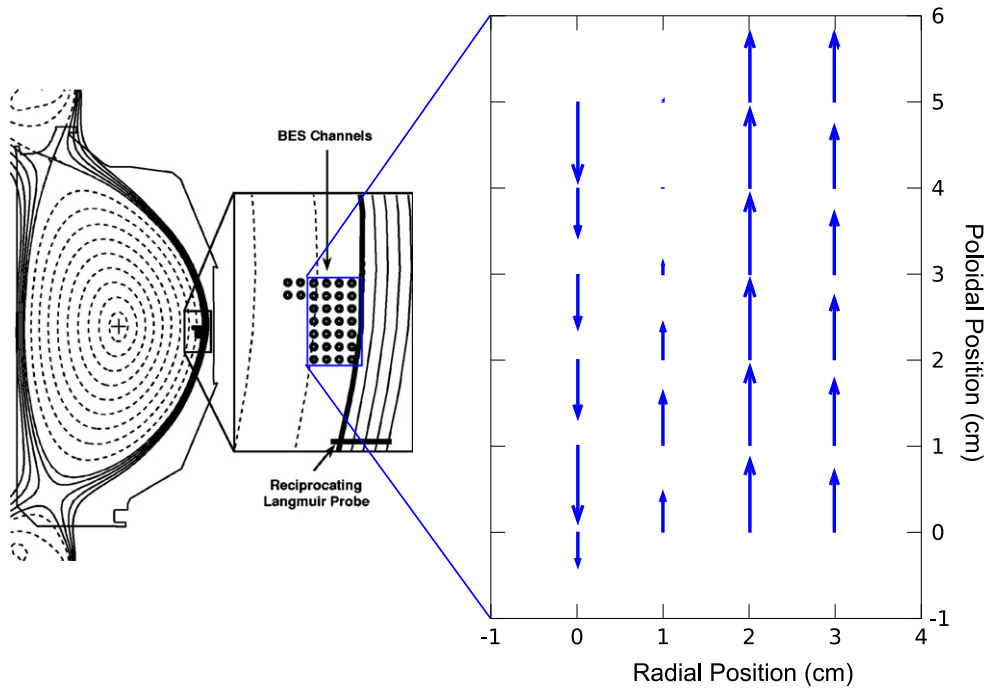**Figure 6.** The poloidal flow velocity associated with the zonal flow (GAM) in the D-IIID tokamak as inferred from the movements of density fluctuations measured by the beam emission spectroscopy (BES) system [37].
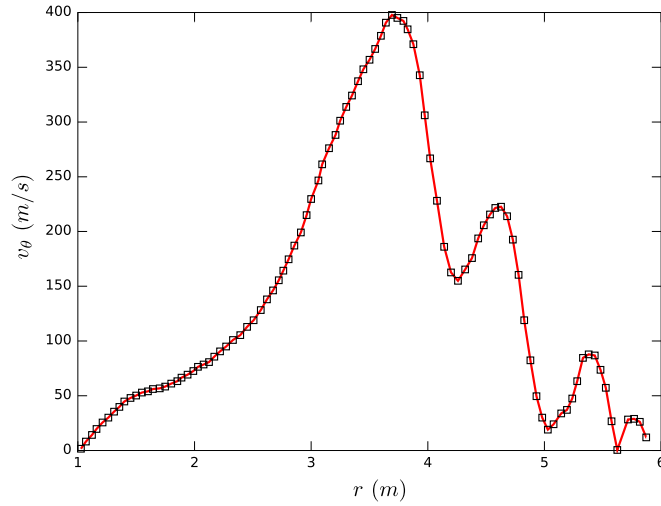

Figure 7. Poloidal ion fluid velocity from CSDX, measured using a mach probe. The original figure in [55] also has error bars roughly of the order of ± 50 m s^{-1} that we dropped for clarity.

dissipative drift instabilities (such as described by the Hasegawa–Wakatani system introduced in section 2.3.2). Using some heating schemes, ITG or electron temperature gradient driven instability (ETG) modes has been reported in some of these basic devices. While stellarators may appear relatively complicated for modeling, linear plasma machines can be modeled rather simply using a cylindrical geometry. A cylindrical plasma device with magnetic field along its axis, is almost a one-to-one analogue to the rotating convection experimental setup discussed in section 1.3. Figure 7 shows the poloidal ion fluid velocity as a function of radius where a 'zonal jet' (associated partly with the diamagnetic velocity due to background density gradient) and smaller zonal flow structures can be observed.

2. Turbulence in fusion plasmas

The primary goal of the magnetic fusion programme is to achieve sufficiently long time confinement of plasma particles and heat so that the fusion reaction may start. This is achieved in tokamaks by keeping the effective diffusion of particles and heat across the magnetic field as small as possible. In modern fusion devices, collisions are fairly rare that the heat and particle transport they drive is feeble. This allows, by heating the core of the plasma, to enforce temperature profiles, where the plasma is very hot in the center, which is necessary for the fusion reaction, and relatively much colder where the plasma touches material surfaces, which is important for the preservation of those surfaces. These radially inhomogeneous profiles of temperature and density provide free energy sources for convective instabilities akin to the convective instabilities in rotating convection problem described above (where physical rotation is replaced by diamagnetic rotation). These general class of instabilities are called drift-instabilities. They are classified based on the free energy source, rotation direction and the mechanism for tapping the free energy source.

As a general rule, radially inhomogeneous background profiles drive instabilities that have an inward-outward fluctuating velocity component. This can be explained as the plasma trying to get rid of the excess free energy (i.e. increase entropy), and in the absence of meaningful collisional transport, it can do so by arranging its fluctuating radial $E \times B$ flow such that the $E \times B$ flow is inward when the local temperature fluctuation is negative, and outward when the local temperature fluctuation is positive (at least for the case when the free energy source is the temperature gradient). This way the hotter plasma is carried outward and the cooler plasma inward, leading to an increase of entropy. This tendency, selects a linearly most unstable mode with finite poloidal wavenumber $k_y \neq 0$, and usually a vanishing radial wavenumber $k_x = 0$ (where x is the radial direction as in the rotating convection problem). This mode that is linearly unstable is characterized by spatial patterns that can be called 'linear streamers'.

Starting from seed levels, such fluctuating flow patterns grow exponentially in time in the linear phase, and saturate via mode coupling in the nonlinear phase. The couplings may be weak, nearly resonant triad interactions between well-defined waves, or strong interactions as in the case of fully developed turbulence, leading to a flux of energy, enstrophy etc through k-space. Furthermore, kinetic physics also contribute to this balance via resonant interactions between waves and particles (Landau damping, Cerenkov emission etc).

Since the goal is the amelioration of confinement, and in the MHD sense a basic state of confinement is already achieved, the primary subject of plasma turbulence in magnetized fusion is the study of the transport that the turbulence drives.
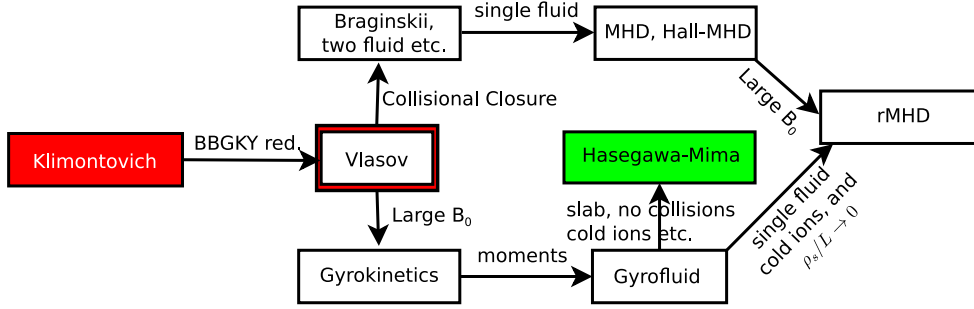
Figure 8. The connections between different types of formulations in plasma turbulence. The most general formulation being that of Klimontovich, and the simplest ones being Hasegawa–Mima and reduced MHD. Only the crucial assumptions that are required are written at each step, even though there are others. BBGKY stand for the Bogoliubov–Born–Greene–Kirkwood–Yvon hierarchy. One interesting observation is that while rMHD seems to require a collisional fluid closure, one may obtain it also based on a large Magnetic field (which localize the particles, via Larmor rotation and play the role of short mean free path).

2.1. Description of plasma turbulence

While its classical description is rather simple, its collective nonlinear nature make the general problem of plasma turbulence, one of the most complex issues that the nature confronts us with. It is, for instance, notably more complicated than the turbulence in neutral fluids due to couplings to electromagnetic fields and kinetic effects such as Landau damping. There are a pleithora of descriptions relevant for plasma problems, from the full Klimontovich description to simple reduced fluid models such as Hasegawa–Mima or Hasegawa–Wakatani systems (see figure 8).

2.1.1. Klimontovich description.
In a classical formulation, point particles follow trajectories that are fully determined by the forces acting on them. Given a collection of such point particles, the probability of finding a particle at a given time at a given position with a given speed is either one or zero, depending on whether or not a particle trajectory coincides with that point in phase space. This can be formulated using the probability distribution function

$$F_s(\mathbf{r}, \mathbf{v}, t) = \sum_{j=1}^{N_s} \delta\big(\mathbf{r} - \mathbf{r}_j(t)\big)\delta\big(\mathbf{v} - \mathbf{v}_j(t)\big), \tag{14}$$

where $\mathbf{r}_j(t)$ and $\mathbf{v}_j(t)$ constitute the trajectory of the jth particle. Taking the derivative of this expression with respect to time gives:

$$\frac{\partial F_s}{\partial t} = \sum_{j=1}^{N_s} \left(\overbrace{\frac{\mathrm{d}\mathbf{r}_j}{\mathrm{d}t}}^{\mathbf{v}_j} \cdot \frac{\partial F_s}{\partial \mathbf{r}_j} + \frac{\mathrm{d}\mathbf{v}_j}{\mathrm{d}t} \cdot \frac{\partial F_s}{\partial \mathbf{v}_j} \right),$$

where the trajectories are determined by the equations of motion for the particles:

$$\frac{\mathrm{d}\mathbf{v}_j}{\mathrm{d}t} = \frac{q_s}{m_s}\left[\mathbf{E}\big(\mathbf{r}_j, t\big) + \frac{\mathbf{v}_j}{c} \times \mathbf{B}\big(\mathbf{r}_j, t\big) \right] \equiv \mathbf{K}_s\big(\mathbf{r}_j, \mathbf{v}_j, t\big) \tag{15}$$

with q_s being the electrical charge for the species s, not to be confused with the PV (also denoted by q in this paper). Noting that $\sum_j \frac{\partial}{\partial \mathbf{r}_j} F(\mathbf{r}, \mathbf{v}, t) = -\frac{\partial}{\partial \mathbf{r}} F(\mathbf{r}, \mathbf{v}, t)$ and $\sum_j \frac{\partial}{\partial \mathbf{v}_j} F(\mathbf{r}, \mathbf{v}, t) = -\frac{\partial}{\partial \mathbf{v}} F(\mathbf{r}, \mathbf{v}, t)$, because of the form of (14), and using (15), we obtain the Klimontovich equations:

$$\frac{\partial F_s}{\partial t} + \mathbf{v} \cdot \frac{\partial F_s}{\partial \mathbf{r}} + \mathbf{K}_s(\mathbf{r}, \mathbf{v}, t) \cdot \frac{\partial F_s}{\partial \mathbf{v}} = 0. \tag{16}$$

For each species s, which are coupled to the Maxwell's equations [56] for the fields with the sources given by:

$$\mathbf{J}(\mathbf{r}, t) = \sum_s \sum_j q_s \mathbf{v}_j \delta(\mathbf{r} - \mathbf{r}_j) = \sum_s q_s \int \mathbf{v} F_s(\mathbf{r}, \mathbf{v}, t) \mathrm{d}^3 \mathbf{v},$$

$$\rho(\mathbf{r}, t) = \sum_s \sum_j q_s \delta(\mathbf{r} - \mathbf{r}_j) = \sum_s q_s \int F_s(\mathbf{r}, \mathbf{v}, t) \mathrm{d}^3 \mathbf{v}.$$

This formulation is in fact nothing but a trivial re-writing of the equations of motion in a compatible form with probabilistic descriptions. Thus, it provides no simplification whatsoever in the insurmountable initial task of solving N_s equations of motion for each species coupled with the Maxwell equations.

One interesting, maybe somewhat philosophical point, is that *turbulence* as a phenomenon of multiscale disorder is nowhere to be found in this formulation of perfectly deterministic motion of classical point particles. Nonetheless, the couplings between particles in the above equation, which take place through K_s that is determined by the phase space distribution of all the other charged particles via the Maxwell's equations open the door to the possibility of complicated motions that form the basis of what we call plasma turbulence.

2.1.2. Vlasov equation. One problem with the Klimontovich formulation, among others, is that $F_s(\mathbf{r}, \mathbf{v}, t) = F_s(\mathbf{r}, \mathbf{v}, t | \mathbf{r}_j, \mathbf{v}_j, 0)$ depends on the initial positions and velocities of all the particles of all species, since one needs the initial conditions for solving the equations of motion in order to find the trajectories. Since neither the determination of all the initial conditions, nor the computation of all the trajectories is possible, a statistical description is the only option.

In order to achieve this, consider the average of $F_s(\mathbf{r}, \mathbf{v}, t | \mathbf{r}_j, \mathbf{v}_j, 0)$ over a statistical ensemble of possible initial conditions:

$$f_s(\mathbf{r}, \mathbf{v}, t) = \left\langle F_s(\mathbf{r}, \mathbf{v}, t | \mathbf{r}_j, \mathbf{v}_j, 0) \right\rangle.$$

The distribution function $f_s(\mathbf{r}, \mathbf{v}, t)$ defined this way is naturally independent of the initial conditions, and is formally called a 'single particle distribution function'. We can write down the equation for the evolution of $f_s(\mathbf{r}, \mathbf{v}, t)$ by averaging the Klimontovich equation (16) over a statistical ensemble:

$$\frac{\partial f_s}{\partial t} + \mathbf{v} \cdot \frac{\partial f_s}{\partial \mathbf{r}} + \left\langle \mathbf{K}_s(\mathbf{r}, \mathbf{v}, t) \cdot \frac{\partial F_s}{\partial \mathbf{v}} \right\rangle = 0. \tag{17}$$

The Klimontovich acceleration involves only the electromagnetic fields that are solutions of the Maxwell's equations. Since those are linear, they can be solved using a response function in terms of the charges and currents, which are themselves functions of the distribution function F_s. Therefore the last term in (17) describing the correlations between particles can be reduced in two ways. If one drops correlations altogether, and considers only the mean

fields (that is the particles interact with eachother only via their interactions with the collectively generated mean electromagnetic fields), one obtains the Vlasov equation:

$$\frac{\partial f_s}{\partial t} + \mathbf{v} \cdot \frac{\partial f_s}{\partial \mathbf{r}} + \frac{q_s}{m_s}\left[\mathbf{E}(\mathbf{r}, t) + \frac{\mathbf{v}}{c} \times \mathbf{B}(\mathbf{r}, t)\right] \cdot \frac{\partial f_s}{\partial \mathbf{v}} = 0$$

in contrast, if one considers only local interactions (i.e. direct collisions), one obtains the Boltzman equation. In general, both of them together leads to the inclusion of a collision operator in the Vlasov equation above. Taking the moments of the Vlasov equation and using a simple collisional closure, one can obtain different fluid closures such as the Braginskii equations, or the two-fluid system of equations, which can be thought of as the basis for further reduction (see section 2.1.5 for a discussion).

2.1.3. Freezing in laws of two-fluid description.   Consider the ion equation of motion:

$$\left(\frac{\partial}{\partial t} + \mathbf{v}_i \cdot \nabla\right)\mathbf{v}_i = \frac{e}{m_i}\left(\mathbf{E} + \frac{\mathbf{v}_i}{c} \times \mathbf{B}\right) - \frac{\nabla P}{m_i n_i} \tag{18}$$

and continuity

$$\left(\frac{\partial}{\partial t} + \mathbf{v}_i \cdot \nabla\right)n_i + n_i \nabla \cdot \mathbf{v}_i = 0$$

for ions.

Note that (18) is isomorphic to equation (1), with Lorentz force replacing the Coriolis force. Taking the curl of the identity: $\nabla(\mathbf{v} \cdot \mathbf{v}) = 2\mathbf{v} \cdot \nabla\mathbf{v} + 2\mathbf{v} \times (\nabla \times \mathbf{v})$ we obtain $\nabla \times [\mathbf{v} \cdot \nabla\mathbf{v}] = -\nabla \times [\mathbf{v} \times (\nabla \times \mathbf{v})]$, which can be used to rewrite (18) as:

$$\frac{\partial}{\partial t}\Omega_i^g = \nabla \times \left(\mathbf{v}_i \times \Omega_i^g\right) + \frac{1}{m_i n_i^2}\nabla n_i \times \nabla P_i, \tag{19}$$

where $\Omega_i^g \equiv \omega_i + \frac{e\mathbf{B}}{m_i c}$ is the 'ion plasma absolute vorticity', which is a sum of the ion plasma vorticity $\omega_i = \nabla \times \mathbf{v}_i$ and the cyclotron frequency $e\mathbf{B}/m_i c$. Since (19) has the form of a freezing in law, we can write it as

$$\frac{\mathrm{d}}{\mathrm{d}t}\left(\nabla\chi \cdot \frac{\Omega_i^g}{n}\right) = \frac{1}{m_i n_i^2}\nabla n_i \times \nabla P_i \cdot \nabla\chi. \tag{20}$$

Considering an equation of heat of the form

$$\frac{\partial}{\partial t}P + \mathbf{v}_i \cdot \nabla P + \Gamma P \nabla \cdot \mathbf{v}_i = 0.$$

Which actually implies conservation of:

$$\left(\frac{\partial}{\partial t} + \mathbf{v}_i \cdot \nabla\right)s = 0,$$

where $s = P/n^\Gamma$ is the specific entropy. Now by choosing $\chi = s$ (or a function of s) causes the right hand side of (20) to vanish, resulting in the general definition of ion plasma PV as:

$$q_i \equiv \left(\frac{\omega_i + \frac{e\mathbf{B}}{m_i c}}{n_i}\right) \cdot \nabla s$$

advected by the ion velocity $\mathbf{v}_i$. We will see later that simply using this definition with a drift approximation, actually gives the correct definition of PV for various models such as Hasegawa–Mima, Hasegawa–Wakatani or slab ITG.

Note that one can write a similar conservation law separately for the electron fluid, advected by the electron velocity

$$\mathbf{v}_e = \mathbf{v}_i - \frac{\mathbf{J}}{ne},$$

where $\mathbf{J}$ is the plasma current density. Assuming for instance that the electrons have constant temperature (or have a temperature proportional to their density):

$$q_e \equiv \left(\frac{\omega_e - \dfrac{e\mathbf{B}}{m_e c}}{n_e} \right) \cdot \nabla\chi,$$

where χ is a constant of motion of the electron fluid.

2.1.4. Dual PV conservation in Hall MHD. If we consider the usual limit $m_e \ll m_i$, and the definition of the $\mathbf{v}_e = \mathbf{v}_i - \frac{c \nabla \times B}{4\pi ne}$, we can write dual freezing in laws as [57]

$$\partial_t \Omega_j = \nabla \times \left(\mathbf{u}_j \times \Omega_j \right), \quad (j = R, L)$$

with the pair of generalized vorticities and velocities defined as:

$$\Omega_R = \frac{e\mathbf{B}}{m_e c}, \quad \mathbf{u}_R = \mathbf{v} - \frac{c}{4\pi ne} \nabla \times \mathbf{B},$$

$$\Omega_L = \frac{e\mathbf{B}}{m_i c} + \nabla \times \mathbf{v}, \quad \mathbf{u}_L = \mathbf{v},$$

where $\mathbf{v}$, the ion velocity plays the role of plasma velocity. Since $\nabla \cdot \mathbf{J} = 0$, the equation of continuity with the ion and electron fluids become the same with the quasi-neutrality condition $n_e = n_i$:

$$\frac{\partial n}{\partial t} + \nabla \cdot (n\mathbf{v}_i) = \frac{\partial n}{\partial t} + \nabla \cdot (n\mathbf{v}_e) = 0$$

which means that density is conserved both by ions and electrons, which allows us to write a PV pair:

$$q_R = \frac{1}{n} \frac{e\mathbf{B}}{m_e c} \cdot \nabla\chi, \quad \mathbf{u}_R = \mathbf{v} - \frac{c}{4\pi ne} \nabla \times \mathbf{B}$$

$$q_L = \frac{1}{n} \left(\frac{e\mathbf{B}}{m_e c} + \nabla \times \mathbf{v} \right) \cdot \nabla s, \quad \mathbf{u}_L = \mathbf{v}$$

such that

$$\left(\frac{\partial}{\partial t} + \mathbf{u}_j \cdot \nabla \right) q_j = 0, \quad (j = R, L).$$

Left fluctuations are expected to dominate the ion scales, while the right fluctuations dominate the electron scales. This has actually been verified in a direct numerical simulation of incompressible Hall-MHD [58].

2.1.5. Drift-fluid description and PV conservation. For spatial scales larger than the gyro-radius and time scales slower than the cyclotron frequency, one may consider the plasma as a reduced fluid that moves around with drift velocities. The reduction that leads to this reduced fluid description is in fact a reduction in particle orbits approximating them using drift velocities. Since the dynamics of its individual elements define the nature of a 'fluid' (as a continuum approximation to a discrete system with very large degrees of freedom) the fact that the individual particles move in drift orbits leads to a description of a drift-fluid. Plasma in these scales act approximately as a drift-fluid as long as local kinetic equilibrium is established. In the case where kinetic physics is important, we use a drift-kinetic description whose moments would correspond to the drift-fluid description of desired complexity depending on the closure of the fluid hierarchy.

One interesting aspect of reduced descriptions (especially for plasmas) is that multiple reductions based on very different assumptions may lead to same or very similar reduced models even though the justifications are based on completely different hypotheses. One example is that, one can obtain reduced MHD equations either by making a fluid closure (strictly justified only when the collisions dominate) and than taking a strong magnetic field to force the system to become 2D or directly by assuming a strong magnetic field and building a fluid-like closure via the effect of the Lorentz force dominating the dynamics [59]. The reason for that is the second step making the first simplifying assumption obsolete, but somehow still respecting the final result (to a certain extent). So in this sense for instance the standard MHD may be seen as an unnecessary but simplifying intermediate step.

In the same vein, the drift-fluid equations can actually be derived from two-fluid equations (which are normally justified based on collisional closures à la Braginskii). For this reason, some people call these drift-Braginskii closures. One may however also derive them by directly taking the moments of the gyrokinetic equation leading to what is known as the gyrofluid [16] description and then going to the drift limit by dropping higher order finite Larmor radius effects.

Based on this justification, we will use two-fluid equations. An asymptotic expansion of the small parameter ω/Ω_i (using the fact that the background magnetic field is very strong) leads to what is known as the drift expansion. Doing this separately for ions and electrons and making the usual assumptions of quasi-neutrality and $m_e \ll m_i$ leads to simple tractable fluid models [60]. However, since the starting point for this derivation is the two-fluid equations. The exact conservation of PV for the two-fluid system leads to the conservation of an expanded approximate PV for the drift-fluid, with an advection velocity given by the drift velocities.

For instance considering the dominant order ion velocity of the form $\mathbf{v}_i = \mathbf{v}_E$, where $\mathbf{v_E}$ is the $\mathbf{E} \times \mathbf{B}$ velocity gives directly:

$$\left(\frac{\partial}{\partial t} + \mathbf{v}_E \cdot \nabla_\perp \right)\left(\left[\frac{\zeta_i + \Omega_i}{n_i} \right] \right) = 0$$

now where $\zeta_i = \nabla \times \mathbf{v}_E \cdot \hat{\mathbf{b}} = \frac{c}{B}\nabla_\perp^2 \Phi$ is the parallel component of the ion plasma vorticity, and Ω_i is the ion cyclotron frequency. It is interesting to note that this gives the Hasegawa–Mima equation that will be discussed in the next section when density is expanded as a linearly varying (i.e. in *x*) background and a small fluctuation around that. Note that in this approach, one need not to consider the nondivergence-free higher order correction to the plasma velocity (which is the polarization drift in the case of magnetized plasmas) explicitly.

2.1.6. Gyrokinetic equation and the PV. An honest description of turbulent phenomena in fusion plasmas unfortunately requires a way to treat kinetic effects. In order to describe kinetic evolution of plasmas under the influence of strong magnetic fields, we use the
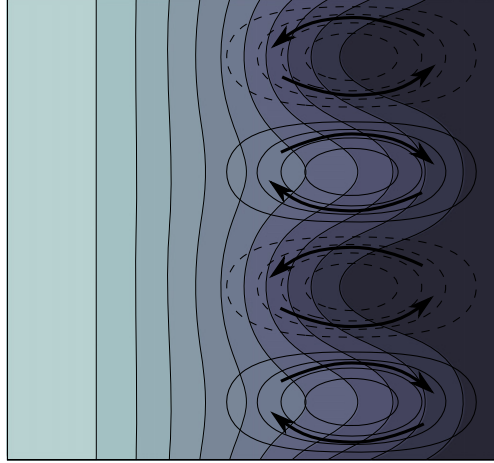
Figure 9. The basic mechanism of the drift wave. Here filled contours of density is shown, which is the sum of a background profile decreasing in the x direction plus a fluctuating sinusoidal component, which is proportional to the fluctuating electrostatic potential due to the adiabatic electron response. This gives an $E \times B$ flow as shown, which is inward just below the density maximum and outward just above it. Since the outward flow increase the density (by carrying high density plasma from the core) and the inward plasma decrease it, the density maximum ends up moving upward.

gyrokinetic equation. Gyrokinetic equation in its full glory tends to be rather complicated. However in most cases it can be written in the form of a conservation law for the guiding center distribution function $F_i = F_i \left(X, p_\parallel, \mu, t \right)$:

$$\frac{\partial}{\partial t} \left[B_\parallel^* F_i \right] + \frac{\partial}{\partial X} \cdot \left(\dot{X} F_i B_\parallel^* \right) + \frac{\partial}{\partial p_\parallel} \left(\dot{p}_\parallel F_i B_\parallel^* \right) = 0,$$

where μ, the adiabatic invariant is simply a label (since $d\mu/dt = 0$). If we want to define a quantity similar to PV, we can define:

$$N_i \equiv \int B_\parallel^* F_i dv_\parallel d\mu$$

which is actually a normalized ion guiding center density. It becomes proportional to the usual PV in the limit of slab with adiabatic electrons and $k_\perp \rho_s \ll 1$.

2.2. Role of turbulence in fusion plasmas, turbulent transport etc

The possibility of transport driven by plasma microturbulence (called anomalous transport due to historical reasons), and the difficulty this poses to the magnetized fusion was recognized rather early on in the development of the fusion programme. Different kinds of instabilities, with different characteristics have been identified over the years. One important class of instabilities that drive transport in tokamaks is the drift waves [61].

2.3. Drift waves, and instabilities

The basic drift wave is a density fluctuation on top of an inhomogeneous background density profile (see figure 9) that propagate because the radial fluctuating $E \times B$ velocity that this

density fluctuation generates, moves the high (low) density plasma outward just above a density peak (hole), and low (high) density plasma inward just below it, leading to a movement of the density peak (hole) upward in the y direction.

For dynamics at ion scales, this wave nature relies on the adiabatic electron response:

$$\frac{\tilde{n}}{n_0} = \frac{e\widetilde{\Phi}}{T_e} \tag{21}$$

which comes from the parallel (to the magnetic field) component of the electron equation of motion (Ohm's law).

$$-\nabla_{\parallel} P_e + en\nabla_{\parallel}\Phi = 0$$

with $P_e = nT_e$, actually gives:

$$\nabla_{\parallel}\left(\frac{n}{n_0} - \frac{e\Phi}{T_e} \right) = 0. \tag{22}$$

Note that (22) has two classes of solutions. The first class, can have a functional dependence on the parallel component but obeys (21). The second class where there is no relation between n and Φ, but both of them are independent of the parallel component z. Drift waves belong to the first class, whereas zonal flows belong to the second.

Another interesting point of the drift wave dynamics is that if one introduces a phase difference between the density and electrostatic fluctuations (for example due to collisions, or trapped electrons), which amounts to moving the flow pattern in figure 9 downwards, since now there will be an outward motion of high density plasma at the maximum of the density (before there was no radial motion at the peak location), in addition to the upward wave propagation there will also be an increase of the amplitude of the sinusoidal fluctuation. This is one of the mechanisms by which the basic drift instability is excited.

The ITG mode is an ion Larmor radius scale drift-instability that has an overall phase speed in the ion diamagnetic direction and is driven unstable due to the ion temperature gradient. The ITG can be unstable even with a perfectly adiabatic electron response. The collisionless, or dissipative trapped electron modes (TEM) are ion Larmor radius scale, electron drift instabilities (i.e. they move in the electron diamagnetic direction), where the free energy source is the electron density and temperature and the instability arises due to the nonadiabatic response of trapped electrons. Dissipative drift instability is an ion Larmor radius scale electron drift instability, where the free energy source is the density gradients and the mechanism for accessing it is the nonadiabatic electron response of passing electrons due to collisions. Finally the ETG mode is an electron Larmor radius scale drift-instability, where the free energy source is the electron temperature gradient. ETG can be unstable even with adiabatic ion response. We will not go further into details of these different types of instabilities and try to focus on their common aspects.

2.3.1. The generalized Hasegawa–Mima system. As in the geophysical setting, one can define a simplified PV for the plasma turbulence:

$$q = \frac{(\zeta + \Omega_i)}{n} = \frac{1}{n}\left[\frac{\nabla_{\perp}^2 \Phi}{B}c + \frac{eB}{mc} \right]$$

using

$$q \approx \frac{1}{n_0 \left(1 - \frac{x}{L_n} + \frac{\tilde{n}}{n_0}\right)} \left(\frac{\nabla_\perp^2 \Phi}{B}c + \frac{eB}{mc}\right)$$

$$\approx \frac{1}{n_0} \frac{\nabla_\perp^2 (\widetilde{\Phi} + \overline{\Phi})}{B} c + \frac{1}{n_0} \frac{eB}{mc}\left(1 + \frac{x}{L_n} - \frac{\tilde{n}}{n_0}\right)$$

whose conservation gives two equations when the fluctuating and mean components are separated:

$$\left(\frac{\partial}{\partial t} + \hat{\mathbf{b}} \times \nabla\overline{\Phi} \cdot \nabla\right)\left(\widetilde{\Phi} - \nabla_\perp^2 \widetilde{\Phi}\right) + \frac{\rho_s}{L_n}\frac{\partial}{\partial y}\widetilde{\Phi} = \delta\left(\hat{\mathbf{b}} \times \nabla\widetilde{\Phi} \cdot \nabla \nabla_\perp^2 \widetilde{\Phi}\right)$$

(23)

$$\left(\frac{\partial}{\partial t} + \hat{\mathbf{b}} \times \nabla\overline{\Phi} \cdot \nabla\right)\nabla_\perp^2 \overline{\Phi} = -\left\langle \hat{\mathbf{b}} \times \nabla\widetilde{\Phi} \cdot \nabla \nabla_\perp^2 \widetilde{\Phi}\right\rangle,$$

(24)

where $\delta\left(\tilde{a}\tilde{b}\right) \equiv \tilde{a}\tilde{b} - \langle\tilde{a}\tilde{b}\rangle$, and we have used the adiabatic electron response (21) and scaled temporal and spatial variables by Ω_i^{-1} and ρ_s respectively. We have also used the dimensionless electrostatic potential $\frac{e\Phi}{T_e}$. This system is called the generalized Hasegawa–Mima (or sometimes generalized Charney–Hasegawa–Mima) equations. Its nontrivial nonlinear structure follows from the fact that the electron response to the fluctuations are adiabatic, the electrons can not respond to $\overline{\Phi}$ who is independent of the parallel coordinate. Note that a term similar to the last term on the left hand side of (23) is dropped from the equation for $\overline{\Phi}$, who is taken to be a function only of the radial coordinate x. However, for more general convective cells, such a term should be added to (24).

2.3.2. The Hasegawa–Wakatani system. Consider the PV for the drift wave problem:

$$q = \frac{\left(\zeta + \Omega_i\right)}{n},$$

where $\zeta = \frac{\nabla_\perp^2 \Phi}{B}c$ as before, coupled to the equation for electron density (note that by quasi-neutrality $n = n_i = n_e$), which can be written as:

$$\left(\frac{\partial}{\partial t} + \mathbf{v}_E \cdot \nabla\right)n = \frac{1}{e}\nabla_\parallel J_\parallel$$

we can write the vorticity equation by eliminating the density from $dq/dt = 0$:

$$\left(\frac{\partial}{\partial t} + \mathbf{v}_E \cdot \nabla\right)(\zeta + \Omega_i) = \frac{\left(\zeta + \Omega_i\right)}{ne}\nabla_\parallel J_\parallel$$

which basically says that the plasma absolute vorticity increases with a parallel current that increase with the parallel coordinate since such a current profile leads to an accumulation of electrons and thus an increase of plasma density. An increase in plasma density in turn increases the vorticity, since the PV is conserved.

The Hasagawa–Wakatani system of equations follow if we use the Ohm's Law with a finite parallel resistivity instead of the adiabatic electron response:

$$\frac{e\eta}{T_e}J_\| = \nabla_\| \left(e\frac{\Phi}{T_e} - \frac{n}{n_0} \right)$$

which gives:

$$\left(\frac{\partial}{\partial t} + \hat{\mathbf{b}} \times \nabla\widetilde{\Phi} \cdot \nabla \right)\tilde{n} + \frac{\rho_s}{L_n}\partial_y\widetilde{\Phi} - D\nabla^2\tilde{n} = c\nabla_\|^2\left(\widetilde{\Phi} - \tilde{n} \right) \qquad (25)$$

$$\left(\frac{\partial}{\partial t} + \hat{\mathbf{b}} \times \nabla\widetilde{\Phi} \cdot \nabla \right)\nabla_\perp^2\widetilde{\Phi} - \nu\nabla^4\widetilde{\Phi} = c\nabla_\|^2\left(\widetilde{\Phi} - \tilde{n} \right), \qquad (26)$$

where we have scaled the parallel variable by L_n and defined $c \equiv \frac{1}{\Omega_i}\frac{T_e}{n_0 L_n^2 e^2 \eta}$ in addition to using the dimensionless variables of section 2.3.1 and added model diffusion terms with diffusion coefficients D and ν that are supposed to represent damping processes.

2.4. ITG

While a discussion of all the various different electrostatic micro-instabilities of the drift type in tokamaks is certainly out of the scope of this review, the ITG mode should probably be mentioned as the most prominent ion Larmor radius scale instability.

The kinetic physics of the ITG mode is sufficiently complex that even the basic linear dispersion relation, with various usual simplifying assumptions such as adiabatic electrons and fluctuations being strongly localized to the low field side etc requires numerical approach for finding the zeroes of a plasma dielectric function which has to be evaluated numerically. Furthermore, even such a (relatively complicated) numerical calculation is well known to overestimate the growth rate of the ITG mode approximately by a factor of two. This means the full poloidal eigenmode problem has to be solved numerically. This is a rather fusion specific exercise and has no place in a general review such as the current one.

While its accuracy in reproducing the linear physics would be poor, a reduced fluid ITG model can be used to study the nonlinear behavior of this mode. The use of such a model may be justified retrospectively by the existence of zonal flows which tend to weaken the balooning mode structure.

ITG requires either the parallel dynamics (cylindrical) or the curvature effects in order to be unstable. We start with the PV budget (11) as in the rotating convection problem:

$$\frac{dq}{dt} = P_q - D_q,$$

where, we write the dissipation as $D_q = -\nu\nabla_\perp^2 q$.

The PV for the simple slab ITG system can be defined as

$$q = \frac{(\zeta + \Omega_i)P^{1/\Gamma}}{n}$$

considering $P = P_0\left(1 - \frac{x}{L_P} + \frac{\widetilde{P}}{P_0} \right)$, $n = n_0\left(1 - \frac{x}{L_n} + \frac{\tilde{n}}{n_0} \right)$, and $\zeta \approx \frac{c}{B}\nabla^2\widetilde{\Phi}$:

$$q \approx \frac{P_0^{1/\Gamma}}{n_0}\left[\frac{c}{B}\nabla^2\widetilde{\Phi} + \Omega_i\left(1 - \left[\frac{\tilde{n}}{n_0} - \frac{x}{L_n} \right] + \frac{1}{\Gamma}\left[\frac{\widetilde{P}}{P_0} - \frac{x}{L_P} \right] \right) \right]$$

which basically is equivalent to $q = \nabla^2\Phi - n + \frac{P}{\Gamma}$ in dimensionless form when the constant is dropped. The conservation of PV implies:

25

$$\left(\frac{\partial}{\partial t} + \hat{\mathbf{b}} \times \nabla \Phi \cdot \nabla \right) \left[\nabla^2 \widetilde{\Phi} - \tilde{n} + \frac{\widetilde{P}}{\Gamma} \right] + \left(\frac{\rho_s}{L_n} - \frac{\rho_s}{\Gamma L_p} \right) \frac{\partial \widetilde{\Phi}}{\partial y} = 0.$$

2.5. General formulation based on PV advection

In all the systems above, the problem can be reduced to a PV equation coupled to some other equations through the baroclinic (or other) drive term.

For instance the inviscid limit of the Hasegawa–Wakatani equations given above, can be written as two equations, one for PV advection, and the other for density. The PV equation is 'independent' of the density equation (i.e. we can solve for PV without knowing the value of the density), however the density equation involves the electrostatic potential (i.e. the stream function). The electrostatic potential can be written as a function of PV and the density (i.e. $\widetilde{\Phi} = \nabla^{-2}(q + n)$, which is a nonlocal integral and thus includes the boundary conditions as well). This is known as the problem of invertibility and is trivially solved in the adiabatic limit (since in this limit $\widetilde{\Phi} = \tilde{n}$). However in the general case, the invertibility becomes a more complicated problem since now given q, we need to solve an integro-differential equation (i.e. equation (25) with $\partial_y \widetilde{\Phi}$ replaced by $\partial_y \nabla^{-2}(q + n)$) to obtain $\tilde{n}$ and hence n, which we can use to obtain $\widetilde{\Phi}$. While this complicates the full problem, in principle the fact that it is doable allows us to focus on the PV dynamics, which is nicely decoupled from density or any other quantity as long as there is no drive. In contrast, the case of rotating convection where the coupling to the temperature equation is via the baroclinic term, or the case of ITG where the coupling is via the temperature gradient drive are cases where the PV equation is only partially decoupled and we have a quasi-conservation instead of an exact conservation.

Note that mesoscale flows defined as $\overline{\mathbf{v}} = \hat{\mathbf{b}} \times \nabla \overline{\Phi}$ in section 2.3.1, and mesoscale PV which can be denoted by $\overline{q}$, can be added to all the simple systems that are considered above, while we avoided adding them explicitly to avoid cumbersome notation.

The general structure of the PV equation in this case becomes:

$$\left(\frac{\partial}{\partial t} + \hat{\mathbf{b}} \times \nabla \overline{\Phi} \cdot \nabla \right) \tilde{q} + \hat{\mathbf{b}} \times \nabla \widetilde{\Phi} \cdot \nabla \left(q_0 + \overline{q} \right) + \delta \left(\hat{\mathbf{b}} \times \nabla \widetilde{\Phi} \cdot \nabla \tilde{q} \right) = 0, \qquad (27)$$

$$\left(\frac{\partial}{\partial t} + \hat{\mathbf{b}} \times \nabla \overline{\Phi} \cdot \nabla \right) \overline{q} + \hat{\mathbf{b}} \times \nabla \overline{\Phi} \cdot \nabla q_0 + \langle \hat{\mathbf{b}} \times \nabla \widetilde{\Phi} \cdot \nabla \tilde{q} \rangle = 0 \qquad (28)$$

note that we recover (23) and (24) by using $\tilde{q} = \nabla^2 \widetilde{\Phi} - \widetilde{\Phi}$ and $\overline{q} = \nabla^2 \overline{\Phi}$. One can add injection and dissipation to these in order to apply them to cases where there is only a quasi-conservation. Note also that the middle term in (28) usually drops when we consider flows that are perfectly zonal.

3. Formation of zonal flows

Zonal flows form in all the physical systems discussed in the previous sections through similar mechanisms. The fluctuations that are driven unstable by some mechanism provide the Reynolds stress, which drive large scale flows, which in turn modify the underlying turbulence that is driving them. There are different ways to express this both in common language and in mathematical formulation. In particular different aspects of this phenomenon of turbulence self-regulation via zonal pattern formation are described using different mathematical frameworks.

3.1. Zonal flows and PV mixing

Various problems in geophysical fluid dynamics, plasma physics, and laboratory experiments of rotating convection can be formulated using a PV quasi-conservation, where the injection is via the baroclinic, or temperature gradient driven instabilities and the dissipation is due to small scale stresses. Therefore general rules about the tendencies of PV dynamics are very useful for understanding the common features of such systems.

One rather interesting, general observation of PV dynamics is that as long as the initial configuration has closed contours of time averaged PV (i.e. $\langle q \rangle \equiv q_0 + \bar{q}$ in the formulation of (27), (28)), the final state will consist of homogenized patches of PV connected by large gradients. Similar conclusion can also be drawn for contours of mean flow (streamlines), since to the lowest order these two are functionally related. This can be shown in different ways [1] here we only mention the demonstration using the integral around a closed PV contour.

First note that the basic background steady state solution of (28), suggests that

$$\hat{\mathbf{b}} \times \nabla\overline{\Phi} \cdot \nabla \langle q \rangle \approx 0$$

which means that to the lowest order, there is a functional relation between the mean PV and the mean electrostatic potential:

$$\langle q \rangle = Q(\overline{\Phi}) + O(\epsilon). \tag{29}$$

Note also that for any function f, the integral over an area A enclosed by a mean streamline

$$\int_A \hat{\mathbf{b}} \times \nabla\overline{\Phi} \cdot \nabla f \, \mathrm{d}s = \oint_C \hat{\mathbf{b}} \times \nabla\overline{\Phi} f \cdot \mathrm{d}\vec{\ell} = 0, \tag{30}$$

where C is the closed contour around the streamline (i.e. $\mathrm{d}\vec{\ell} = \nabla\overline{\Phi}\mathrm{d}\ell/|\nabla\overline{\Phi}|$).

Using this and (28), we can write:

$$\int_C \langle \hat{\mathbf{b}} \times \nabla\overline{\Phi}\tilde{q} \rangle \cdot \mathrm{d}\vec{\ell} \approx 0 \tag{31}$$

in the steady state. Now using an eddy viscosity hypothesis:

$$\langle \hat{\mathbf{b}} \times \nabla\overline{\Phi}\tilde{q} \rangle_i \sim -\kappa_{ij}\frac{\partial}{\partial x_j}\langle q \rangle.$$

And the perturbation expansion (29), we can write

$$-\frac{\partial Q}{\partial\overline{\Phi}} \int_C \kappa_{ij}\frac{\partial}{\partial x_i}\overline{\Phi}\frac{\partial}{\partial x_j}\overline{\Phi}\frac{\mathrm{d}\ell}{|\nabla\overline{\Phi}|} \approx 0$$

which implies that as long as κ_{ij} is positive $\frac{\partial Q}{\partial\overline{\Phi}} \approx 0$ for any closed streamline. This means that the PV does not vary from one streamline to another on such a closed contour, which means that the steady state solution of the problem defined by (27) and (28) is simply:

$$\langle q \rangle = \bar{q} + q_0 = \text{const.} + O(\epsilon)$$

in a region where the initial condition contained a closed contour of mean PV.

However since this is in opposition to the background variation of the PV for example due to background density gradient in the drift wave problem. The flat region of PV would have to be connected to the next flat region by a strong gradient. When many of such regions are connected, the result is what can be called a PV staircase.

Notice that the nonlinear term vanishes for a homogenized PV profile. There is a close analogy between the homogenization of the PV and the phenomenon of flux expulsion in

MHD and eventually to the phenomenon of dynamic alignment which leads to generation of large regions of aligned or counter-aligned velocity and magnetic field profiles which are connected by sheets or filaments where the alignment changes rapidly.

3.1.1. Rhines scale and its applicability to fusion plasmas.   The Rossby wave turbulence in the atmosphere as described by the Charney equations is rather similar to the 2D turbulence described by the Euler equations. This is true in particular for small scales where the equation basically becomes an Euler equation apart from the β effect.

If one compares the linear and the nonlinear terms in (10), noting that the nonlinear term scales dimensionally as U^2/L^2 and the linear term as $\beta'U$ it is clear that for a given β' and U, the two terms balance each other at a length scale given in dimensional units by:

$$L_R \equiv \left(\frac{U}{\beta} \right)^{1/2}$$

or a wave-number $k_R \equiv (\beta/U)^{1/2}$, where U is interpreted as a characteristic (rms) velocity of the fluid (sometimes a rather arbitrary factor such as 2 or π may be introduced at the denominator). For scales larger than this scale (wavenumbers smaller than k_R), the linear term which represents the β effect will dominate, and wave turbulence, which leads to formation of zonal flows will result. Whereas for smaller scales (i.e. wave-numbers larger than k_R), the nonlinear term dominates and fully developed 2D turbulence will result. Notice that if the Rossby deformation radius $R = \sqrt{h_0 g} f_0^{-1}$ is already much larger than this critical length scale, we can treat small scale turbulence by using Euler equation directly.

The usual description of fully developed 2D turbulence involves a dual cascade where the enstrophy cascades forward and the energy cascades inversely. Therefore, another way to view the Rhines scale is as a scale where the 2D inverse cascade terminates since the turbulence changes character beyond this scale. Therefore it is common to talk about the 'arrest' of inverse energy cascade at the Rhines scale, even though it is open to debate whether the 2D turbulence really generates a local inverse cascade or if this inverse cascade is really arrested at the Rhines scale.

When the dispersion relation is anisotropic as in the case for Rossby or drift waves, the Rhines scale generalizes to a curve in k space inside of which the interactions with zonal flows dominate. This can be demonstrated for drift waves as follows (see [62] for the Rossby wave version):

$$u_{rms}^2 k_R^2 = \omega^2 = \left(\frac{\rho_s}{L_n} \right)^2 \frac{\rho_s^2 k_{Ry}^2}{\left(1 + \rho_s^2 k_R^2 \right)^2} \Omega_i^2$$

$$\left(\rho_s k_R \right)^2 \left(1 + \rho_s^2 k_R^2 \right)^2 = \left(\frac{\rho_s}{L_n} \right)^2 \frac{\left(\sin \alpha_R \right)^2}{\left(e\Phi_{rms}/T_e \right)^2} \tag{32}$$

note that we have defined $\sin \alpha_R \equiv k_{Ry}/k_R$. The curve is represented in figure 10. Inside this curve, weak wave turbulence and therefore wave-like modes interacting mainly via the zonal flows dominate, and outside the curve we have a classical fully developed 2D turbulence. Since the energy is usually injected inside the curve for drift instabilities (which usually has a most unstable mode with finite k_y and $k_x \approx 0$), and couples to zonal flows which fall outside the curve, the role of the Rhines scale in drift-wave turbulence is quite different from the
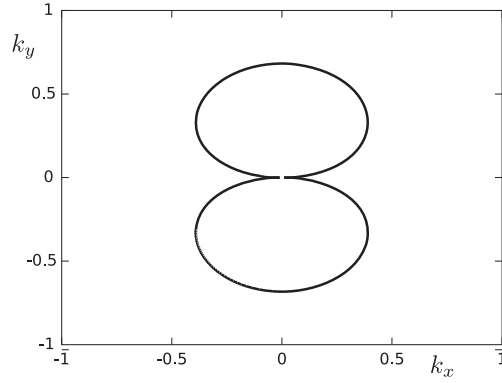
Figure 10. Anisotropic Rhines scale for drift wave turbulence. Inside the curve, the turbulence has a wave-like character and interactions with the zonal flows dominate, outside it has the character of a classical fully developed 2D turbulence.

arrest of the 2D inverse cascade picture. Note that as an order of magnitude $\left(e\Phi_{\mathrm{rms}}/T_e\right)^2 \sim \left(\frac{\rho_s}{L_n}\right)^2$ in drift wave turbulence (i.e. the mixing length estimate).

While the applicability or the importance of the Rhines scale to fusion plasma turbulence may be questionable, the curve given in figure 10 can be interpreted as the boundary between anisotropic turbulence at 'large' scales and the isotropic turbulence at 'small' scales. When the energy is injected within the above curve, it will excite a drift wave which has the form of a streamer (i.e. $k_x \ll k_y$ mode), this mode couples naturally to an isotropic mode (with $k_x \sim k_y$, sometimes called a Kelvin–Helmholtz-like mode, but we think that this terminology is misleading) and a zonal mode. The interaction in a fusion device is actually a 4-wave interaction where the two satellites of the primary pump mode (i.e. the streamer) couple to give the zonal mode. We will discuss how this can be described in the framework of modulational instability in the following sections.

However note that as the energy goes to the zonal flow, the zonal flow transfers some of this energy to a smaller (or larger) scale $k_x \sim k_y$ mode and a smaller (or larger) scale streamer-like mode. Sometimes called a tertiary instability. However since the smaller scale streamer that is driven by the 'tertiary instability' then drives smaller scale zonal flows leading to a cascade of enstrophy through the k-space via these particular triads, it is in fact simply a part of an hierarchy of interactions. We think that within the context of turbulence calling it an 'instability' is misleading unless one sees each step in the cascade as an instability of the previous scale. In contrast it is clear that for single wave-packet whose characteristics actually evolve in time, the tertiary instability has a clear meaning.

3.1.2. Rhines scale versus mixing length versus critical balance. There are various examples in the literature where people consider the balance between the linear and the nonlinear terms as we have discussed above to define the Rhines scale. The mixing length idea commonly used in fusion to estimate the fluctuation level is indeed a balance between the linear and the nonlinear terms. For instance for the Hasegawa–Mima case:

$$\frac{\rho_s}{L_n}\rho_s\frac{\partial}{\partial y}\left(\frac{e\widetilde{\Phi}}{T}\right) \approx \rho_s^4 \hat{\mathbf{b}} \times \nabla\left(\frac{e\widetilde{\Phi}}{T}\right) \cdot \nabla \nabla_\perp^2\left(\frac{e\widetilde{\Phi}}{T}\right)$$

which gives (for $\rho_s k_\perp \sim \rho_s k_y \sim 1$ which is roughly true for the most unstable mode):

$$\frac{e\widetilde{\Phi}}{T} \sim \frac{\rho_s}{L_n}$$

this is the basic mixing-length estimate of the fluctuation level for drift-wave turbulence. A more detailed version can be used to determine the maximum of the turbulence k-spectrum by arguing that the maximum occurs when the linear growth rate is balanced by the nonlinear decorrelation rate (i.e. eddy damping):

$$\gamma_k \approx D_k^{nl} k_\perp^2,$$

where $D_k^{nl} \propto |\frac{e\widetilde{\Phi}_k}{T}|^2$ is the nonlinear diffusion coefficient that appears in turbulent fluxes of density and particles [63]. The maximum of the spectrum can be obtained by solving:

$$\max\left(\left|\frac{e\widetilde{\Phi}_k}{T}\right|^2\right) \approx \max\left(\frac{\gamma_k}{k_\perp^2}\right)$$

for k. Since the functional form of γ_k can in principle be obtained maximizing $\gamma_k/k_\perp^2$ one obtains the mixing length maximum of the spectrum. It is interesting to note that this seems to work rather well for turbulence in tokamak plasmas even with the complicating effects of curvature, magnetic shear etc [124]. The reason is probably that most of the complicating effects change the form of γ_k in this argument, but do not change the fact that the γ_k is balanced by an effective turbulent diffusion near the most unstable mode. Note that while one uses the same basic idea of balancing linear and nonlinear terms, the mixing length considers the energy budget (so the energy injected by the linear instability is equal to the energy extracted by the nonlinear transfer), whereas the Rhines scale argument is based on a comparison between the eddy turnover rate and the wave propagation in the original equation.

Yet another famous balance between the linear and the nonlinear terms is the so-called critical balance [64] in 3D MHD turbulence. The idea is very similar to how one obtains the Rhines scale but considering parallel propagating Alfvén waves with a fully developed 2D perpendicular spectrum. By balancing the Alfvén wave transit rate in the parallel direction with the eddy turnover rate in the perpendicular direction, one obtains:

$$v_A k_\parallel \approx u(k_\perp)k_\perp.$$

Notice that in standard 3D MHD there is no process which would break the isotropy on the perpendicular plane (i.e. k_x versus k_y), however there is a rather important source of anisotropy in the parallel versus perpendicular directions. Since the spectral energy density in the perpendicular direction for a 2D forward cascade is $E(k_\perp) \propto \varepsilon^{2/3} k_\perp^{-5/3}$ or $u(k_\perp) \sim E(k_\perp)^{1/2} k_\perp^{1/2} \propto \varepsilon^{1/3} k_\perp^{-1/3}$, the critical balance gives the relation:

$$k_\parallel \propto \frac{\varepsilon^{1/3}}{v_A} k_\perp^{2/3}.$$

This is usually interpreted as a strongly anisotropic spectrum with $k_\parallel$ following the $k_\perp$ cascade scale by scale until it reaches the critical balance. It can be generalized for an arbitrary dispersion relation by replacing v_A with the parallel phase velocity $v_{ph\parallel}(k)$. The idea can be applied to various systems with parallel propagating waves.

3.1.3. PV and its importance in DW/ZF dynamics.

As discussed above, a number of plasma and geophysical fluid dynamics models can be formulated using a description based on PV
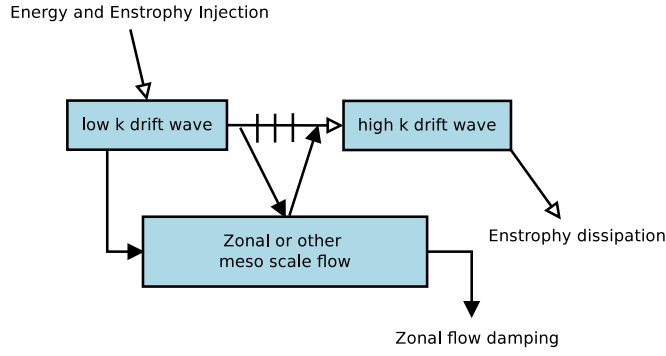
Figure 11. Forward potential enstrophy cascade mediated by large scale flow structures.
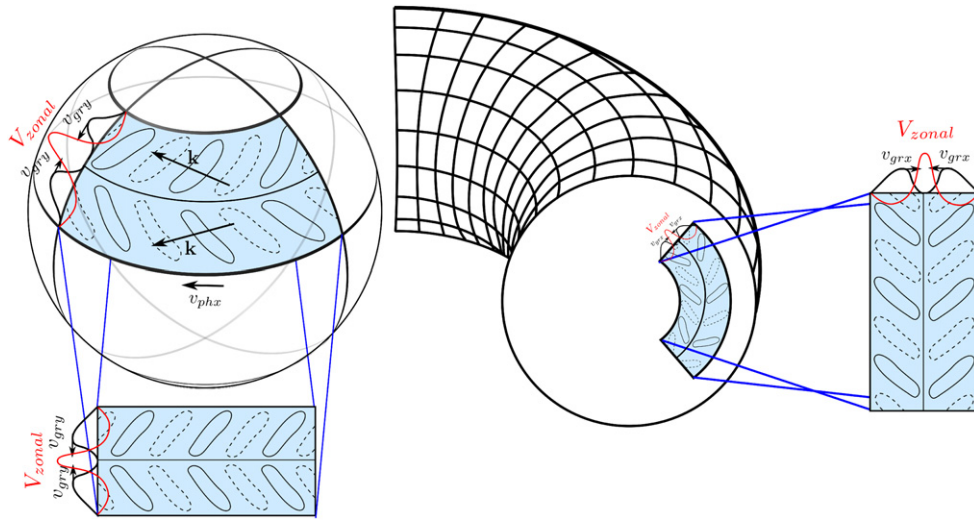

Figure 12. Simple mechanism for the zonal flow reinforcement.

evolution. Advection of PV, coupled to other equations such as that of entropy density or pressure via the baroclinic term or via curvature effects when there are additional sources of free energy. Notice however that in general the quadratic quantity that is conserved by the nonlinear dynamics of co-evolving drift waves and zonal flows, as described for instance by (23) and (24), is the PE.

$$ W \equiv \langle q^2 \rangle = \langle |\widetilde{q}|^2 \rangle + \bar{q}^2 = \left\langle \left| \left(1 - \nabla^2 \right) \widetilde{\varPhi} \right|^2 \right\rangle + \left\langle | \nabla^2 \overline{\varPhi} |^2 \right\rangle. $$

In other words the nonlinear system described by (23) and (24), the zonal flows and the drift waves exchange PE and not energy. So it is the PE that is conserved between the drift waves and the zonal flows, since it is the PV that is advected. However local interactions among the drift waves still conserve energy and enstrophy leading to a dual cascade.

3.1.4. Forward enstrophy cascade and ZF formation. One interesting point is that while it is common to talk about zonal flow formation informally as a process of 'inverse cascade', in

reality the anisotropic mechanism that leads to the formation of zonal flows does not really have the character of a local cascade where the energy moves to larger and larger scales. The mechanism can be described better as a nonlocal interaction in k-space where the zonal flow acts on all scales diffracting the fluctuations to smaller and smaller wave-numbers (see figure 11).

From a spatial, 'pattern formation' point of view, the same process can be explained by looking at the dispersion relations for drift or Rossby waves. Consider the setup in figure 12, for Rossby waves as the first example. The basic Rossby wave has a mainly westward phase motion, with a phase velocity given by:

$$\mathbf{v}_{\mathrm{ph}} = -\frac{\beta' k_x}{k^4}\mathbf{k}$$

while its latitudinal group velocity, v_{gx}, can be in either direction, its meridional group velocity, v_{gy}, is in the opposite direction to its meridional phase velocity, making it a backwards wave in the meridional direction:

$$v_{gy} = \frac{\partial}{\partial k_y}\left(-\frac{\beta' k_x}{k^2}\right) = \frac{2\beta' k_x k_y}{k^4}.$$

Similarly for drift waves the main phase velocity propagation direction is counter-clockwise in the geometry of figure 12 if the magnetic field is in the out of plane direction. The radial group velocity

$$v_{gx} = \frac{\mathrm{d}}{\mathrm{d}k_x}\left[\frac{\rho_*}{L_n}\frac{k_y}{\left(1 + k^2\right)}\right] = -\frac{\rho_*}{L_n}\frac{2k_x k_y}{\left(1 + k^2\right)^2}$$

which is also backwards with respect to its radial phase propagation (i.e. $v_{\mathrm{ph}x} = \frac{\rho_*}{L_n}\frac{k_y k_x}{\left(1 + k^2\right)k^2}$). Note that while Rossby waves carry negative wave momentum away from the stirring region, the drift waves carry positive wave momentum towards the stirring region resulting in the same basic effect of momentum convergence towards this region.

One very interesting point is that if an infinitesimal velocity shear which has the profile given in figure 12 is introduced, the sheared flow leading to a tilting of the eddies resulting in a radial (meridional in the case of Rossby waves) group propagation which leads to momentum convergence towards the maximum of the flow.

3.2. The wave-kinetics formulation

Self-regulating drift/Rossby wave turbulence, can be described using the wave kinetic equation in a weakly inhomogeneous medium [65–67]:

$$\frac{\partial}{\partial t}N_{\mathbf{k}}(\mathbf{X}, t) + \nabla_{\mathbf{k}} \cdot \left[\left(\omega - \overline{\mathbf{V}} \cdot \mathbf{k}\right)\nabla_X N_{\mathbf{k}}(\mathbf{X}, t)\right]$$
$$- \nabla_{\mathbf{X}} \cdot \left[\left(\omega - \overline{\mathbf{V}} \cdot \mathbf{k}\right)\nabla_{\mathbf{k}}N_{\mathbf{k}}(\mathbf{X}, t)\right] = C'\left(N_{\mathbf{k}}, N_{\mathbf{k}}\right), \tag{33}$$

where N_k is the wave quanta of the drift waves. The weak inhomogeneity described partly by the dispersion relation and partly by the mean flow $\overline{\mathbf{V}}$ above can be coupled to the slower time scale evolution of the zonal flows using a scale separation approach. Notice that it is also possible to obtain the wave kinetic formulation, and derive explicit expressions for the diffusion coefficients using a Lagrangian correlations approach [68, 69].

When considered by itself the wave-kinetic equation describes the evolution of high frequency drift waves that move around in a medium whose optical index of refraction is determined by the zonal shearing. Recall that the WKB equations can be written as

$$\frac{d\mathbf{x}}{dt} = \frac{\partial}{\partial \mathbf{k}}\left(\omega_k - \overline{\mathbf{V}} \cdot \mathbf{k}\right)$$

and

$$\frac{d\mathbf{k}}{dt} = -\frac{\partial}{\partial \mathbf{x}}\left(\omega_k - \overline{\mathbf{V}} \cdot \mathbf{k}\right)$$

which is the basis for the interpretation of (33) as a 'kinetic' equation. Notice that since zonal flows are narrow banded flow structures, they play the role of wave-guides for drift waves.

The wave kinetic formulation of drift-wave zonal flow interaction is a very powerful tool. As discussed in detail in reference [36], a quasi-linear calculation, based on the wave-kinetic formulation (i.e. using $N_k = \langle N_k \rangle + \delta N_k$ where δN_k is a perturbation) can be used to estimate the zonal flow 'growth rate' (i.e. the rate at which the zonal flows are driven by drift waves):

$$\gamma_q[W_k] = -2q^2 c_s^2 \sum_k \frac{k_y^2 \rho_s^2}{\left(1 + k^2 \rho_s^2\right)^2} R(k, q) k_x \frac{\partial}{\partial k_x} W_k,$$

where $W_k = \left\langle \left(1 + \rho_s^2 k^2\right)^2 |\widetilde{\Phi}_k|^2 \right\rangle$ is the drift wave PE density. Remarkably, the general form of the coupled quasi-linear system of equations that result:

$$\frac{\partial}{\partial t} W_k - \frac{\partial}{\partial k_r}\left[D_k \frac{\partial}{\partial k_r} W_k \right] = \gamma_k W_k - \frac{\Delta \omega_k}{N_0} W_k^2, \tag{34}$$

$$\frac{\partial}{\partial t}\left|\Phi_q\right|^2 = \gamma_q[W_k]\left|\Phi_q\right|^2 - \gamma_d \left|\Phi_q\right|^2 - \gamma_{nl}\left[\left|\Phi_q\right|^2\right]\left|\Phi_q\right|^2. \tag{35}$$

A formal statistical calculation based on the direct interaction approximation between disparate scales for the generalized Hasegawa–Mima system gives essentially the same result also [70]. Notice that the equations (34) and (35) already suggest

(i) that the turbulence drives zonal flows via γ_q,
(ii) that the zonal flows contribute to the forward enstrophy cascade by refracting the drift waves towards smaller k_r. Adding the zonal flow damping, we have roughly all the ingredients for a spectral PP dynamics as described in figure 11.

3.3. Modulational instability framework

Assuming that the spatio-temporal dynamics of large scale flow structures is sufficiently slower than that of drift/Rossby wave turbulence, one can use the modulational instability framework. The complete framework can actually be developed from a Hamiltonian description of nonlinear waves, for which there are already very good books and reviews [71, 72]. Since, the purpose of this paper is to review physical mechanisms, we limit ourselves to a discussion of the modulation instability and discuss the formulation by Newell [73]. Consider the nonlinear system

$$\mathcal{L}\left(\nabla, \partial_t, R\right)\phi = \mathcal{N}\phi\mathcal{M}\phi, \tag{36}$$

where $\mathcal{L}$, $\mathcal{N}$ and $\mathcal{M}$ are operators representing linear terms and nonlinear couplings respectively, and R represents a parameter that determines the stability condition (e.g. the

Rayleigh number for the problem of convention). We obtain the linear dispersion relation for given R by linearizing (36):

$$\mathcal{L}(\mathbf{ik}, -i\omega, R) = 0, \tag{37}$$

where $\omega = \omega_{\mathbf{k}} \equiv \omega_{r\mathbf{k}} + i\gamma_{\mathbf{k}}$ is the complex frequency. One can obtain the stability condition by substituting $\omega = \omega_{\mathbf{k}}(R)$ and setting $\gamma_{\mathbf{k}} = 0$, and solving for $R = R_c(\mathbf{k})$ instead.

In many problems in nature there is a critical scale (the most unstable mode) at which the net energy production has a maximum because the energy production decreases towards larger scales, and the dissipation increases towards smaller scales. This implies that $R_c(k)$ has a minimum at this point. Thus, when the control parameter R is close to, but slightly above its critical value

$$R = R_c\left(1 + \epsilon^2 \chi\right)$$

only a small subset of modes around the most unstable mode are excited (i.e. $k_c \pm O(\epsilon)$). This allows us to consider a wave whose amplitude is slowly modulated:

$$\phi = \Phi\left(\overline{X}, \overline{T}, \tau\right)e^{i\mathbf{k}\cdot\tilde{\mathbf{x}} - i\omega_{r\mathbf{k}}\tilde{t}} + \text{c. c.},$$

where $\Phi(X, T, \tau)$ is the modulated complex amplitude, using the reductive perturbation theory:

$$\phi = \epsilon\left(\phi_0 + \epsilon\phi_1 + \epsilon^2\phi_2 + \cdots\right)$$

with a basic scale separation assumption, which can be regarded as a Taylor series expansion of the operator $\mathcal{L} = \mathcal{L}_0 + \epsilon\mathcal{L}_1 + \epsilon^2\mathcal{L}_2 + \cdots$, around the point $(\tilde{V}, \tilde{\partial}_t, R_c)$ to a neighboring point $\left(\tilde{V} + \epsilon\bar{V}, \tilde{\partial}_t + \epsilon\bar{\partial}_T + \epsilon^2\partial_\tau, R_c\left[1 + \epsilon^2\chi\right]\right)$ in the operator space. For example

$$\begin{aligned}
\mathcal{L}_1 &= \left(\frac{\partial\mathcal{L}_0(\mathbf{ik}, -i\omega, R)}{\partial(-i\omega)}\bar{\partial}_T + \frac{\partial\mathcal{L}_0(\mathbf{ik}, -i\omega, R)}{\partial(\mathbf{ik})} \cdot \bar{V}\right) \\
&= \frac{\partial\mathcal{L}_0(\mathbf{ik}, -i\omega, R)}{\partial(-i\omega)}\left(\bar{\partial}_T + \mathbf{v}_g \cdot \bar{V}\right),
\end{aligned} \tag{38}$$

where we have used the fact that

$$\frac{\partial}{\partial\mathbf{k}}\mathcal{L}_0(\mathbf{ik}, -i\omega, R) = -\frac{\partial\omega}{\partial\mathbf{k}}\frac{\partial}{\partial\omega}\mathcal{L}_0(\mathbf{ik}, -i\omega, R)$$

which can be obtained by differentiating the dispersion relation (37). Note that (38) corresponds to the group motion of the envelope modulation and can be eliminated by transforming to a frame of reference moving with the group velocity.

Similarly

$$\mathcal{L}_2 = -\frac{1}{2}\frac{\partial^2\mathcal{L}_0}{\partial\omega^2}\bar{\partial}_{TT} + \frac{\partial^2\mathcal{L}_0}{\partial k_i \partial\omega}\bar{\partial}_T\bar{\partial}_i - \frac{1}{2}\frac{\partial^2\mathcal{L}_0}{\partial k_i \partial k_j}\bar{\partial}_i\bar{\partial}_j + i\frac{\partial\mathcal{L}_0}{\partial\omega}\bar{\partial}_\tau + \frac{\partial\mathcal{L}_0}{\partial R}R\chi \tag{39}$$

substituting the following relation, which can be obtained by taking the second derivative of the dispersion relation with respect to k:

$$-\frac{1}{2}\frac{\partial^2\mathcal{L}_0}{\partial k_i \partial k_j} = \frac{1}{2}\frac{\partial^2\omega}{\partial k_i \partial k_j}\frac{\partial\mathcal{L}_0}{\partial\omega} + \frac{1}{2}\frac{\partial\omega}{\partial k_i}\frac{\partial\omega}{\partial k_j}\frac{\partial^2\mathcal{L}_0}{\partial\omega^2} + \frac{\partial\omega}{\partial k_i}\frac{\partial^2\mathcal{L}_0}{\partial k_j \partial\omega} + \frac{1}{2}\frac{\partial^2 R}{\partial k_i \partial k_j}\frac{\partial\mathcal{L}_0}{\partial R} \tag{40}$$

and using the transformation to the group velocity frame that was used to eliminate $\mathcal{L}_1$ (i.e. $\partial_T = -\frac{\partial \omega}{\partial k_i} \bar{\partial}_i$), we note that the first and second terms of (39) are canceled by the second and the third terms on the right hand side of (40) respectively. This leaves:

$$\mathcal{L}_2 = i \frac{\partial \mathcal{L}_0}{\partial \omega} \bar{\partial}_\tau + \frac{1}{2} \frac{\partial^2 \omega}{\partial k_i \partial k_j} \frac{\partial \mathcal{L}_0}{\partial \omega} \bar{\partial}_i \bar{\partial}_j + \frac{1}{2} \frac{\partial^2 R}{\partial k_i \partial k_j} \frac{\partial \mathcal{L}_0}{\partial R} \bar{\partial}_i \bar{\partial}_j + \frac{\partial \mathcal{L}_0}{\partial R} R \chi \qquad (41)$$

which is to be balanced by the nonlinear terms. The exact form of the resulting equations depend on the details of the nonlinear saturation mechanism that balances the envelope modulations that can be described in general using the above formalism. The envelope equation, including the lowest order nonlinear terms takes the form

$$\mathcal{L}_2 \Phi_0 \approx \mathcal{N}_0 \Phi_0 \mathcal{M}_0 \Phi_0.$$

The simplest possible example that results in various physical problems is the so called nonlinear Schrödinger equation, which takes the form:

$$i \bar{\partial}_\tau \Phi + \frac{1}{2} \frac{d^2 \omega}{dk^2} \frac{\partial^2}{\partial x^2} \Phi + \lambda |\Phi|^2 \Phi = 0,$$

where λ is the lowest order coefficient for the perturbation expansion of the nonlinear term. The nonlinear Schrödinger equation is common to a number of interesting physical problems, and its implications are profound. Another thing that is very remarkable about this equation is that, it has actually been solved using the inverse scattering method, which were later on developed into a methodology for solving similar equations. However here we only use it as an example to the large class of possible amplitude equations that can be obtained from the modulational instability framework and refer the reader to the well written books and review papers on the subject [125].

3.3.1. Amplitude equations and their application to basic zonal-flow/drift-wave system.
Consider the nonlinear system (23)–(24) which describes the coupled evolution of simple drift-waves and zonal flows. We can write (23) in the form:

$$\mathcal{L} \widetilde{\Phi} = -\hat{\mathbf{b}} \times \nabla \overline{\Phi} \cdot \nabla \left(\widetilde{\Phi} - \nabla_\perp^2 \widetilde{\Phi} \right) + \delta \left(\hat{\mathbf{b}} \times \nabla \widetilde{\Phi} \cdot \nabla \nabla_\perp^2 \overline{\Phi} \right),$$

where the linear dispersion relation follows from:

$$\mathcal{L}_0 \left(i\mathbf{k}, -i\omega_k \right) = -i\omega_k \left(1 + k^2 \right) + \frac{\rho_s}{L_n} k_y = 0$$

which gives:

$$\frac{\partial}{\partial \omega_k} \mathcal{L}_0 \left(i\mathbf{k}, -i\omega_k \right) = -i \left(1 + k^2 \right).$$

Note that for this problem, there is no R, since the basic linear dispersion relation is always stable.

Using the reductive perturbation method described above, considering zonal modulations, and flows (i.e. $\partial_Y \to 0$) and assuming further that the zonal electrostatic field varies roughly at the same scale at which the envelope is modulated (i.e. $\widetilde{\Phi}_0 = \Phi_0(X, T, \tau) e^{i(\mathbf{k} \cdot \mathbf{x} - \omega t)}$ and $\overline{\Phi} = \overline{\Phi}(X, T)$), we can write for $\mathcal{L}_2$ from (41):

$$\left(i\partial_\tau + \frac{1}{2} \frac{\partial^2 \omega}{\partial k_x \partial k_x} \partial_{XX} \right) \Phi = k_y \Phi \partial_X \overline{\Phi} \tag{42}$$

which is then coupled to

$$\left(\epsilon \partial_\tau - v_{gx} \partial_X \right) \partial_{XX} \overline{\Phi} = 2 k_x k_y \partial_{XX} |\Phi|^2. \tag{43}$$

Note that a scaling $\Phi \sim O(\epsilon)$, $\overline{\Phi} \sim O(\epsilon)$ is suggested if the term on the right hand side of (42) is to be of the same order as the term on the left hand side, while the group velocity term in (43) is to be of the same order as the term on the right hand side. In this case we can solve (43) by neglecting the the higher order $\epsilon \partial_\tau$ term and substitute the result into (42), which gives:

$$i\partial_\tau \Phi + \frac{1}{2} \frac{\partial^2 \omega}{\partial k_x \partial k_x} \partial_{XX} \Phi + \frac{2 k_x k_y^2}{v_{gx}} |\Phi|^2 \Phi = 0 \tag{44}$$

which is again the nonlinear Schrödinger equation (NLS), which we write as

$$i\partial_\tau \Phi + \beta \partial_{XX} \Phi + \alpha |\Phi|^2 \Phi = 0, \tag{45}$$

where

$$\beta \equiv \frac{1}{2} \frac{\partial^2 \omega}{\partial k_x \partial k_x} \quad \text{and} \quad \alpha \equiv \frac{2 k_x k_y^2}{v_{gx}}. \tag{46}$$

Consider the following perturbed homogeneous solution:

$$\Phi = \left(\Phi_0 + \delta\Phi \right) e^{i\alpha |\Phi|^2 \tau}$$

which, without the $\delta\Phi$ is a homogeneous plane wave with a nonlinear frequency shift. Looking at the linear stability of $\delta\Phi \sim \delta\Phi_0 e^{i\left(q_x X - \omega_Z \tau \right)}$, one obtains the dispersion relation:

$$\omega_{zf}^2 = \beta^2 q_x^4 - 2\alpha\beta q_x^2 |\Phi_0|^2.$$

The instability condition for this dispersion relation is basically that

$$q_x^2 < 2\frac{\alpha}{\beta} |\Phi_0|^2$$

when the mode is unstable, we can write:

$$\gamma_{zf}\left(q_x \right) = \sqrt{2\alpha\beta q_x^2 |\Phi_0|^2 - \beta^2 q_x^4}$$

which allows us to compute the most unstable zonal mode, (i.e. by setting $\gamma_{zf}'\left(q_x \right) = 0$):

$$q_x^2 = \frac{\alpha}{\beta} |\Phi_0|^2 \tag{47}$$

and with this the growth rate of the most unstable mode:

$$\gamma_{zf}\left(q_x \right) = |\alpha| |\Phi_0|^2 = \frac{c_s |k_y| \left(1 + \rho_s^2 k^2 \right)^2}{\rho_s / L_n} \left| \frac{e\Phi_0}{T_e} \right|^2$$

in dimensional form.

It is interesting to note that, the modulational instability framework, defines a specific characteristic 'most unstable' wave-number for the zonal flows (i.e. (47)). While the final 'steady state' (if there ever is a steady state) value of the zonal flow wave-number depends

also on the way it is dissipated, which we will discuss in section 4, the most unstable wave-number would give an indication about the characteristic radial size of the zonal flows. It is interesting to note that as to the knowledge of current authors, this was never used as a basis for comparison, at least in fusion experiments.

3.4. Pattern selection in electron scales by modulational instability

Using the general framework of modulational instability, we consider a two field model of small scale drift turbulence driven by ETG. Both because it was done initially for this system and due to the its direct similarity to the rotating convection problem discussed in section 1.3. Here we also demonstrate the application of the modulational instability framework to the question of 2D pattern selection in plasma turbulence. We consider a reduced fluid ETG system as a working model:

$$\left(\partial_t + \hat{\mathbf{z}} \times \nabla \Phi \cdot \nabla\right)\left(1 - \nabla^2\right)\Phi + \partial_y(\Phi + P) + \nu \nabla^4 \Phi = 0, \tag{48}$$

$$\left(\partial_t + \hat{\mathbf{z}} \times \nabla \Phi \cdot \nabla\right)P - \chi \nabla^2 P - r\partial_y \Phi = 0, \tag{49}$$

where the following dimensionless drift wave variables are used:

$$\Phi \to \frac{e\phi}{T_i \epsilon_{*i}}, \quad P \to \frac{\epsilon_B P_{e1}}{\epsilon_{*i}^2 P_{i0}}, \quad t \to \Omega_e \epsilon_{*i} t, \quad \mathbf{x} \to \mathbf{x}/\sqrt{\tau} \rho_e$$

$$\epsilon_{*i} = \frac{\sqrt{\tau} \rho_e}{L_n} = \frac{v_{*i}}{c_{se}}, \quad \epsilon_{*e} = -\frac{\sqrt{\tau} \rho_e}{L_{p_e}} = \frac{v_{*e}}{c_{se}},$$

$$\epsilon_B = \frac{\sqrt{\tau} \rho_e}{L_B} = \frac{v_B}{c_{se}}, \quad r = \frac{\epsilon_B \epsilon_{*e}}{\epsilon_{*i}^2}$$

and $\tau = T_i/T_e$. In order to apply the modulational instability framework, we separate the fluctuations and mean flows/fields. The mean flow equations, dropping the dissipative terms, can be written as

$$\partial_T\left(1 - \nabla^2\right)\bar{\Phi} + \partial_Y\left(\bar{\Phi} + \bar{P}\right) = \langle \hat{\mathbf{z}} \times \nabla \tilde{\Phi} \cdot \nabla \nabla^2 \tilde{\Phi}\rangle, \tag{50}$$

$$\partial_T \bar{P} - r\partial_Y \bar{\Phi} = \langle \hat{\mathbf{z}} \times \nabla \tilde{P} \cdot \nabla \tilde{\Phi}\rangle, \tag{51}$$

and the two equations for the fluctuations can be combined as:

$$\underbrace{\left[\partial_t\left(\partial_t\left(1 - \nabla^2\right) + \partial_y\right) + r\partial_{yy}\right]}_{L\left(\partial_t, \partial_y, \partial_x\right)}$$

$$\times \widetilde{\Phi} \underbrace{-\left(\hat{\mathbf{z}} \times \mathbf{k} \cdot \nabla\right)\left(\left(\omega\left(1 + 2k_y^2\right) - rk_y\right)\bar{\Phi} - k_y\bar{P}\right)\widetilde{\Phi}}_{N\left(\bar{\Phi}, \bar{P}\right)} = 0 \tag{52}$$

by dropping the direct interactions between fluctuations and dissipation.

The Reynolds stress for a modulated monochromatic wave in general can be written as:

$$\langle \hat{\mathbf{z}} \times \nabla \tilde{\Phi} \cdot \nabla \nabla^2 \tilde{\Phi}\rangle \approx 2\left(\hat{\mathbf{z}} \times \mathbf{k} \cdot \nabla\right)(\mathbf{k} \cdot \nabla)\,|\Phi|^2$$
$$+ \left(\hat{\mathbf{z}} \times \mathbf{k} \cdot \nabla\right)(\nabla \cdot \mathbf{J}) - (\mathbf{k} \cdot \nabla)(\nabla \times \mathbf{J})_z, \tag{53}$$

where,

$$\mathbf{J} = \mathrm{i}\left(\Phi \nabla \Phi^* - \Phi^* \nabla \Phi \right)$$

is the Schrödinger intensity flux density, and Φ is the complex amplitude. Similarly for the advection of pressure,

$$\langle \hat{\mathbf{z}} \times \nabla \tilde{P} \cdot \nabla \tilde{\Phi} \rangle \approx \nabla \cdot \left(\hat{\mathbf{z}} \times \mathrm{i}\mathbf{k}\left[\Phi^* P - P^* \Phi \right] + \hat{\mathbf{z}} \times \left[\Phi^* \nabla P - P^* \nabla \Phi \right] \right). \tag{54}$$

The phase difference between Φ and P can be calculated from (49), by including slow modulations. When we consider a particular perturbation expansion (53) and (54) will be further simplified.

It is easy to see, from (52) that the linear dispersion relation has two solutions, and the unstable mode has a maximum at $k_x = 0$. This means that the monochromatic drift-wave around which we perform the modulational instability has $k_x = 0$ but finite k_y.

3.4.1. Initially isotropic modulations. In order to see what kind of elongated patterns form among zonal flows with $\Delta X \ll \Delta Y$, streamers with $\Delta X \gg \Delta Y$, or isotropic convective cells with $\Delta X \sim \Delta Y$, we start the analysis with isotropic modulations and see in which direction the system evolves. The amplitude equation in this case can be written as:

$$\mathrm{i}\partial_\tau \Phi + \frac{1}{2}\frac{\partial^2 \omega}{\partial k_y^2}\partial_{YY}\Phi + \frac{1}{2}\frac{\partial^2 \omega}{\partial k_x^2}\partial_{XX}\Phi + \alpha k_y^2 \partial_{XX}\left(|\Phi|^2 \right)\Phi = 0. \tag{55}$$

It is also possible to rewrite this with the scalings $X \to X/\sqrt{|\beta_x|}$, $Y \to Y/\sqrt{|\beta_y|}$, $\Phi \to (k_y\sqrt{|\alpha/\beta_x|})\Phi$, where $\beta_x = (1/2)\partial^2\omega/\partial k_x^2$ and $\beta_y = (1/2)\partial^2\omega/\partial k_y^2$, and replacing $\Phi \to \Phi^*$ if $\beta_x < 0$, which gives:

$$\mathrm{i}\partial_\tau \Phi + \partial_{YY}\Phi + \partial_{XX}\Phi + \sigma\partial_{XX}\left(|\Phi|^2 \right)\Phi. \tag{56}$$

This scaling uses the fact that the signs of β_x and β_y are the same. Here $\sigma = \pm 1$ is the overall sign of (α/β_x), where $\sigma = -1$ corresponds to an attractive nonlinearity and $\sigma = +1$ to a repulsive one. The total Hamiltonian for (56):

$$H = \int \mathrm{d}V\left[|\partial_X \Phi|^2 + |\partial_Y \Phi|^2 + \frac{\sigma}{2}\left(\partial_X\left(|\Phi|^2 \right) \right)^2 \right] \tag{57}$$

is conserved. Following Talanov, we write the evolution equation for the radial and poloidal variance (defined as $\langle X^2 \rangle = \int X^2 |\Phi|^2 \mathrm{d}X\mathrm{d}Y$ and $\langle Y^2 \rangle = \int Y^2 |\Phi|^2 \mathrm{d}X\mathrm{d}Y$ respectively):

$$\frac{\mathrm{d}^2\langle X^2 \rangle}{\mathrm{d}t^2} = 4H + 4\int\left[\sigma\left(\partial_X|\Phi|^2 \right)^2 + \left(|\partial_X \Phi|^2 - |\partial_Y \Phi|^2 \right) \right]\mathrm{d}X\mathrm{d}Y, \tag{58}$$

$$\frac{\mathrm{d}^2\langle Y^2 \rangle}{\mathrm{d}t^2} = 4H + 4\int\left[|\partial_Y \Phi|^2 - |\partial_X \Phi|^2 \right]\mathrm{d}X\mathrm{d}Y. \tag{59}$$

As these are explicit differential equations for the second derivatives of these quantities (akin to acceleration), one may qualitatively interpret them as Newton's equations of motion. For $H < 0$, which is possible for $\sigma = -1$, the total variance V is always 'pulled' towards zero, leading to a collapse. However it is easy to see that for $H < 0$ $V_x - V_y$ is always 'pulled' towards the negative axis. This means $\langle X^2 \rangle$ is always 'pulled' more strongly than $\langle Y^2 \rangle$. Since an initially isotropic state corresponds to $\langle X^2 \rangle \sim \langle Y^2 \rangle$, one arrives at the conclusion that the
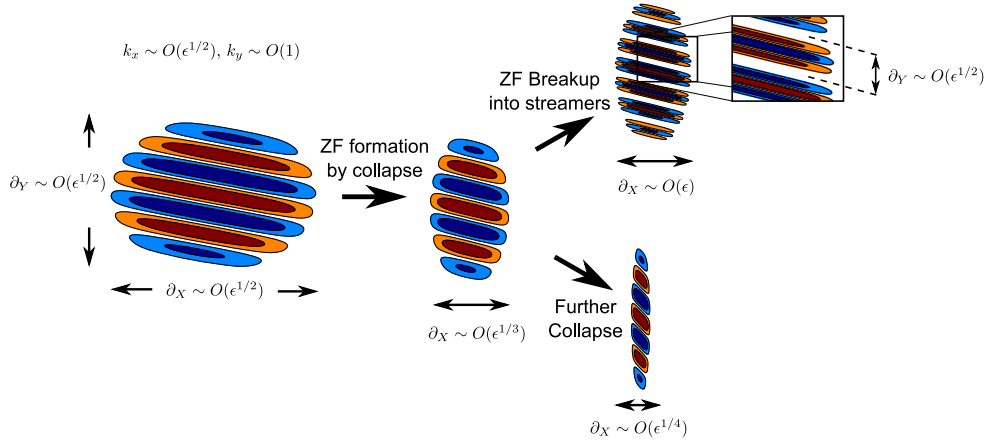
Figure 13. Evolution of an initial isotropic modulation (i.e. $\partial_X \sim \partial_Y$) of a mode with $k_x \ll k_y$. Note that while the modulational instability framework describes the modulations of complex amplitude (i.e. amplitude and phase), we have only depicted modulations of real amplitude and for simplicity in this figure.

final state will have $\langle X^2 \rangle \ll \langle Y^2 \rangle$ or $\partial_X \gg \partial_Y$. Notice that $H < 0$ is a condition on the initial data that allows the finite time singularity formation.

The collapse of the initial data to a singular layer in the perturbation analysis suggests that the wave amplitude becomes larger and ∂_X becomes smaller than it is assumed in the perturbation expansion corresponding to the initial isotropic modulation. The complete evolution of an initially isotropic amplitude modulation can be seen in figure 13. The perturbation expansion breaks down as the system collapses in the radial direction, resulting in a poloidally elongated (i.e. $\partial_X \gg \partial_Y$) modulation (and flow) structure. However, we can continue the analysis by choosing a new scaling.

3.4.2. Further anisotropic evolution. An equation describing the further evolution of the structure in the limit $\partial_X \gg \partial_Y$ may be derived similarly to the isotropic case. The main problem is that if the scaling is such that $\partial_Y \sim \partial_X^2$, one can no longer neglect the divergence of intensity flux density term $k_y(\partial_x \nabla \cdot \mathbf{J})$ in the calculation of the Reynolds stress. It is possible that this term nonlinearly damps the zonal flow, balancing the self focusing tendency. Thus, the critical scaling $\partial_X \sim O(\epsilon^{1/4})$, corresponds on the scale at which the collapse possibly stops (see figure 13). Using ϵ_{*i} as a crude estimate for ϵ we get $\Delta X \sim \rho_{es}^{3/4} L_n^{1/4}$ for the radial scale of the final meso-scale structure. If this is the zonal flow (i.e. no breakup into smaller scale structures occurs), then this would be the radial size of the zonal flow. However, as mentioned before, it is also possible that breakup into smaller scale structures occurs, then, this estimate would correspond to the radial size of these 'small scale' structures resulting from a tertiary instability.

Before the critical scaling however there is an intermediate scaling. Since this corresponds to a poloidally collapsed state of an initially isotropic field, the scaling of ∂_Y should be kept as before (i.e. $\partial_Y \sim O(\epsilon^{1/2})$, $\partial_X \sim O(\epsilon^{1/3})$, $k_x \sim O(\epsilon^{1/2})$ and $k_y \sim O(1)$) avoiding the critical scaling $\partial_x \sim O(\epsilon^{1/4})$, in order to be able to neglect the divergence of the intensity flux density term. This, in turn, results in a scaling of the mean field as $\bar{\Phi} \sim O(\epsilon^{1/3})$, and time as $\partial_T \sim O(\epsilon^{1/2})$ and $\partial_\tau \sim O(\epsilon^{2/3})$. Then, the dynamics of fluctuations in a frame

moving with velocity $\mathbf{v} = v_{gy}\hat{\mathbf{y}}$, can be described with a simple amplitude equation as before.

$$i\partial_\tau \Phi + \beta_x \partial_{XX} \Phi + \alpha k_y^2 \partial_{XX}\left(|\Phi|^2\right)\Phi = 0.$$

There are two possible end results (probably coexisting in actual turbulence): (a) the zonal flow structure can break up into streamers, in which case we can continue our analysis for streamer structures, (b) the modulations continue to collapse and form a shear layer. The size of such a shear layer will be determined by the competition between the tendency of the nonlinearity to collapse, and the effect of dissipation or higher order nonlinearities that play the role of dissipation.

3.4.3. Streamer formation. For the ETG mode, the possibility that the zonal flows are damped or balanced during the isotropic phase due to other physical processes [74] should also be considered. In this case V_x will remain fixed (or oscillate) after some initial collapse, while V_y would continue collapsing, after the fluctuations reach a certain level. This leads us to the state in which the anisotropy of the drive and the modulations are the same (i.e. $k_x\partial_Y \sim k_y\partial_X$). Choosing the scaling as $\partial_X \sim O(\epsilon)$, $\partial_Y \sim O(\epsilon^{1/2})$, $k_x \sim O(\epsilon^{1/2})$ and $k_y \sim O(1)$, and going through a similar analysis as in the isotropic case, one can write down the amplitude equation:

$$i\partial_\tau \Phi + \frac{1}{2}\frac{\partial^2\omega}{\partial k_y^2}\partial_{YY}\Phi - \frac{1}{2}\frac{\partial^2\omega}{\partial k_x^2}k_x^2\Phi + \alpha\Phi\left(\hat{\mathbf{z}}\times\mathbf{k}\cdot\nabla\right)^2|\Phi|^2 = 0. \tag{60}$$

Notice that apart from resonance (i.e. considerable enhancement of α, near marginal stability), the terms in this equation can only be balanced by choosing an expansion of the form: $\widetilde{\Phi} = \epsilon^{-1/2}\widetilde{\Phi}_0 + \epsilon^{1/2}\widetilde{\Phi}_1 + \dots$, which is a rather strong scaling of the field, producing $e\Phi/T_i \sim O(\epsilon_{*i}/\epsilon^{1/2})$. For this to be meaningful, it should be true that $1 \gg \epsilon \geqslant \epsilon_{*i}^2$. Physically, since we still neglect the ITG effects, our 'large scale' structures are smaller then the ion Larmor radius. The above condition effectively requires the large scale structures to be smaller then the density gradient length scales. This should still be very well satisfied for the ETG system. Also, for $\epsilon \sim \epsilon_{*i}$, as a crude estimate for the expansion parameter, the fluctuation level is estimated to be $e\Phi/T_e \sim O(\epsilon_{*i}^{1/2})$.

Defining α, β_x and β_y as before, we can write down a single soliton solution of (60):

$$\Phi(X, Y, \tau) = \left(\frac{|G_0|^2}{m} + \frac{X^2}{2\sigma\beta_y}\right)^{1/2} \frac{1}{k_x}\sqrt{\frac{2a}{|\alpha/\beta_y|}} \ \text{sech}\left[\sqrt{a/\beta_y}\left(Y + \frac{k_x}{k_y}X\right) - \left(\frac{U^2}{4} - a\right)\tau\right]$$

$$\times e^{i\left(\frac{U}{2\sqrt{\beta_y}}\left(Y + \frac{k_x}{k_y}X\right) - \left(\frac{U^2}{4} - a + \beta_x k_x^2\right)\tau\right)}.$$

$$\tag{61}$$

This is a self-sheared soliton solution of (60), with a and U being measures of amplitude and velocity of the soliton in the $\eta = \left(Y + \frac{k_x}{k_y}X\right)\Big/\sqrt{|\beta_y|}$ direction, respectively.

4. Damping of zonal flows

Zonal flow damping is the key parameter that determines the 'fitness' of the zonal flow as a complex structure. Therefore, it also is one of the key parameters that determine the steady state of the complex nonlinear system consisting of interacting drift/Rossby-waves and zonal

flows. Since it is the zonal flow that regulates the drift wave turbulence, the level of zonal flow defines the steady state (if it exists), or the characteristics of dynamics (if the system does not have a well defined steady state). Thus, the dissipation via zonal flow damping rate is at least as important as the energy injection by the (linear) instability of the drift wave turbulence. However, the understanding of the actual mechanisms of zonal flow damping in fusion plasmas is rudimentary compared to that of the primary instability.

In the case of quasi-geostrophic fluids, the primary source of zonal flow damping is the bottom drag [26], which is usually taken as Ekman friction. Bottom drag controls the final characteristics of zonal flows such as their characteristic scale and the spectrum of the quasi-geostrophic turbulence that results [75].

In the case of fusion plasmas, the picture is more complicated due to the possibility of coupling to kinetic physics. While all the physical effects that have been discussed previously could be described within a fluid or a gyrofluid model even if applied to plasma turbulence, zonal flow damping may have an inherently kinetic nature. In fusion turbulence research, the main justification for using the much more expensive gyrokinetic simulations instead of the cheaper gyrofluid ones is the fact that the gyrofluid codes, even when some closure that imitates linear Landau damping is used, could not get the zonal flow damping right [76]. This means even if a particular description can describe the instability and the nonlinear physics reasonably correctly, if it can not describe the damping of zonal flows, it is not very useful in predicting the fluctuation levels and therefore the resulting transport.

4.1. Linear damping

There are various mechanisms that can damp poloidal flows in tokamak devices. For instance, in the core region, a certain class of oscillating zonal flows, called GAMs, are damped due to Landau damping. However, GAM physics is particular to toroidal geometry, and standard zonal flows are not subject to Landau damping. This means they are damped mainly by collisional processes. A complete theory of how the collisional processes function in toroidal geometry, especially in the presence of particles that are trapped in the low field side of the toroidal magnetic confinement geometry, called the 'neoclassical theory' were developed in the early stages of fusion research [126].

The main linear damping mechanism on zonal flows in the regime of weak collisionality is the damping due to what are called 'banana particles', which are particles that are trapped in the low field side (the outer part) of the torus and follow trajectories that somewhat resemble bananas. (see figure 14). The mechanism works as a drag between trapped particles and zonal flows.

The short time response of the zonal flow due to effects of collisional drag, can be computed exactly (with certain simplifying assumptions such as large aspect ratio, circular concentric flux surfaces etc) using a variational principle within a boundary layer defined by the passing/trapping boundary. The result is the short time response kernel (i.e. $\mathcal{K}_k^{(s)}(t) \equiv \overline{\Phi}_k(t) / \overline{\Phi}_k(0)$, where $t \ll \tau_{ii}$) [127]:

$$\mathcal{K}_k^{(s)}(t) = \left(1 - \frac{1}{\alpha}\right) e^{-\nu_G t} \cos(\omega_G t) + \frac{1}{\alpha} e^{\frac{\beta(t)^2}{\alpha^2} t} \operatorname{erfc}\left(\frac{\beta(t)}{\alpha} t^{1/2}\right), \tag{62}$$

where $\omega_G = v_{thi}/R$ and $\nu_G = \omega_G e^{-q^2}$ are the GAM frequency and damping rate respectively (due to Landau damping), $\alpha = 1 + 1.6 q^2/\varepsilon^{1/2}$ and $\beta(t) = 3\pi q^2 \bar{\nu}^{1/2} / \left(\varepsilon \Lambda(t)^{3/2}\right)$. Note that here $\Lambda(t) \approx \ln\left(16\left(\varepsilon/[\bar{\nu}t]\right)^{1/2}\right)$, $\bar{\nu} = 0.61/\tau_{ii}$, and the standard fusion notation is used so that q is the safety factor, τ_{ii} is the ion–ion collision time, v_{thi} is the ion thermal speed, R is the
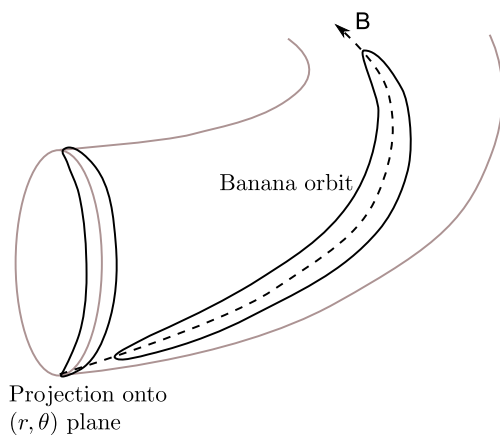
Figure 14. A banana orbit in the toroidal geometry of a tokamak and its projection onto the (r, θ) plane.
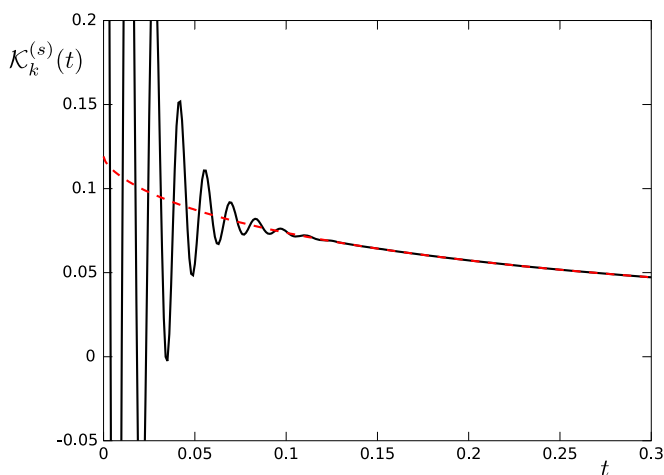

Figure 15. The short time collisional response kernel (62), as a function of time (normalized to ion–ion collision time τ_{ii}). The solid line shows the full kernel whereas the dashed line shows the second term in (62), which corresponds to the damping of zonal flows. Note that initial oscillations correspond to GAM oscillations that are rapidly damped via Landau damping.

major radius and ε is the aspect ratio. The figure 15 depicts this kernel for $\varepsilon = 0.18$, $q = 1.4$ and $\nu_{*i} = 0.04$.

A similar linear, collisional mechanism due to friction between passing and trapped electrons for ETG turbulence has been suggested as a mechanism for damping of small scale electron zonal flows [128] whose formation is discussed in section 3.4. It should be noted that electron heat transport due to ETG turbulence remains a controversial problem, where the experimental measurements are scarce and gyrokinetic simulations disagree with one another. Therefore, at least for now, it remains difficult to make an objective assessment of the importance of zonal flows, or their damping in ETG turbulence.

4.2. Nonlinear damping

As is usually the case with linear phenomena, the collisional drag for zonal flows in tokamaks and geostrophic fluids of different kinds have no similarities. This is due to the fact that the analogy between the different systems are limited to the forms of reduced partial differential equations that are used to describe these different systems and the similarity does not extend to the effects of boundary layers or geometry, or the nature and the effects of collisions (classical versus neo-classical for example).

In contrast the basic effects of nonlinearities are almost exactly the same in these very different physical systems, since the way the nonlinear interactions function is rather universal. It is the nonlinearity, for instance, that allows the formation of zonal flows through a modulational instability. There are also higher order nonlinear terms that may contribute to their damping. The basic idea that higher order nonlinear terms cause the collisionless damping of zonal flows exist in various forms. Coupling to 'damped eigenmodes' [77] or parallel and perpendicular stresses acting in opposition [78], are suggested examples of such ideas for fusion plasmas.

Note that, since within the modulational instability picture, the zonal flow formation is realized through a collapse of the modulation envelope, a nonlinear diffusion effect that simply causes the envelope to smooth out, will also oppose the collapse.

Another way the zonal flow can be nonlinearly damped is the phenomenon of 'tertiary instability', which may take the form of a Kelvin–Helmholtz instability of the sheared flow pattern that is formed by the zonal flow.

4.3. Nonacceleration: Charney–Drazin theorem

Taking dimensionless form for the fluctuating part of (9):

$$\tilde{q} \approx \tilde{\zeta} - \tilde{h}$$

we can define the zonally averaged latitudinal PV flux as:

$$\left\langle \tilde{q}\tilde{v}_y \right\rangle = \frac{\partial}{\partial y}\left\langle \partial_y \tilde{h} \partial_x \tilde{h} \right\rangle$$

which is in fact equivalent to the Taylor identity. This allows us to write:

$$\partial_t \bar{v}_x - \left\langle \tilde{q}\tilde{v}_y \right\rangle = \bar{F}_x - \langle D \rangle_v. \tag{63}$$

Considering the equation for the evolution of zonally averaged PE:

$$\frac{\partial}{\partial t}\langle \tilde{q}^2 \rangle + \left\langle 2\tilde{q}\tilde{v}_y \right\rangle \frac{\partial}{\partial y}\left(\bar{q} + q_0 \right) + \partial_y \left\langle \tilde{v}_y \tilde{q}^2 \right\rangle = 2\left\langle \tilde{q}\tilde{P}_q \right\rangle - 2\left\langle \tilde{q}\tilde{D}_q \right\rangle \tag{64}$$

and combining (63) and (64) in order to cancel the second terms on the left hand sides:

$$\left[\frac{1}{2}\frac{1}{\frac{\partial}{\partial y}\left(\bar{q} + q_0 \right)}\frac{\partial}{\partial t}\langle \tilde{q}^2 \rangle + \frac{\partial}{\partial t}\bar{v}_x \right] = \frac{1}{\frac{\partial}{\partial y}\left(\bar{q} + q_0 \right)}\left[\left\langle \tilde{q}\tilde{P}_q \right\rangle - \left\langle \tilde{q}\tilde{D}_q \right\rangle \right] + \bar{F}_x - \langle D \rangle_v. \tag{65}$$

Dropping the highest order terms in $\tilde{q}/\bar{q}$, and forcing and dissipation, once can write

$$\bar{v}_x + \frac{1}{2}\frac{\langle\tilde{q}^2\rangle}{\frac{\partial}{\partial y}\left(\bar{q}+q_0\right)} = \text{const}$$

which is a statement of conservation of total meridional momentum including zonal flows and waves. In other words, (65) implies that the meridional momentum due to waves and zonal flows can increase or decrease (locally) only as a result of forcing and dissipation at that spatial position. In particular, local meridional forcing, and drag that modify the zonal flow momentum or local PE injection and dissipation that modify the wave momentum can eventually increase or decrease total meridional momentum by transfer to the other 'species' via the action of turbulent PV flux. The same reasoning can be applied to drift waves [79].

5. Shearing effects on turbulence

5.1. Shear decorrelation

As discussed in the earlier sections, self-regulated large/meso-scale sheared flow structures emerge from the natural dynamical evolution of certain types of turbulence. Those systems that can develop flow shear, such as magnetized plasmas and fluids subjected to strong rotation, are naturally more effective in enduring large amounts of external free energy than others. In such a turbulent system, the initial instability acts merely as a catalyst that transfers the free energy from the external agent to the large scale flows, since the generated large scale flow shear reacts back on the turbulence and eventually suppresses its own driver.

While the end result may be a statistical quasi-steady state with flows and turbulence, it may also lead to intermittent cycles à la PP oscillations between the growth of the primary instability and the growth of the secondary flow structures and a consequent decay of the primary instabilities [80].

The stages of these oscillations are (i) the initial growth of the primary instability, (ii) the secondary growth of the meso-scale sheared flow structures (iii) the supression of the primary instability by the flow shear via shear decorrelation, and (iv) the damping of the sheared flow. An important part of research on magnetized fusion has historically been dedicated to the identification and classification of linear instabilities. Therefore this is not really addressed in this paper beyond a basic mention of characteristics of drift instabilities. Zonal flow formation, and its various aspects has already been discussed in some detail in section 3. Damping of zonal flows, both linear and nonlinear, are discussed in section 4. This leaves us with the question of shear decorrelation.

While it is part of the bigger picture of coupled co-evolution of flows and turbulence, in order to focus on physics of shear decorrelation itself, in this section we drop the requirement of self-consistency and consider an externally imposed flow shear. As such the approach is more directly applicable to a stationary sheared radial electric field, or an imposed sheared flow in a rotating convection experiment. Nonetheless it gives us useful information about the nature of the shear decorrelation process which plays a role also in the zonal-flow/turbulence interaction.

The basic idea of shear decorrelation is that a sheared flow can stretch an initially isotropic eddy to a length that is much larger than its initial length sufficiently rapidly that the eddy size hits the turbulence correlation length and thus the eddy gets decorrelated faster. For given free energy source, the faster decorrelation implies lower fluctuation intensity and hence a reduction of turbulent transport [81]. The subject is reviewed previously [82] with

detailed references. Our purpose here is not to repeat the existing review but to present the formulation of the [81] (BDT henceforth) in an understandable way.

In order to see the effect of sheared flow on turbulence, consider the following equation:

$$\left[\frac{\partial}{\partial t} + v_{Ey}(x)\frac{\partial}{\partial y} + \tilde{v} \cdot \nabla \right] \tilde{q}(x, y, t) = \tilde{P} - \tilde{D} \tag{66}$$

which has the basic form of PV advection, with $\tilde{P}$ being the production and $\tilde{D}$ the dissipation of $\tilde{q}$ (it is clear that $\tilde{q}(x, y, t)$ need not have to be the PV and may be another fluctuating field as well). Note that we are using slab geometry unlike the original BDT calculation, which uses a cylindrical geometry. An equation for the two-point correlation $C_{12}(t) \equiv \langle \tilde{q}_1 \tilde{q}_2 \rangle$ can be written by multiplying the equation for $\tilde{q}_1 \equiv \tilde{q}(x_1, y_1, t)$ by $\tilde{q}_2 \equiv \tilde{q}(x_2, y_2, t)$, and vice versa and adding and statistically averaging the two equations:

$$\left[\frac{\partial}{\partial t} + v_{Ey}(x_1)\frac{\partial}{\partial y_1} + v_{Ey}(x_2)\frac{\partial}{\partial y_2} \right] C_{12}(t) + N = L,$$

where $N = \langle \tilde{q}_2 \tilde{v}_1 \cdot \nabla \tilde{q}_1 \rangle + \langle \tilde{q}_1 \tilde{v}_2 \cdot \nabla \tilde{q}_2 \rangle$ represents the nonlinear terms, and $L = \langle \tilde{P}_1 \tilde{q}_2 \rangle + \langle \tilde{P}_2 \tilde{q}_1 \rangle - \langle \tilde{D}_1 \tilde{q}_2 \rangle - \langle \tilde{D}_2 \tilde{q}_1 \rangle$ represents linear production and dissipation terms. In order to describe stretching, we consider the sum and difference coordinates: $x_+ = (x_1 + x_2)/2$, $x_- = (x_1 - x_2)/2$. Taylor expanding the mean $E \times B$ flow as $v_{Ey}(x_1) \approx v_{Ey}(x_+) + x_- v'_{Ey}(x_+)$ and $v_{Ey}(x_2) \approx v_{Ey}(x_+) - x_- v'_{Ey}(x_+)$ and using $\partial_{y_1} = \left(\partial_{y_+} + \partial_{y_-} \right)/2$ and $\partial_{y_2} = \left(\partial_{y_+} - \partial_{y_-} \right)/2$ and assuming that the two point correlation is homogeneous (i.e. a function only of the difference variable), we obtain:

$$\left[\frac{\partial}{\partial t} + x_- v'_{Ey}(x_+)\frac{\partial}{\partial y_-} \right] C_{12}(t) + N = L,$$

where N and L denote the nonlinear and the linear terms in the resulting equation respectively. Dropping the linear terms and using an eddy diffusivity to represent the nonlinear ones, we arrive at:

$$\left[\frac{\partial}{\partial t} + x_- v'_{Ey}(x_+)\frac{\partial}{\partial y_-} \right] C_{12}(t) - \frac{\partial}{\partial x_-} D \frac{\partial}{\partial x_-} C_{12}(t) = 0. \tag{67}$$

In order to describe the evolution of average distance between two points, we consider the equation for x_-^2, $x_- y_-$ and y_-^2 moments of (67) using $D = D_0 \left(x_-^2 / \Delta x_t^2 + y_-^2 / \Delta y_t^2 \right)/2 \sim \Delta \omega_t \left(x_-^2 + \Delta x_t^2 k_{0y}^2 y_-^2 \right)/2$, and defining $\omega_s \equiv v'_{Ey} k_{0y} \Delta x_t$, which gives:

$$\frac{\mathrm{d}}{\mathrm{d}t} \left\langle x_-^2 \right\rangle = \Delta \omega_t \left(3 \left\langle x_-^2 \right\rangle + \Delta x_t^2 k_{0y}^2 \left\langle y_-^2 \right\rangle \right)$$

$$\frac{\mathrm{d}}{\mathrm{d}t} \left\langle x_- y_- \right\rangle = \omega_s \left(k_{0y} \Delta x_t \right)^{-1} \left\langle x_-^2 \right\rangle + \Delta \omega_t \left\langle x_- y_- \right\rangle$$

$$\frac{\mathrm{d}}{\mathrm{d}t} \left\langle y_-^2 \right\rangle = 2\omega_s \left(k_{0y} \Delta x_t \right)^{-1} \left\langle x_- y_- \right\rangle.$$
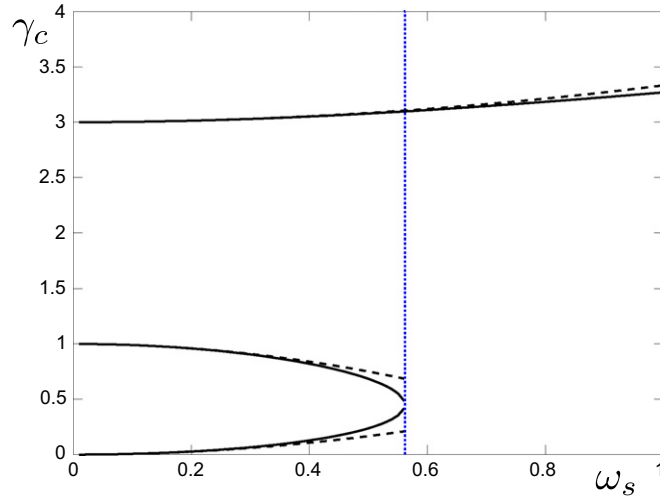
Figure 16. Numerical (solid lines) and approximate analytical (dashed lines) solutions of the dispersion relation (68).

The solution of this linear system is given by the solution of the dispersion relation:

$$\gamma_c \left(\gamma_c - \Delta\omega_t \right)\left(\gamma_c - 3\Delta\omega_t \right) = 2\omega_s^2 \Delta\omega_t \tag{68}$$

In the limit of nonzero $\Delta\omega_t$ but small ω_s, the solution can be expanded around the solutions for $\omega_s \to 0$, to find the three roots:

$$\gamma_c^{(1)} \approx \Delta\omega_t \left(1 - \frac{\omega_s^2}{\Delta\omega_t^2} \right)$$

$$\gamma_c^{(2)} \approx \frac{2}{3} \frac{\omega_s^2}{\Delta\omega_t}$$

$$\gamma_c^{(3)} \approx 3\Delta\omega_t \left[1 + \frac{1}{9} \frac{\omega_s^2}{\Delta\omega_t^2} \right].$$

The asymptotic solution on the other hand actually approaches:

$$\gamma_c \approx \frac{4\Delta\omega_t}{3} + 2^{1/3}\omega_s^{2/3}\Delta\omega_t^{1/3}$$

which is a continuation of the $\gamma_c^{(3)}$ root and has the scaling $\gamma_c \sim 2^{1/3}\omega_s^{2/3}\Delta\omega_t^{1/3}$ for $\omega_s \gg \Delta\omega_t$. See figure 16 for how the asymptotic expressions compare with the numerical solution of (68). Note also that two of the weak shear roots (i.e. $\gamma_c^{(1)}$ and $\gamma_c^{(2)}$) vanish as one increases the shear. The exact point where the first root disappears can be computed as:

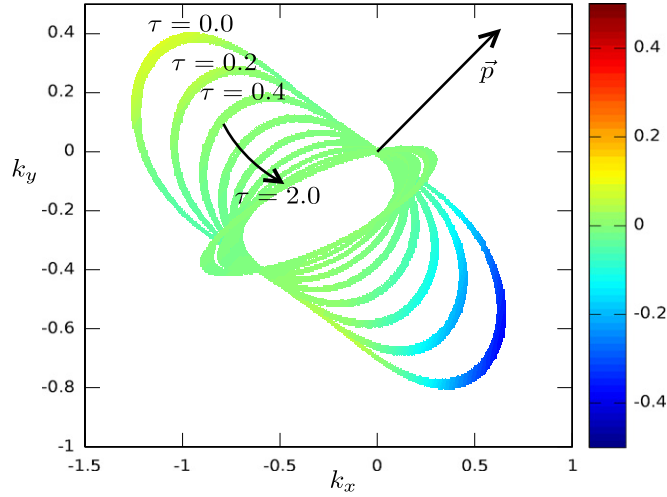$$\frac{\omega_s}{\Delta\omega_t} = \frac{\sqrt{7^{3/2} - 10}}{3^{3/2}} \approx 0.562.$$

46

Figure 17. The resonant manifold $\Delta\omega \equiv \omega(\mathbf{p}) + \omega(\mathbf{q}) + \omega(\mathbf{k}) \approx 0$, with $\mathbf{q} = -\mathbf{k} - \mathbf{p}$, in shearing coordinates as a function of time τ for $p_x = 0.6$, $p_y = 0.4$. The color codes indicate the strength of the nonlinear interaction coefficient M_{kpq}. The figure shows that while initially this mode was coupled to two other modes roughly $k_x \sim -1$, $k_y \sim 0.3$ and $k_x \sim 0.6$, $k_y \sim -0.6$, later on, both the size of the resonant manifold and the nonlinear interaction coefficient on the resonant manifold diminish. This suggests that the three wave interactions become very ineffective.

5.2. Effect on the resonance manifold

The resonance manifold, that defines how the wave-like fluctuations can interact with each-other efficiently is the key ingredient of the description of weak wave turbulence. A given wave-number $\mathbf{p}$ interacts with two other wave-numbers $\mathbf{q}$ and $\mathbf{k} = -\mathbf{p} - \mathbf{q}$ (since the interacting wavenumbers form a triangle). Thus, if $\mathbf{p}$ and $-\mathbf{p} - \mathbf{q}$ are on the manifold defined by the Manley–Rowe relations $\Delta\omega \equiv \omega(\mathbf{p}) + \omega(\mathbf{q}) + \omega(-\mathbf{p} - \mathbf{q}) = 0$ (using the convention that frequency is taken as negative if the wavenumber is negative).

Consider for instance the resonance manifold given by the dispersion relation for the Charney–Hasegawa–Mima equation: $\omega_k = k_y/\left(1 + k^2\right)$:

$$\Delta\omega(\mathbf{p}, \mathbf{q}) \equiv \frac{p_y}{\left(1 + p^2\right)} + \frac{q_y}{\left(1 + q^2\right)} - \frac{p_y + q_y}{\left(1 + p^2 + q^2 + 2\mathbf{q}\cdot\mathbf{p}\right)} = 0.$$

To consider the effect of constant shear, one can introduce the so-called shearing coordinates [83]:

$$\tau = (t - t_0), \quad \xi = x, \quad \eta = y - v'_{Ey}x(t - t_0). \tag{69}$$

The other key element in computing the efficiency of three wave interactions is the interaction coefficient. For the CHM system, it can be written as:

$$M_{kpq} = \frac{\hat{\mathbf{z}} \times \mathbf{p} \cdot \mathbf{q}\left(q^2 - p^2\right)}{1 + k^2}.$$

The effect of a constant shear on the resonance manifold and the interaction coefficient can be seen in figure 17.

It is well known that in plasmas and quasi-geostrophic fluids, weaknesses in resonant interactions (i.e. that the manifold is small and the interaction coefficient vanishes on a large portion of that manifold) is one of the primary reasons for the generation of large scale flow structures. In other words, as the resonance manifold is weakened the only remaining interaction that remains is via the large scale flow that satisfies the Manley–Rowe relations in a trivial way.

It is therefore interesting to see that the action of flow shear, indeed weakens the resonance manifold in time, hence a time averaged 'effective' resonant manifold also gets weaker. This leads to the turbulence being forced to couple even more to the large scale flow. In other words, while at the beginning of the shearing transformation the turbulence may have been coupling to other modes, as the time increases, the eddies are tilted and they can only couple to the large scale flow.

Physically this corresponds to tilting and absorption of small scale vortices by the sheared flow as discussed in [84]. This is a self-enhancing nonlinear mechanism that amplifies the initial shear as opposed to the vortex break up. This observation is interesting for control, because if we impose external flow shear, the same level of turbulence will generate more zonal flows under the action of large scale shear because the eddies can not couple to anything else other than the zonal flows due to the destruction of the resonance manifold. This means that for quasi-2D turbulence, by applying an external flow shear we can increase self generated flow shear structures as well.

5.3. Self amplification

We have discussed various mechanisms by which a shear flow amplifies itself. First we discussed the simple process of radial group velocity propagation of the waves that are tilted in a certain direction giving rise to sheared flows which increase the tilt and hence the Reynolds stress. Then there is the basic mechanism of modulational instability; a seed sheared flow which acts on fluctuations by modulating their amplitude results in 'negative viscosity' and hence finite time singularity. Finally we discussed the effect of sheared flow on the three-wave interaction resonance manifold, noting that while initially the manifold is reasonably populated, as the sheared flow acts, the three wave interactions become less and less efficient, favoring the coupling with the zonal flows.

These are all different ways of describing a common phenomenon; that of the self amplification of the zonal flow by its effect on turbulence. This usually corresponds to the initial phase of the zonal flow growth and works until the fluctuations start to be seriously modified by the zonal shear that they are unable to sustain their energy.

6. PP dynamics

6.1. Basic PP dynamics

The fact that the zonal flow feeds on the energy of turbulent fluctuations, while suppressing those same fluctuations that drive it, via shear decorrelation, suggests an analogy between the dynamics of the zonal flow/drift wave system and that of a predator and a prey species. In this analogy, the zonal flow acts as a predator, whose increased population becomes a threat to the drift wave that play the role of the prey. The zonal flow damping is then a key control parameter that determines, once the prey is gone, how long will the predators last. This is the key parameter, along with the available free energy that sets the dynamics of the system. The basic Lotka–Volterra equations for zonal-flow drift-wave system can be obtained by
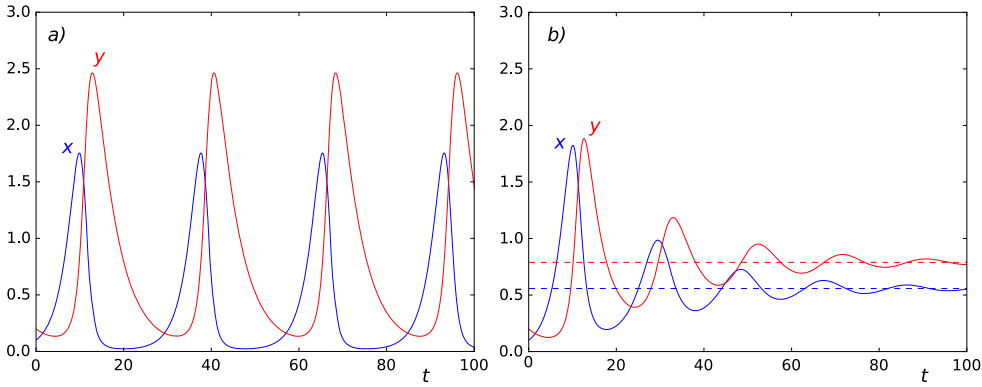
Figure 18. Temporal evolution of the Lotka–Volterra system (on the left) and its basic generalization that is used in plasma turbulence (on the right), where the fixed points given in (72) are shown as dashed lines. Here the variable x correspond to the primary turbulence (prey) and the variable y corresponds to the zonal flow (the prey).

considering the zero-dimensional limit of the wave-kinetic formulation described in section 3.2:

$$\frac{\partial N}{\partial t} = \gamma N - \alpha E_V N - \Delta\omega N^2, \tag{70}$$

$$\frac{\partial E_V}{\partial t} = \alpha N E_V - \nu_F E_V - \gamma_{nl}(E_V)E_V, \tag{71}$$

where N indicates the wave-quanta density and E_V indicates the energy associated with zonal shear. Various coupling coefficients such as γ, the linear growth rate, α shearing efficiency, $\Delta\omega$, nonlinear decorrelation rate, ν_F, the zonal flow damping and γ_{nl} define the characteristics of the model.

It is clear that the evolution of the turbulent fluctuations coupled to zonal flow energy as described by the simplified model given by (70) and (71) describes the dynamics of a PP system. The prey species N has an internal growth as well as a nonlinear damping (due to 'eddy' diffusion), while the predator species has linear damping but nonlinear growth -that is proportional to the population of the prey- as well as a higher order nonlinear damping (which is not really necessary for a minimal model).

A PP cycle thus has four phases dominated subsequently by these four terms. It starts with the initial growth phase where the fluctuations grow exponentially. This is followed by a predation phase, where the zonal flows grow rapidly feeding off of the free energy of the fluctuations. This phase is characterized by modulational instability or self-enhanced growth of initially weak zonal perturbations. The next phase, characterized by shear suppression is the phase where intense zonal flow shear scatters turbulence energy to high-k where it gets dissipated. In this phase the fluctuation intensity decreases. The final phase in the PP cycle is the zonal flow damping phase. Physically this is usually the slowest phase, and therefore it determines the period of PP oscillations.

6.1.1. Lotka–Volterra. The basic Lotka–Volterra equations are given by

$$\frac{\mathrm{d}x}{\mathrm{d}t} = ax - bxy$$

$$\frac{\mathrm{d}y}{\mathrm{d}t} = -cy + dxy,$$

where x correspond to drift waves (prey) and y to zonal flows (predator). The system has two fixed points for each variable given by $x = 0$, $y = 0$, $x = c/d$, $y = a/b$. The resulting oscillation is shown in figure 18.

6.1.2. The zonal flow variant. The equation

$$\frac{\mathrm{d}x}{\mathrm{d}t} = ax - bxy - ex^2$$

$$\frac{\mathrm{d}y}{\mathrm{d}t} = -cy + dxy - fy^2$$

has the fixed points defined by

$$x(a - by - ex) = 0$$

$$-y(c - dx + fy) = 0$$

which gives the nontrivial solution

$$x = \frac{cb + fa}{db + ef}, \quad y = \frac{da - ec}{db + ef} \tag{72}$$

as we can see in figure 18, the system saturates by approaching this solution. While the dynamics of this simple model is representative of the similar dynamics in tokamaks, it is not clear if the fixed point remains meaningful even after considerable modeling effort to estimate the coefficients. The model is actually a rather qualitative model that is used to develop insight into the tendencies rather than as a quantitative model.

6.2. PP and forward enstrophy cascade

When the zonal flows become important dynamically, low k drift wave spectrum is dominated mainly by nonlocal interactions with the zonal flow. These interactions are anisotropic in nature and are nonlocal in k-space in that the zonal shearing, can act on small scales directly by transferring some of the PE in the drift waves (which is a conserved quantity of the zonal flow–drift wave interaction) to smaller scales.

However since the zonal flow obtains energy by transforming the PE of the low-k drift wave to the high-k one it becomes stronger, and as it becomes stronger it leads to more and more spectral flux being dumped to small scales and dissipated. However as the zonal flow becomes too effective in moving the PE to dissipation range, it starts to deplete its source. With some zonal flow damping, this leads to cycles of 'bursts' in the spectral evolution equation of the zonal flow.

Consider for example the basic spectral budget for PE:

$$\frac{\partial}{\partial t}W(k) + \frac{\partial}{\partial k}\Pi_{n\ell}^{W}(q, k) + \frac{\partial}{\partial k}\Pi_{\ell}^{W}(k) = P_W(k) - \varepsilon_W(k), \tag{73}$$

where $\Pi_\ell^W(k)$ is the usual k-space flux of PE, driven by local interactions and $\Pi_{n\ell}(q, k)$ is the part of the flux that is driven by nonlocal interaction with the zonal mode (of wave-number q). P_W and ε_W are the production and the dissipation of PE.

6.2.1. Spectrum with nonlocal interactions. Basic dimensional analysis suggests that

$$\Pi_{n\ell}^W(q, k) = \tau_{zf}^{-1}(q, k) W(k) k$$

$$\tau_{zf}^{-1}(q, k) \propto k E(q)^{1/2} q^{1/2}$$

now considering a constant nonlocal flux, we obtain:

$$W(k) = \frac{\beta k^{-2}}{u_{\mathrm{rms}}(q)}, \tag{74}$$

where $u_{\mathrm{rms}}(q) = E(q)^{1/2} q^{1/2}$ is the root mean square velocity of the zonal flow. Note that here we took the zonal flow as a more general two-dimensional structure and considered the isotropized energy spectrum in order to preform a dimensional analysis. The basic scalings should work as long as there is an additional mechanism which isotropize the fluctuations at smaller scales.

Remarkably, the spectrum

$$\Phi_k^2 \propto n_k^2 \propto \frac{k^{-3}}{\left(1 + k^2\right)^2}$$

one obtains from (74) for $W(k) \sim \Phi_k^2 k \left(1 + k^2\right)^2$ (note that the extra k is an integration factor) seem to agree reasonably well with experimental observations of density fluctuations in Tore Supra, especially for high-k where the turbulence is expected to be relatively isotropic, using the Doppler back-scattering diagnostic system.

7. Role of zonal and mean flows in L–H transition

Recent observations of the intermediate phase (I-phase) that appear between L and H-mode states and display limit cycle oscillations between turbulence intensity and mean flows point out the key role that the zonal flows play in the formation of transport barriers.

The basic role of $E \times B$ shear in H-mode is rather well understood. In a quasi-steady state, the energy injection rate + the energy generated by the fusion reactions (which is usually weak compared to the injected energy in current tokamaks, but will hopefully become important in the future ones) has to be balanced by the heat flux. However the heat transport in tokamaks is mainly turbulent, and since $E \times B$ shear reduces turbulence, and thus the turbulent diffusion coefficients, if a Fick's law is used to estimate the turbulent heat transport as the diffusion coefficient goes down, in order to keep the heat flux constant, the temperature gradient has to go up. A similar argument can be made for the density. In fact there are a number of simple transport models, which can 'describe' the L–H transition qualitatively using this basic idea [85].

7.1. Modeling the L–H transition.

The minimum model that can describe the L–H transition involves the $E \times B$ shear suppression mechanism where the $E \times B$ shear is somehow linked to either the temperature gradient via the neoclassical expression for toroidal velocity [86], or density gradient times

temperature gradient via the radial force balance [85]. The minimal model, which has relevant physics for the H-mode is a setup, somewhat related to a 1-D double diffusive convection problem encountered in the study of salinity transport in the ocean.

Consider a set of radial transport equations for density $n(r, t)$ and pressure $P(r, t)$:

$$\frac{\partial}{\partial t}n + \frac{1}{r}\frac{\partial}{\partial r}\left[r\Gamma_n\right] = S_n(r)$$

$$\frac{3}{2}\frac{\partial}{\partial t}P + \frac{1}{r}\frac{\partial}{\partial r}[rQ_p] = H(r),$$

where a slow 'transport time scale' dynamics is assumed for the evolution of the profiles which are averaged over the flux surfaces (in θ and ϕ directions around the torus), so that fluctuations smooth out. It is further assumed that a basic closure for the heat and particle fluxes can be implemented such that:

$$\Gamma_n = -D_0\frac{\partial n}{\partial r} - D_1\mathcal{E}\frac{\partial n}{\partial r}$$

$$Q_p = -\chi_0\frac{\partial P}{\partial r} - \chi_1\mathcal{E}\frac{\partial P}{\partial r},$$

where D_0 and χ_0 corresponds respectively to the residual part of the particle and heat diffusivities usually thought to be due to neoclassical diffusion, and $D_1\mathcal{E}$ and $\chi_1\mathcal{E}$ are the turbulent particle and heat diffusivities respectively, which are explicitly proportional to the turbulence intensity $\mathcal{E}$. A simple shear suppression rule in the spirit of section 5.1, which correspond to the weak shear limit of reference [81], is usually used:

$$\mathcal{E} = \frac{\mathcal{E}_0}{1 + \alpha v_{Ey}'^2}$$

to imitate the suppression of the turbulence due to sheared flow.

Where usually an approximate form of the radial force balance for the ions:

$$E_r = -\frac{v_\theta}{c}B_\phi + \frac{v_\phi}{c}B_\theta + \frac{\nabla P}{en}$$

such as

$$v_{Ey}' = \frac{c}{eBn_i^2}\frac{dn}{dr}\frac{dP}{dr}$$

is used (recall that $v_{Ey} = -cE_r/B$) [85]. The heat source $H(r)$ is localized in the center and the particle source $S(r)$ is localized near the edge of the plasma. This system of equations solved with the boundary conditions $n(a) = n_a$, $P(a) = P_a$ and $\partial_t\partial_x n(0) = \partial_t\partial_x P(0) = 0$ (and possibly with other boundary conditions as well), gives a rather clear L–H transition (see figure 19).

Many similar models have been developed, explaining the details of the bifurcation phenomenon [87], including angular momentum transport to explain intrinsic rotation [88, 89], including turbulence spreading [90] and turbulence-zonal flow PP evolution to explain the L–I–H transition [90–92]. In our current understanding of the phenomenon, the zonal flows play an important role during the transition.
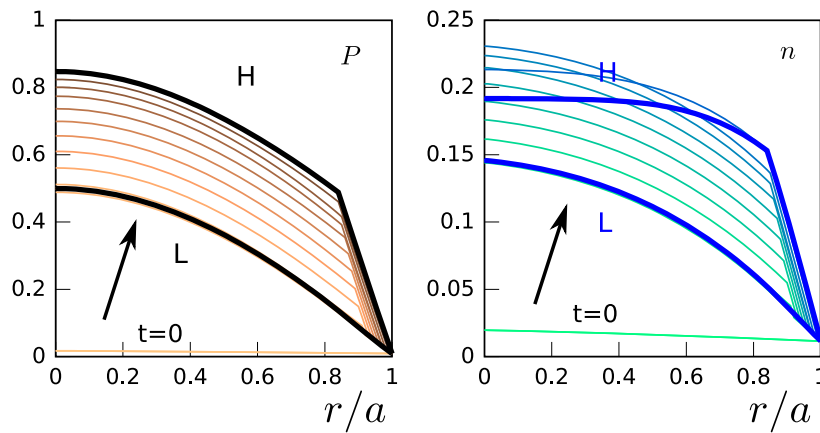
Figure 19. Dynamics and the final steady state of the basic transport model, showing the establishment of the L-mode profiles (denoted with L) slightly below the critical threshold at $q_a = 2.9$ and the H-mode profiles (denoted with L) slightly above it at $q_a = 3.0$ for pressure (on the left) and density (on the right). It is remarkable that the L-mode profile is established very rapidly while the transition to H-mode takes time in this formulation.
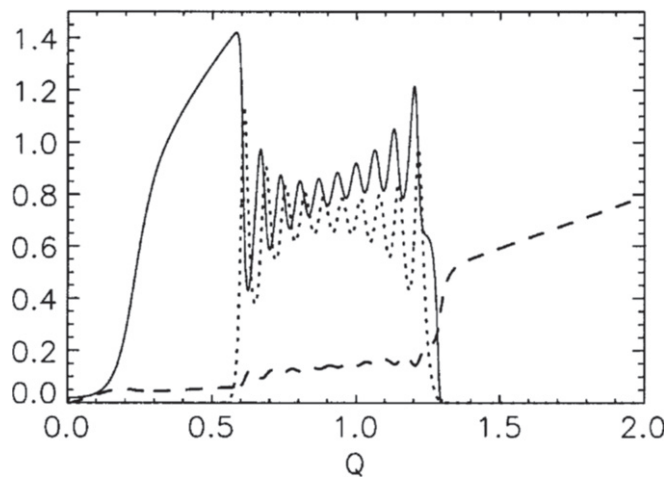

Figure 20. Limit cycle oscillations before an L–H transition as predicted by a simple meso-scale model [100], the solid line corresponds to turbulence intensity, the dotted line to zonal flows and the dashed line corresponds to the mean flow (or equivalently the pressure gradient). Figure used with permission from Kim E-J and Diamond P H 2003 *Phys. Rev. Lett.* **90** 185006. Copyright 2003 American Physical Society.

7.2. Models including PP dynamics

Recent observations of, slow coupled oscillations between plasma fluctuations and large scale flow structures, display certain characteristics of PP dynamics. Such 'limit cycle oscillations' have been observed in TJ-II stellerator [93], and HL-2A [94], ASDEX-Upgrade [95], D-IIID [96], EAST [97] and Alcator C-Mod [98] tokamaks and point to zonal flows as a universal trigger to the L–H transition [99].

While the experimental observations of the phenomenon are relatively new, the idea has been around for a while. Most notably, Kim and Diamond had predicted the limit cycle oscillations [100] from a simple L–H transition model that includes zonal-flow turbulence interactions (see figure 20). The models have recently been extended in a series of papers by Miki and Diamond *et al* in the form of reduced meso-scale models of zonal flow triggering of the L–H transition [92, 101–103]. Similarly coupling a shell model of drift-wave turbulence (which incorporates naturally the PP evolution) to a transport model has given a qualitatively consistent picture of meso-scale evolution leading to pedestal formation [90].

The basic picture which arise from these theoretical studies and experimental observations is that the zonal flows and therefore the meso-scale dynamics associated with them, such as avalanches, turbulence spreading, spatial and spectral evolution of turbulence intensity into regions of phase-space that are not linearly excited is an essential part of the dynamical self-regulation leading up to the L–H transition. Dominant paradigms based on a fixed background gradient driving micro-turbulence, whose only effect is to define a turbulent diffusion coefficient can not capture the PP behavior as a result of either the lack of or a strong damping of mesoscale phenomenon. This suggests that a direct approach to modeling the turbulent transport is more difficult than initially thought, since it requires a direct numerical simulation of the evolution of the full gyro-kinetic distribution function where the free energy sources are not the gradients but rather explicit heating terms written in terms of fluxes. Such a 'flux-driven' simulation effort, has indeed been undertaken, but has shown to be rather difficult with current resources, for realistic practical applications for tokamak plasmas [129].

This justifies the use of simpler models as discussed in this review, sometimes as the only source of prediction, as most direct numerical simulations are based on fixed imposed profiles, which work only when the plasma is not dynamically evolving and basically has no hope of simulating a multi-scale dynamical phenomenon such as an L–I–H transition.

7.3. Staircases and sandpiles

PV staircases are a well known feature of the Earth's atmosphere related to zonal jets in different planets shown in figures 1 and 2 in section 1. They are also a key feature of the thermohaline, and provide a barrier for the thermal transport across different layers of the ocean. They also probably exist in tokamaks and act as a seed for the formation of the actual transport barrier.

While staircases reduce transport across them due to the flow shear associated with them, they don't completely suppress turbulence. As a result the flux that is slightly reduced leads to an accumulation of the transported quantity leading to a sharpening of its gradient and hence the possibility of a sudden burst of transport. This dynamical coupling between a forming staircase pattern and a sudden burst of transport (an 'avalanche') is a secondary meso-scale dynamics of plasma turbulence that has important implications on the dynamics of the profiles (i.e. transport) especially formation and destruction of barriers.

An interesting aspect of avalanche dynamics is its relation to self organized criticality (SOC) and thus sandpiles. One may intuitively expect that the plasma when driven far from equilibrium drives sheared flows and other complex mesoscale structures to bring itself near a self-organized critical 'equilibrium'. In this dynamical state, the plasma would be in a state of locally marginal equilibrium hovering slightly above and slightly below this self-organized marginal stability curve.

Leaving the question of what this marginal equilibrium is and how it is established aside, we may describe the evolution of the profiles around this equilibrium. Noting that the joint reflection symmetry $x \rightarrow -x$, $\delta P \rightarrow -\delta P$ is respected [104] by the flux near an SOC

equilibrium state (such that $P = P_{\text{SOC}} + \delta P$), one can consider a combination of the simplest possible forms of the flux as $\Gamma(\delta p) \approx (\lambda/2)\delta P^2 - \chi\frac{\partial}{\partial x}\delta P$. This gives the following equation for the deviation from the SOC state for the plasma pressure [105]:

$$\frac{\partial}{\partial t}\delta P + \frac{\partial}{\partial x}\left(\frac{\lambda}{2}\delta P^2\right) - \frac{\partial}{\partial x}\left(\chi\frac{\partial}{\partial x}\delta P\right) = 0$$

which can be recognized as the Burgers equation. Since the Burger's equation leads to formation of shocks, and a slower process of PV homogenization counters this tendency, it is not surprising that the system generates 'staircase' patterns.

The effect of a mean sheared flow on this basic Burgers dynamics can be included by adding another direction to consider a flow in the y direction that is sheared in the x direction. This gives a 'transport' equation of the form:

$$\frac{\partial}{\partial t}\delta P + v_E' x\frac{\partial}{\partial y}\delta P + \frac{\partial}{\partial x}\left(\frac{\lambda}{2}\delta P^2\right) - \frac{\partial}{\partial x}\left(\chi\frac{\partial}{\partial x}\delta P\right) - \frac{\partial}{\partial y}\left(\chi\frac{\partial}{\partial y}\delta P\right) = 0$$

which is still consistent with the joint reflection symmetry.

8. Nonlocality, radial propagation

Another mechanism by which the zonal flow/drift wave system can saturate is through spatial propagation. We have already seen a glimpse of that in the modulational instability framework as we made a transformation to the frame of reference, moving radially at the radial group velocity. The zonal flow, which does not move is then retarded in this reference frame and it is this effect that balances the Reynolds stress at the lowest order. However in reality the coupling of spatial propagation and zonal flows is not as simple. Since modulations that are generated in different spatial positions with different characteristics and can propagate either inward or outward both due to linear and nonlinear effects.

In nature, turbulence is never local. If a local perturbation injects energy to a turbulent field locally in space, the resulting fluctuations spread throughout the system. The phenomenon while obvious from a turbulence perspective, may appear counter-intuitive from a magnetized plasma perspective where the particles are well localized due to small Larmor radii.

However since turbulent transport allow the particles or heat to be transported radially due to phase relations of fluctuating fields, the generated turbulence can also propagate via these same turbulent mechanisms. The phenomenon that is called 'turbulence spreading' is usually described using Fokker–Planck formulations resulting in Fischer–Kolmogorov type nonlinear equations, such as:

$$\frac{\partial}{\partial t}\mathcal{E} + \frac{\partial}{\partial x}\left[v_g\mathcal{E} - D_0\mathcal{E}\frac{\partial}{\partial x}\mathcal{E}\right] = \gamma\mathcal{E} - \gamma_{n\ell}\mathcal{E}^2, \tag{75}$$

where $\mathcal{E}(x, t)$ is a measure of the turbulent fluctuation level (usually a nonlinearly conserved quantity such as energy, or PE).

The equation can also be obtained by a systematic reductive perturbation method based on the two scale direct interaction approximation, which is applicable to two and more field models of turbulence [106]. The equation (75) has a number of exact solutions for certain forms of γ and $\gamma_{n\ell}$ that are physically relevant solutions, such as self-similar spreading or ballistic fronts [107].

A detailed derivation of a similar equation can be done, starting from the drift-kinetic equation, where the flux can be written as an integral over the velocity space of the flux of free-energy density, instead of the particular form (i.e. $\Gamma_{\mathcal{E}} = v_g \mathcal{E} - D_0 \mathcal{E} \frac{\partial}{\partial x} \mathcal{E}$) that was taken above:

$$
\Gamma_{\mathcal{E}} \equiv \int \left(\frac{\left\langle \tilde{\mathbf{v}}_E \widetilde{f}^2 \right\rangle}{2\overline{f}} + \frac{\left\langle \widetilde{f}^2 \right\rangle}{2\overline{f}} \hat{\mathbf{b}} v_{\parallel} \right) d^3 v, \tag{76}
$$

where $\overline{f}$ and $\widetilde{f}$ being the slowly evolving and the rapidly fluctuating parts of the drift kinetic distribution function.

Basic effect of large scale flow shear can be included in this equation by including the physics of advection by a radially sheared poloidal flow:

$$
\frac{\partial}{\partial t} \mathcal{E} + v_E' x \frac{\partial}{\partial y} \mathcal{E} + \frac{\partial}{\partial x} \left[v_g \mathcal{E} - D_0 \mathcal{E} \frac{\partial}{\partial x} \mathcal{E} \right] = \gamma \mathcal{E} - \gamma_{n\ell} \mathcal{E}^2.
$$

A formulation of this form is not self consistent unless one includes the effect of fluctuations on driving the $E \times B$ shear. It may however be useful in the case, when the $E \times B$ shear is sufficiently strong and steady that it can be considered as an external one. The H-mode in tokamaks would satisfy this condition.

However for the transition, current understanding suggests that the spatio-temporal PP like dynamics of turbulent fluctuations and zonal flows with mean $E \times B$ shear acting as a reservoir of kinetic energy play the dominant role. While the fluctuations can recover from zonal shear suppression due to zonal flow damping, mean shear eventually acquires enough energy and suppresses the turbulent fluctuations sufficiently, reducing the transport coefficients considerably leading to a state of high confinement.

It should be noted however that the simple PP idea described above, which will be discussed in more detail below, does not take into account the spatial propagation. Nonetheless, both the fluctuations and the zonal flows actually propagate as they are nonlinearly coupled forming complex interaction patterns. A description of this phenomenon using simple models is possible and interesting in its own right. However even the simplest model ends up with 4-5 partial differential equations describing spatio-temporal evolution of different quantities.

8.1. Telegraph equation, traffic flow, and turbulent elasticity

8.1.1. Telegraph equation. In the standard formulation of plasma transport, the response of the flux to the gradient is usually taken to be local and instantaneous There is a direct relation between the heat flux and the temperature gradient (i.e. with adiabatic electrons and zero rotation with symmetric $k_{\parallel}$ spectrum):

$$
Q = -\chi_i \frac{\partial T}{\partial r}. \tag{77}
$$

This relation is called the Fick's law (or the Fourier law of heat conduction in the case of solids), and it implies that the flux responds *infinitely rapidly* and *perfectly locally* to the gradients. In contrast, 'the second sound' [108], in solids at very fast time scales [109], and in reactive fluids, a commonly used relation is the following (e.g. [110]):

$$\tau \frac{\partial Q}{\partial t} + \chi_i \nabla_r T + Q = 0, \tag{78}$$

where τ can be considered as a new coefficient of transport physics, which physically corresponds to the response time of the flux to the gradient. This relation, which is called the Maxwell–Cattaneo relation, incorporates the fact that *if the gradient is suddenly changed, the heat flux would respond in some finite response time (i.e. τ)*. Notice that, the steady state limit of (78) is indeed (77). In order to understand 'transient' transport, we actually need both τ and χ_i even though τ may be as fast as a few turbulent decorrelation times.

However since the plasma transport is driven mainly by turbulence, the response of the flux is not a simple 'transient', because by the time the flux is saturated to its mixing length level, the gradient is also changed via the transport equation for heat:

$$\frac{\partial T_i}{\partial t} + \nabla_r \cdot Q_i = H(r, t), \tag{79}$$

where $H(r, t)$ is the net heating, and this allows a dynamical coupling between the flux and the gradient. For example expanding around an equilibrium (i.e. $\nabla_r \cdot Q_i = H(r, t)$), it is easy to see that the excess temperature obeys the equation:

$$\frac{\partial^2 \delta T_i}{\partial t^2} + \frac{1}{\tau} \frac{\partial}{\partial t} \delta T_i - \nabla_r \cdot \left[\frac{\chi_i}{\tau} \nabla_r \delta T \right] = 0 \tag{80}$$

which is actually *the telegraph equation*. This equation is well known to describe the time evolution of the transport in reactive fluids and in problems of population growth, more accurately than a simple diffusion equation [111, 112]. It is the simplest formulation that describes the phenomenon of diffusion in a medium, which describes not only the positions, but also the momenta of the basic elements [113] that constitute that medium. It is clear that as $\tau \to 0$, the first term in (80) becomes negligible and we recover the usual diffusion equation. Note that this is a singular limit where the highest order derivative with respect to time drops.

In contrast, for finite τ, the wave character of the equation suggests a radial propagation speed $v_r = \sqrt{\chi_i / \tau}$, which is consistent with the spreading phenomenology $v_{\text{spr}} \sim \sqrt{2\gamma D_{\mathcal{E}}}$ (where γ is the growth rate), except that the diffusion coefficient for turbulence intensity $D_{\mathcal{E}}$ is replaced in this coupled formulation by the heat diffusivity χ_i [107, 114–116].

If the flux response is not perfectly local, but rather smoothed out (i.e. a discontinuity in the gradients, does not generate a step function flux), we can write:

$$\tau \frac{\partial Q}{\partial t} + \tau \nabla_r \Gamma_Q + \chi_i \nabla_r T + Q = 0, \tag{81}$$

where a local closure for the flux of heat flux:

$$\Gamma_Q = -D \frac{\partial Q}{\partial r} \tag{82}$$

can be proposed, which gives the so-called Guyer–Krumhansl constitutive relation [117], which is sometimes referred to as a 'weakly nonlocal' relation. Obviously, if the radial group velocity of the waves that are responsible for transport is finite, it should be added to Γ_Q (i.e. as $v_{gr} Q$).

Note that this formulation of the transport now has three coefficients, namely the heat diffusivity χ_i, flux response time τ and the flux penetration length $\lambda = \sqrt{D\tau}$. Note that (81) is simply the Cattaneo relation with the added diffusion of heat flux. However since, the

transport is anomalous in fusion plasmas, the coefficients χ, τ and D are functions of turbulence intensity, rendering the constitutive relation nonlinear as will be discussed.

The effect of mean shear can be introduced into the equation for the heat flux by moving to two dimensions as:

$$\tau \left(\frac{\partial}{\partial t} + v_E' x \frac{\partial}{\partial y} \right) Q + \tau \nabla_r \Gamma_Q + \chi_i \nabla_r T + Q = 0.$$

8.1.2. Turbulent elasticity and PP waves. The basic approach that has been outlined in the previous section for weakly nonlocal evolution of the heat flux can be applied to other quantities that are transported in a plasma, such as particles and momentum. A full matrix formulation is discussed in appendix B as a starting point for this generalization. However since such a formulation is by definition 'meso-scale' both in time and in space, other meso-scale phenomena, and in particular zonal flows has to be included in the same footing. While the zonal flows are special in the sense that they suppress the underlying turbulence, they are driven by a perpendicular momentum flux, just as any other flow can be driven by momentum flux. In fact the zonal momentum flux evolution can be obtained simply by taking the corresponding moment of the wave-kinetic equation. Following [118], we consider the wave kinetic equation (33), which can be written as:

$$\frac{\partial}{\partial t} N_k + v_{g,k} \frac{\partial}{\partial x} N_k - k_y v_E' \frac{\partial}{\partial k} N_k = -\gamma_{N,k} \left(N_k - N_{0,k} \right) \tag{83}$$

coupled to the spatio-temporal evolution of the zonal+mean flow:

$$\frac{\partial}{\partial t} v_E + \frac{\partial}{\partial x} \Pi_y = -\nu_F \left(v_E - v_{E,0} \right).$$

The wave-quanta density N_k is driven towards $N_{0,k}$, which is the steady state k-spectrum due to eddy damping, and v_E, which is the zonal $E \times B$ velocity is driven towards $v_{E,0}$ -the $E \times B$ flow implied by the radial force balance- due to ZF damping mechanisms discussed above. Here

$$\Pi_y = \left\langle \tilde{v}_x \tilde{v}_y \right\rangle$$

is the radial flux of zonal momentum and using the equivalence of wave-particle momenta [79] is equivalent to wave-momentum, which can be computed by multiplying (83) by $v_{g,k} k_y$ and integrating over k as:

$$\frac{\partial \Pi_y}{\partial t} + \frac{\partial}{\partial x} \Gamma_{\Pi y} + \alpha \frac{\partial}{\partial x} v_E = -\gamma_N \left(\Pi_y - \Pi_{y0} \right). \tag{84}$$

Here γ_N is the expectation value of $\gamma_{N,k}$ over the 'distribution' $\delta N_k = N_k - N_{0,k}$. The local, steady-state limit of (84), gives a Fick's law like expression for the zonal flow:

$$\Pi_y = \Pi_{y0} - \frac{\alpha}{\gamma_N} \frac{\partial}{\partial x} v_E,$$

where Π_{y0} plays the role of a residual momentum flux [89, 119] in the absence of $E \times B$ shear. One can get a simple telegraph equation for the zonal flow, even by dropping the $\frac{\partial}{\partial x} \Gamma_{\Pi y}$ term altogether (i.e. considering a delayed response, but no spatial coupling).

$$\frac{\partial \widetilde{\Pi}_y}{\partial t} + \alpha \frac{\partial}{\partial x} \tilde{v}_E = -\gamma_N \widetilde{\Pi}_y$$

$$\frac{\partial}{\partial t} \tilde{v}_E + \frac{\partial}{\partial x} \widetilde{\Pi}_y = -\nu_F \tilde{v}_E,$$

where $\widetilde{\Pi}_y = \Pi_y - \Pi_{y0}$ and $\tilde{v}_E = v_E - v_{E0}$ are the meso-scale time evolving components. The two equations can be combined simply as:

$$\left(\frac{\partial}{\partial t} + \nu_F \right) \left(\frac{\partial}{\partial t} + \gamma_N \right) \tilde{v}_E - \alpha \frac{\partial^2}{\partial x^2} \tilde{v}_E = 0$$

which suggest damped wave-like solutions independent of the sign and the value of α. This means that in order to excite spatial PP waves, one has to include some form of spatial nonlocality.

Since we are not interested in the temporal evolution of $\Gamma_{\Pi y}$, we can use a flux-limited diffusion [120, 121] expression as a 'closure':

$$\Gamma_{\Pi y} = -\frac{\chi_{\Pi y} \frac{\partial}{\partial x} \Pi_y}{\sqrt{1 + \lambda_{\Pi y} \left(\frac{\partial}{\partial x} \ln \Pi_y \right)^2}}$$

for $\lambda_{\Pi y} \to 0$ or $\frac{\partial}{\partial x} \ln \Pi_y \ll \lambda_{\Pi y}^{-1/2}$, the expression gives the usual Fick's law, but in the opposite limit it gives advection. In this latter limit, the combined equation takes the form of a generalized telegraph equation:

$$\left[\left(\frac{\partial}{\partial t} + \nu_F \right) \left(\frac{\partial}{\partial t} + \gamma_N - v_c \frac{\partial}{\partial x} \right) - \alpha \frac{\partial^2}{\partial x^2} \right] \tilde{v}_E = 0. \tag{85}$$

The modulational instability condition for (85) is $\left| \alpha q^2 / \gamma_N \right| > \nu_F$, which also gives a critical (i.e. most unstable) zonal wave-number as $q_c \approx \left| \nu_F \gamma_N / \alpha \right|^{1/2}$. It is clear that once these radially propagating PP waves establishes, all the fluxes become equally nonlocal, since the local gradients of temperature, density and momentum, will all be determined by the incoming fluxes via this dynamics rather than the other way around.

With this we may be able to say a few words about a current debate in the fusion community about fixed gradient versus flux driven formulations. It is true that the turbulence in fusion devices are excited locally by the free energy in the gradients. However a formulation based on fixed gradients is not very meaningful since the profiles themselves adjust in order to be able to accommodate the injected heat, particles and momentum. This means that a flux-driven formulation (source-driven is usually implied) is critical for describing the evolution of the plasma globally. However a global description necessitates a proper implementation of boundary conditions and different parts of the plasma, such as open and closed field lines. Instead a partially local description can be imagined where the fluxes and the gradients co-evolve in the domain, and the boundary conditions are chosen as the fluxes and the gradients at the boundary of the domain. If the simulated domain does not contain sources, such a partially local formulation may be sufficient for describing the weakly nonlocal dynamics of the plasma turbulence.

Acknowledgments

Appendix A. Derivation of thermal Rossby equations

Considering a viscous fluid in the container depicted in figure 3, the equation of motion can be written as:

$$\left(\frac{\partial}{\partial t} + \mathbf{v} \cdot \nabla\right)\mathbf{v} + 2\Omega\hat{\mathbf{n}} \times \mathbf{v} + \Omega^2\mathbf{r} = -\frac{\nabla P}{\rho} + \nu \nabla^2\mathbf{v}. \tag{A.1}$$

Using a perturbation expansion, $P = P_0 + \delta P$, and $\rho = \rho_0 + \delta\rho$, the zeroth order balance with no flow takes the form

$$\nabla P_0 = -\rho_0 \Omega^2 r_0 \hat{\mathbf{r}}. \tag{A.2}$$

When we substitute these expansions back into (A.1), and use (A.2) to eliminate ∇P_0, we obtain:

$$\left(\frac{\partial}{\partial t} + \mathbf{v} \cdot \nabla\right)\mathbf{v} + 2\Omega\hat{\mathbf{n}} \times \mathbf{v} = -\frac{\nabla \delta P}{\rho_0} - \Omega^2 r_0 \frac{\delta\rho}{\rho_0}\hat{\mathbf{r}} + \nu \nabla^2\mathbf{v}. \tag{A.3}$$

Using the equation of state:

$$\rho = \rho_0\left[1 - \alpha\left(T - T_0\right)\right]$$

we can write $\delta\rho = -\alpha\rho_0\delta T$ where δT is the deviation from an equilibrium profile of temperature, which is the steady state solution of the heat equation:

$$\left(\frac{\partial}{\partial t} + \mathbf{v} \cdot \nabla\right)T = \kappa \nabla^2 T \tag{A.4}$$

which actually becomes the Laplace's equation $\nabla^2 T_0 = 0$, one solution to which is a constant gradient linking the two boundary values of temperature

$$T_0(x) = T_1 + \frac{\Delta T}{D}x. \tag{A.5}$$

Multiplying (A.3) by D^3/ν^2, and using the dimensionless variables $\mathbf{v}' = D\mathbf{v}/\nu$, $t' = \nu t/D^2$, $\mathbf{x}' = \mathbf{x}/D$, $\pi = \frac{D^2}{\nu^2}\frac{\delta P}{\rho_0}$ and $\Theta = \delta T/(\mathcal{P}\Delta T)$:

$$\left(\frac{\partial}{\partial t} + \mathbf{v} \cdot \nabla\right)\mathbf{v} + 2E^{-1}\hat{\mathbf{n}} \times \mathbf{v} = -\nabla\pi + Ra\Theta\hat{\mathbf{r}} + \nabla^2\mathbf{v}, \tag{A.6}$$

where we dropped the primes for convenience and defined

$$Ra \equiv \alpha\frac{D^3\Delta T}{\nu\kappa}\Omega^2 r_0,$$

which is the Rayleigh number, and

$$E \equiv \frac{\nu}{D^2\Omega},$$

which is the Ekman number. The equation for temperature perturbation can be obtained by substituting $T = T_0(x) + \delta T$ with $T_0(x)$ given by (A.5) into the heat equation (A.4):

$$\left(\frac{\partial}{\partial t} + \mathbf{v} \cdot \nabla\right)\delta T + v_x \frac{\Delta T}{D} = \kappa \nabla^2 \delta T$$

multiplying by $D^2/(\nu \Delta T)$ and using the normalization discussed above, we obtain:

$$\mathcal{P}\left(\frac{\partial}{\partial t} + \mathbf{v} \cdot \nabla\right)\Theta + v_x = \nabla^2 \Theta. \tag{A.7}$$

Using $\mathbf{v} = \hat{\mathbf{n}} \times \nabla_\perp \psi$, and the geostrophic balance as described already in section 1.2.3 the system of equations (A.6) and (A.7) can be written as

$$\left(\frac{\partial}{\partial t} + \mathbf{v} \cdot \nabla\right)\zeta + \left(\zeta + 2E^{-1}\right)\left(\nabla_\perp \cdot \mathbf{v}\right) = -Ra\frac{\partial}{\partial y}\Theta + \nabla^2 \zeta$$

using (3) with $h = h(x) = h_0 - 2\eta_0 x$, we can write

$$\left(\frac{\partial}{\partial t} + \mathbf{v} \cdot \nabla\right)\zeta - \eta_* \partial_y \psi = -Ra\frac{\partial}{\partial y}\Theta + \nabla^2 \zeta,$$

where $\eta_* = 4\eta_0/\left(Eh_0\right)$.

Appendix B. Matrix formulation of weakly nonlocal transport

One can formulate general transport equations with evolving fluxes in simple geometry as follows:

$$\frac{\partial}{\partial t}\xi + \nabla_r \cdot \Gamma = \mathbf{S} \tag{B.8}$$

$$\tau \frac{\partial}{\partial t}\Gamma + \left(\Gamma - \Gamma_{\text{res}}\right) + \nabla_r \cdot [\mathfrak{R} \cdot \mathcal{G}] = \mathfrak{M} \cdot \mathcal{F}, \tag{B.9}$$

where

$$\boldsymbol{\xi} = \begin{pmatrix} n \\ nT \\ nv_\phi \end{pmatrix}, \quad \boldsymbol{\Gamma} = \begin{pmatrix} \Gamma_n \\ Q \\ \Pi_\phi \end{pmatrix}$$

$$\boldsymbol{\mathcal{F}} = \begin{pmatrix} \nabla_r n \\ \nabla_r T \\ \nabla v_\phi \end{pmatrix}, \quad \mathfrak{M} = -\begin{pmatrix} D_n & U_{nT} & U_{n\phi} \\ U_{Tn} & \chi_i & U_{T\phi} \\ U_{\phi n} & U_{\phi T} & \chi_\phi \end{pmatrix}$$

$$\boldsymbol{\mathcal{G}} = \begin{pmatrix} \nabla_r \Gamma_n \\ \nabla_r Q \\ \nabla_r \Pi_\phi \end{pmatrix}, \quad \mathfrak{R} = -\begin{pmatrix} D_{\Gamma_n} & U_{\Gamma_n Q} & U_{\Gamma_n \Pi_\phi} \\ U_{Q\Gamma_n} & D_Q & U_{Q\Pi_\phi} \\ U_{\Pi_\phi \Gamma_n} & U_{\Pi_\phi Q} & D_{\Pi_\phi} \end{pmatrix}.$$

Furthermore these can be extended to include temperature anisotropy as well as magnetic curvature and inhomogeneity separating turbulent and neoclassical contributions to the flux [122]. Note that in the above formulation the neoclassical fluxes should appear as offset, not as a modification of the fixed point. In other words, we would say $\Gamma = \Gamma_{\text{neo}} + \Gamma_{\text{turb}}$ and write (B.9) only for the turbulent bit. Here we present this matrix formulation as the basis of an alternative to standard transport frameworks (e.g. [123]).

References

[1] Rhines P B and Young W R 1982 *J. Fluid Mech.* **122** 347–67
[2] Larichev V and Reznik G 1976 *Dokl. Akad. Nauk SSSR* **231** 1077–9
[3] Flierl G R, Stern M E and Jr J A W 1983 *Dyn. Atmos. Oceans* **7** 233–63
[4] Meiss J D and Horton W 1983 *Phys. Fluids* **26** 990–7
[5] Taylor J B 1974 *Phys. Rev. Lett.* **33** 1139–41
[6] Diamond P H and Malkov M 2003 *Phys. Plasmas (1994–present)* **10** 2322–9
[7] Dobrowolny M, Mangeney A and Veltri P 1980 *Phys. Rev. Lett.* **45** 144–7
[8] Grappin R, Frisch U, Pouquet A and Leorat J 1982 *Astron. Astrophys.* **105** 6–14
[9] Boldyrev S 2006 *Phys. Rev. Lett.* **96** 115002
[10] Levin S A 1998 *Ecosystems* **1** 431–6
[11] Frisch U 1995 *Turbulence: The Legacy of A N Kolmogorov* (Cambridge: Cambridge University Press)
[12] Ingersoll A P, Beebe R F, Collins S A, Hunt G E, Mitchell J L, Muller P, Smith B A and Terrile R J 1979 *Nature* **280** 773–5
[13] Maximenko N A, Bang B and Sasaki H 2005 *Geophys. Res. Lett.* **32** L12607
[14] Fujisawa A 2009 *Nucl. Fusion* **49** 013001
[15] Lin Z, Hahm T S, Lee W W, Tang W M and White R B 1998 *Science* **281** 1835–7
[16] Brizard A 1992 *Phys. Fluids* B **4** 1213–28
[17] Hockey T A 1999 *Galileo's Planet : Observing Jupiter Before Photography* (Bristol: Institute of Physics)
[18] Porco C C *et al* 2003 *Science* **299** 1541–7
[19] García-Melendo E, Pérez-Hoyos S, Sánchez-Lavega A and Hueso R 2011 *Icarus* **215** 62–74
[20] Peek B M 1958 *The Planet Jupiter* (London: Faber and Faber) http://archive.org/details/ThePlanetJupiter
[21] García-Melendo E and Sánchez-Lavega A 2001 *Icarus* **152** 316–30
[22] NASA/JPL/University of Arizona 2000 PIA02863: Planetwide Color Movie http://photojournal.jpl.nasa.gov/catalog/PIA02863
[23] Maximenko N A, Melnichenko O V, Niiler P P and Sasaki H 2008 *Geophys. Res. Lett.* **35** L08603
[24] Richards K J, Maximenko N A, Bryan F O and Sasaki H 2006 *Geophys. Res. Lett.* **33** L03605
[25] Rossby C G 1940 *Q. J. R. Meteorol. Soc.* **66** 68–87
[26] Vallis G K 2006 *Atmospheric and Oceanic Fluid Dynamics: Fundamentals and Large-scale Circulation* 1st edn (Cambridge, UK: Cambridge University Press)
[27] Pedlosky J 1987 *Geophysical Fluid Dynamics* 2nd edn (New York: Springer)
[28] Hoskins B J, McIntyre M E and Robertson A W 1985 *Q. J. R. Meteorol. Soc.* **111** 877–946
[29] Fultz D and Nakagawa Y 1955 *Proc. R. Soc.* A **231** 211–25
[30] Hide R 1958 *Phil. Trans. R. Soc.* A **250** 441–78
[31] Chandrasekhar S 1953 *Proc. R. Soc.* A **217** 306–27
[32] Read P L, Yamazaki Y H, Lewis S R, Williams P D, Miki-Yamazaki K, Sommeria J, Didelle H and Fincham A 2004 *Geophys. Res. Lett.* **31** L22701
[33] Busse F H 2004 *Chaos* **14** 803
[34] Busse F H and Or A C 1986 *J. Fluid Mech.* **166** 173–87
[35] Chandrasekhar S 1961 *Hydrodynamic and Hydromagnetic Stability (Dover Classics of Science and Mathematics)* (New York: Dover)
[36] Diamond P H, Itoh S-I, Itoh K and Hahm T S 2005 *Plasma Phys. Control. Fusion* **47** R35–161
[37] McKee G R *et al* 2003 *Phys. Plasmas* **10** 1712–9
[38] Tynan G R, Moyer R A, Burin M J and Holland C 2001 *Phys. Plasmas* **8** 2691–9
[39] Moyer R A, Tynan G R, Holland C and Burin M J 2001 *Phys. Rev. Lett.* **87** 135001
[40] Xu G S, Wan B N, Song M and Li J 2003 *Phys. Rev. Lett.* **91** 125001
[41] Fujisawa A, Itoh K, Iguchi H *et al* 2004 *Phys. Rev. Lett.* **93** 165002
[42] Estrada T *et al* 2009 *Plasma Phys. Control. Fusion* **51** 124015
[43] Manz P, Ramisch M and Stroth U 2009 *Phys. Rev. Lett.* **103** 165004
[44] Tynan G R *et al* 2006 *Plasma Phys. Control. Fusion* **48** S51
[45] Sokolov V, Wei X, Sen A K and Avinash K 2006 *Plasma Phys. Control. Fusion* **48** S111
[46] Fujisawa A, Itoh K, Shimizu A *et al* 2008 *Phys. Plasmas* **15** 055906
[47] Jakubowski M, Fonck R J and McKee G R 2002 *Phys. Rev. Lett.* **89** 265003

[48] Schmitz L, Wang G, Hillesheim J C, Rhodes T L, Peebles W A, White A, Zeng L, Carter T A and Solomon W 2008 *Rev. Sci. Instrum.* **79** 10F113
[49] Hamada Y, Nishizawa A, Ido T, Watari T, Kojima M, Kawasumi Y, Narihara K, Toi K and Group J I 2005 *Nucl. Fusion* **45** 81
[50] Conway G D, Scott B, Schirmer J, Reich M, Kendl A and the ASDEX Upgrade Team 2005 *Plasma Phys. Control. Fusion* **47** 1165
[51] Nagashima Y *et al* 2005 *Phys. Rev. Lett.* **95** 095002
[52] Vershkov V, Shelukhin D, Soldatov S, Urazbaev A, Grashin S, Eliseev L, Melnikov A and the T-10 team 2005 *Nucl. Fusion* **45** S203
[53] Zhao K J *et al* 2006 *Phys. Rev. Lett.* **96** 255004
[54] Vermare L, Hennequin P, Gürcan Ö D and the Tore Supra Team 2012 *Nucl. Fusion* **52** 063008
[55] Yu J, Holland C, Tynan G, Antar G and Yan Z 2007 *J. Nucl. Mater.* **363–5** 728–32
[56] Jackson J D 1998 *Classical Electrodynamics Third Edition* 3rd edn (New York: Wiley) ISBN 047130932X
[57] Yoshida Z and Mahajan S M 2002 *Phys. Rev. Lett.* **88** 095001
[58] Meyrand R and Galtier S 2012 *Phys. Rev. Lett.* **109** 194501
[59] Chew G F, Goldberger M L and Low F E 1956 *Proc. R. Soc.* A **236** 112–8
[60] Hasegawa A and Wakatani M 1983 *Phys. Rev. Lett.* **50** 682–6
[61] Horton W 1999 *Rev. Mod. Phys* **71** 735–78
[62] Vallis G K and Maltrud M E 1993 *J. Phys. Oceanogr.* **23** 1346–62
[63] Balescu R 2005 *Aspects of Anomalous Transport Plasmas (Series in Plasma Physics)* (Bristol: Institute of Physics)
[64] Goldreich P and Sridhar S 1995 *Astrophys. J.* **438** 763–75
[65] Carnevale G F and Martin P C 1982 *Geophys. Astrophys. Fluid Dyn.* **20** 131–64
[66] Dubrulle B and Nazarenko S 1997 *Physica* D **110** 123–38
[67] Smolyakov A I and Diamond P H 1999 *Phys. Plasmas* **6** 4410–3
[68] Balescu R 2003 *Phys. Rev.* E **68** 046409
[69] Balescu R, Petrisor I and Negrea M 2005 *Plasma Phys. Control. Fusion* **47** 2145
[70] Krommes J A and Kim C B 2000 *Phys. Rev* E **62** 8508–39
[71] Zakharov V E and Kuznetsov E A 1997 *Phys. Usp.* **40** 1087
[72] Falkovich G 2011 *Fluid Mechanics: A Short Course for Physicists* 1st edn (Cambridge: Cambridge University Press)
[73] Newell A 1974a *Nonlinear Wave Motion (Lectures in Applied Mathematics)* (Providence, RI: American Mathematical Society) p 15
[74] Kim E j, Holland C and Diamond P H 2003 *Phys. Rev. Lett.* **91** 075003
[75] Manfroi A J and Young W R 1999 *J. Atmos. Sci.* **56** 784–800
[76] Dimits A M *et al* 2000 *Phys. Plasmas* **7** 969–83
[77] Terry P W, Gatto R and Baver D A 2002 *Phys. Rev. Lett.* **89** 205001
[78] Itoh K, Hallatschek K, Toda S, Sanuki H and Itoh S I 2004 *J. Phys. Soc. Japan* **73** 2921–3
[79] Diamond P H, Gurcan O D, Hahm T S, Miki K, Kosuga Y and Garbet X 2008 *Plasma Phys. Control. Fusion* **50** 124018
[80] Diamond P H, Liang Y M, Carreras B A and Terry P W 1994 *Phys. Rev. Lett.* **72** 2565–8
[81] Biglari H, Diamond P H and Terry P W 1990 *Phys. Fluids* B **2** 1–4
[82] Terry P W 2000 *Rev. Mod. Phys.* **72** 109–65
[83] Goldreich P and Lynden-Bell D 1965 *Mon. Not. R. Astron. Soc.* **130** 125
[84] Manz P, Ramisch M and Stroth U 2009 *Phys. Rev. Lett.* **103** 165004
[85] Hinton F L and Staebler G M 1993 *Phys. Fluids* B **5** 1281–8
[86] Hinton F L 1991 *Phys. Fluids* B **3** 696–704
[87] Malkov M A and Diamond P H 2008 *Phys. Plasmas* **15** 122301
[88] Dominguez R R and Staebler G M 1993 *Phys. Fluids* B **5** 3876–86
[89] Gürcan Ö D, Diamond P H, Hahm T S and Singh R 2007 *Phys. Plasmas* **14** 042306
[90] Berionni V 2014 Etude de l'impact des flux zonaux sur la turbulence plasma, la transition LH et la production d'entropie *PhD Thesis* LPP, Ecole Polytechnique in preparation
[91] Kim E and Diamond P 2003 *Phys. Plasmas* **10** 1698–704
[92] Miki K, Diamond P H, Gürcan Ö D, Tynan G R, Estrada T, Schmitz L and Xu G S 2012 *Phys. Plasmas* **19** 092306
[93] Estrada T, Happel T, Hidalgo C, Ascasibar E and Blanco E 2010 *Europhys. Lett.* **92** 35001
[94] Zhao K J *et al* 2010 *Plasma Phys. Control. Fusion* **52** 124008

J. Phys. A: Math. Theor. **48** (2015) 293001

Topical Review

[95] Conway G D, Angioni C, Ryter F *et al* 2011 *Phys. Rev. Lett.* **106** 065001
[96] Schmitz L, Zeng L, Rhodes T L, Hillesheim J C, Doyle E J, Groebner R J, Peebles W A, Burrell K H and Wang G 2012 *Phys. Rev. Lett.* **108** 155002
[97] Manz P *et al* 2012 *Phys. Plasmas* **19** 072311
[98] Cziegler I *et al* 2013 *Phys. Plasmas* **20** 055904
[99] Tynan G *et al* 2013 *Nucl. Fusion* **53** 073053
[100] Kim E J and Diamond P H 2003 *Phys. Rev. Lett.* **90** 185006
[101] Miki K, Diamond P H, Hahn S H, Xiao W W, Gürcan Ö D and Tynan G R 2013 *Phys. Rev. Lett.* **110** 195002
[102] Miki K *et al* 2013 *Nucl. Fusion* **53** 073044
[103] Miki K, Diamond P H, Schmitz L, McDonald D C, Estrada T, Gürcan Ö D and Tynan G R 2013 *Phys. Plasmas* **20** 062304
[104] Hwa T and Kardar M 1989 *Phys. Rev. Lett.* **62** 1813–6
[105] Diamond P H and Hahm T S 1995 *Phys. Plasmas (1994–present)* **2** 3640–9
[106] Gürcan Ö D, Diamond P H and Hahm T S 2006 *Phys. Plasmas* **13** 052306
[107] Gürcan Ö D, Diamond P H, Hahm T S and Lin Z 2005 *Phys. Plasmas* **12** 032303
[108] Lane C T, Fairbank H A and Fairbank W M 1947 *Phys. Rev.* **71** 600–5
[109] Brorson S D, Fujimoto J G and Ippen E P 1987 *Phys. Rev. Lett.* **59** 1962–5
[110] Chester M 1963 *Phys. Rev.* **131** 2013–5
[111] Méndez V, Fedotov S and Horsthemke W 2010 *Reaction Transport Systems: Mesoscopic Foundations, Fronts and Spatial Instabilities (Springer Series in Synergetics)* 1st edn (Berlin: Springer)
[112] Méndez V and Camacho J 1997 *Phys. Rev. E* **55** 6476–82
[113] Taylor G I 1922 *Proc. Lond. Math. Soc.* **s2-20** 196–212
[114] Garbet X, Laurent L, Samain A and Chinardet J 1994 *Nucl. Fusion* **34** 963
[115] Lin Z and Hahm T S 2004 *Phys. Plasmas* **11** 1099–108
[116] Garbet X, Sarazin Y, Imbeaux F, Ghendrih P, Bourdelle C, Gürcan Ö D and Diamond P H 2007 *Phys. Plasmas* **14** 122305
[117] Guyer R A and Krumhansl J A 1966 *Phys. Rev.* **148** 766–78
[118] Guo Z B, Diamond P H, Kosuga Y and Gürcan Ö D 2014 *Phys. Rev. E* **89** 041101
[119] Diamond P H, McDevitt C J, Gürcan Ö D, Hahm T S and Naulin V 2008 *Phys. Plasmas* **15** 012303
[120] Levermore C D and Pomraning G C 1981 *Astrophys. J.* **248** 321–34
[121] Jou D, Casas-Vazquez J and Lebon G 1999 *Rep. Prog. Phys.* **62** 1035
[122] Garbet X, Abiteboul J, Strugarek A, Sarazin Y, Dif-Pradalier G, Ghendrih P, Grandgirard V, Bourdelle C, Latu G and Smolyakov A 2012 *Plasma Phys. Control. Fusion* **54** 055007
[123] Artaud J F, Basiuk V, Imbeaux F *et al* 2010 *Nucl. Fusion* **50** 043001
[124] Jenko F, Dannert T and Angioni C 2005 *Plasma Phys. Control. Fusion* **47** B195
[125] Sulem C and Sulem P-L 1999 *The Nonlinear Schrödinger Equation: Self-Focusing and Wave Collapse 1st edn.* (New York: Springer-Verlag)
[126] Hinton F L and Hazeltine R D 1976 *Rev. Mod. Phys.* **48** 239
[127] Hinton F L and Rosenbluth M N 1999 *Plasma Phys. Control. Fusion* **41** A653
[128] Kim E-J, Holland C and Diamond P H 2003 *Phys. Rev. Lett.* **91** 075003
[129] Dif-Pradalier G *et al* 2010 *Phys. Rev. E* **82** 025401(R)